

# Proazaphosphatrane and Bench-Stable Carbon-Based Lewis Acids in Frustrated Lewis Pair Chemistry

by

Gabriel Nicholas Jun Hao Wee

A thesis submitted in conformity with the requirements  
for the degree of Master of Science

Department of Chemistry  
University of Toronto

© Copyright by Gabriel N. J. H. Wee 2019

# Proazaphosphatrane and Bench-Stable Carbon-Based Lewis Acids in Frustrated Lewis Pair Chemistry

Gabriel Nicholas Jun Hao Wee

Master of Science

Department of Chemistry  
University of Toronto

2019

## Abstract

$B(C_6F_5)_3$  and  $P(MeNCH_2CH_2)_3N$  form a classical Lewis adduct,  $(C_6F_5)_3BP(MeNCH_2CH_2)_3N$ . Although the adduct does not exhibit spectroscopic evidence of dissociation into its constituent Lewis acid and base, products of frustrated Lewis pair (FLP) addition reactions are observed with  $PhNCO$ ,  $PhCH_2N_3$ ,  $PhNSO$ , and  $CO_2$ . Recently, a bench-stable trityl cation and  $P(MeNCH_2CH_2)_3N$  were also found to form a classical Lewis adduct that does not exhibit spectroscopic evidence of dissociation. This adduct was able to carry out the heterolytic splitting of  $H_2$ . Interestingly, when this and other newly synthesized bench-stable trityl cations were combined with phosphine bases such as  $P(t-Bu)_3$  and  $P(o-tol)_3$ , FLPs capable of heterolytic splitting of  $H_2$  were generated and, in at least one case, reversible activation of  $H_2$  was observed. These recent findings open avenues towards the application of bench-stable carbon-based Lewis acids for FLP mediated hydrogenation.

## Acknowledgments

I would like to express my sincere gratitude to my research supervisor, Prof. Douglas Stephan for his patience, support, guidance and giving me the opportunity to work and be a part of such a wonderful research group. Thank you for taking me on as a student and providing directions for me to grow as a researcher. I am very grateful for the opportunity to work in your lab. My time in your lab has undoubtedly made me a better scientist. I would also like to thank Prof. Datong Song for taking the time to review this thesis.

I am also incredibly fortunate to have had the opportunity to work with some amazing collaborators in the group. I would like to thank Dr. Timothy Johnstone (now Prof.) for helping me get started and established in the lab. I am very grateful for your patience and willingness to help me with chemistry and provide feedback. My experience working closely with you has taught me how to be a better scientist. I would also like to thank Eliar Mosaferi (now Dr.) for his help on solving structures and helpful discussions. Your advice and inputs are truly appreciated. I would also like to extend my gratitude to all members of the Stephan research group for their support and encouragement throughout this degree, especially Karlee Bamford, Alex Waked, Ryan Andrews, Christopher Major, James LaFortune, Jolie Lam and Alvaro Briceno-Strocchia. Thank you for making my time in the lab immensely enjoyable.

Last but not least, I would like to thank my family and friends for their support and encouragement throughout this degree. This would not have been possible without your love and support.

# Table of Contents

Abstract.....	ii
Acknowledgments .....	iii
Table of Contents .....	iv
List of Figures.....	vi
List of Schemes .....	vii
List of Symbols and Abbreviations .....	ix
Chapter 1 .....	1
Introduction .....	1
1.1 Frustrated Lewis Pair Chemistry .....	1
1.2 Group 14 Lewis Acids.....	7
1.3. Scope of Thesis.....	11
Chapter 2 .....	13
Accessing Frustrated Lewis Pair Chemistry from a Spectroscopically Stable and Classical Lewis Adduct .....	13
2.1 Introduction .....	13
2.2 Results and Discussion.....	15
2.3 Conclusion.....	24
2.4 Experimental Section.....	24
2.4.1 General Consideration .....	24
2.4.3 X-ray crystallography .....	31
Chapter 3 .....	33
Bench-Stable Carbon-Based Lewis Acids in Frustrated Lewis Pair Chemistry .....	33
3.1 Introduction .....	33
3.2 Results and Discussion.....	39
3.2.1 Reactivity of Bench-Stable Trityl Cations with Proazaphosphatrane .....	39
3.2.2 Reactivity of Bench-Stable Trityl Cations with Phosphines .....	49
3.3 Conclusion.....	55
3.4 Experimental Section.....	56
3.4.1 General Consideration .....	56
3.4.2 Synthesis of Starting Materials.....	57
3.4.3 X-ray crystallography .....	60
References .....	62

## List of Tables

Table 1: X-ray crystallographic data for <b>2-1 – 2-5</b> .....	32
Table 2. X-ray crystallographic data for <b>3-1</b> .....	61

## List of Figures

Figure 1: Frontier molecular orbital depiction of a classical Lewis pair reactivity resulting in adduct formation.....	1
Figure 2: Frontier molecular orbital depiction of a frustrated Lewis pair reactivity resulting in no adduct formation.....	3
Figure 3: Transannular distance in a proazaphosphatrane-electrophile adduct.....	15
Figure 4: Crystal structure of <b>2-1</b> .....	16
Figure 5: $^{19}\text{F}\{^1\text{H}\}$ NMR and $^{19}\text{F}$ - $^{19}\text{F}$ EXSY NMR spectrum of a 1:1 mixture of <b>2-1</b> and $\text{B}(\text{C}_6\text{F}_5)_3$ .....	17
Figure 6: Solid-state structure of <b>2-2</b> . C: grey, N: blue, O: red, B: green, F: pink, P: orange, S: yellow, H: white .....	19
Figure 7: Solid-state structure of <b>2-3</b> . C: grey, N: blue, O: red, B: green, F: pink, P: orange, S: yellow, H: white .....	20
Figure 8: Solid-state structure of <b>2-4</b> . C: grey, N: blue, O: red, B: green, F: pink, P: orange, S: yellow, H: white .....	21
Figure 9: Solid-state structure of <b>2-5</b> . C: grey, N: blue, O: red, B: green, F: pink, P: orange, S: yellow, H: white .....	22
Figure 10: Relaxed potential energy surface scan along the P-B distance of <b>2-1</b> (B3LYP/def2-TZVPP).....	23
Figure 11: Solid-state structure of <b>3-2</b> . C: grey, N: blue, O: red, B: pink, F: yellow, P: orange...42	
Figure 12: A comparison of the reactivity and $^{31}\text{P}$ NMR shifts of various trityl cations and $\text{B}(\text{C}_6\text{F}_5)_3$ with $\text{P}(\text{MeNCH}_2\text{CH}_2)_3\text{N}$ .....	49
Figure 13: HD scrambling experiment with $\text{PMe}_3$ and <b>3-7</b> FLP .....	55

## List of Schemes

Scheme 1: Non-classical reactivity of sodium trityl and THF-triphenylborane adduct.....	2
Scheme 2: Non-classical reactivity of sodium trityl and triphenylborane.....	2
Scheme 3: Intramolecular reactivity of an aminoborane compound.....	3
Scheme 4: Reversible metal-free activation of H <sub>2</sub> .....	4
Scheme 5: Enantioselective hydrogenation catalyzed by chiral FLP salt .....	4
Scheme 6: Proposed mechanism of the catalytic hydrogenation of ketones in ethereal solvent.....	5
Scheme 7: Small molecule activation by frustrated Lewis pair chemistry.....	6
Scheme 8: Nucleophilic aromatic substitution of a trityl cation by a sterically hindered base.....	7
Scheme 9: Activation of H <sub>2</sub> and NH <sub>3</sub> by an (alkyl)(amino)-carbene .....	8
Scheme 10: FLP-mediated heterolytic cleavage of diphenyl disulfide by a carbon-based Lewis acid .....	8
Scheme 11: Activation of H <sub>2</sub> by an all-carbon FLP .....	9
Scheme 12: Proposed mechanism of the catalytic hydrogenation of imines using Ru-η <sup>6</sup> -arene complex as a carbon-based Lewis acid .....	10
Scheme 13: FLP activation of H <sub>2</sub> using a methylated acridinium salt .....	10
Scheme 14: Reactions of FLP derived from [Ph <sub>3</sub> C] <sup>+</sup> and P(o-tolyl) <sub>3</sub> .....	11
Scheme 15: H <sub>2</sub> activation by a dynamic intramolecular FLP.....	14
Scheme 16: Synthesis of <b>2-1</b> .....	15
Scheme 17: Formation of FLP addition products from <b>2-1</b> .....	18
Scheme 18: Deactivation pathways of B(C <sub>6</sub> F <sub>5</sub> ) <sub>3</sub> by H <sub>2</sub> O .....	34
Scheme 19: Proposed mechanism for hydrogenation of imines by activation of H <sub>2</sub> using either a) THF solvent or b) substrate as a frustrated Lewis base.....	35
Scheme 20: Catalytic hydrogenation of ketones and aldehydes in toluene.....	35

Scheme 21: Moisture-tolerant hydrogenation of acetone.....	36
Scheme 22: a) Previously reported FLP-catalyzed borylation of heteroarenes b) Synthesis of bench-stable fluoroborate precatalysts .....	37
Scheme 23: Reductive amination catalyzed by BPh <sub>3</sub> or B(C <sub>6</sub> F <sub>5</sub> ) <sub>3</sub> .....	38
Scheme 24: FLP reductive amination of carbonyl compounds using water-tolerant borane as catalyst.....	39
Scheme 25: Synthesis of <b>3-1</b> .....	40
Scheme 26: Reaction of P(MeNCH <sub>2</sub> CH <sub>2</sub> ) <sub>3</sub> N with <b>3-1</b> .....	41
Scheme 27: Synthesis of <b>3-3</b> .....	43
Scheme 28: Synthesis of <b>3-4</b> .....	44
Scheme 29: Reaction of P(MeNCH <sub>2</sub> CH <sub>2</sub> ) <sub>3</sub> N with <b>3-4</b> .....	45
Scheme 30: Heterolytic cleavage of H <sub>2</sub> by FLP <b>3-5</b> .....	47
Scheme 31: Synthesis of <b>3-6</b> .....	47
Scheme 32: Reaction of P(MeNCH <sub>2</sub> CH <sub>2</sub> ) <sub>3</sub> N and <b>3-6</b> .....	48
Scheme 33: Heterolytic cleavage of H <sub>2</sub> by P(MeNCH <sub>2</sub> CH <sub>2</sub> ) <sub>3</sub> N and <b>3-6</b> FLP.....	49
Scheme 34: Heterolytic cleavage of H <sub>2</sub> by P(t-Bu) <sub>3</sub> and <b>3-4</b> FLP .....	50
Scheme 35: Heterolytic cleavage of H <sub>2</sub> by P(o-tolyl) <sub>3</sub> and <b>3-4</b> FLP .....	51
Scheme 36: Heterolytic cleavage of H <sub>2</sub> by PMes <sub>3</sub> and <b>3-1</b> FLP .....	52
Scheme 37: Synthesis of <b>3-7</b> .....	52
Scheme 38: Heterolytic cleavage of H <sub>2</sub> by PMes <sub>3</sub> and <b>3-7</b> FLP .....	53

## List of Symbols and Abbreviations

°C	degree Celsius
{ <sup>1</sup> H}	proton-decoupled
Å	angstrom, 10 <sup>-10</sup> m
atm	atmosphere
B C F H N O P S	boron carbon fluorine hydrogen nitrogen oxygen phosphorus sulfur
C <sub>6</sub> D <sub>5</sub> CD <sub>3</sub>	deuterated toluene
C <sub>6</sub> D <sub>6</sub>	deuterated benzene
C <sub>6</sub> F <sub>5</sub>	pentafluorophenyl
calcd	calculated
CD <sub>2</sub> Cl <sub>2</sub>	deuterated dichloromethane
CDCl <sub>3</sub>	deuterated chloroform
C <sub>6</sub> H <sub>6</sub>	benzene
DART	direct analysis in real time
DCM	dichloromethane
DFT	density functional theory
d	doublet
dd	doublet of doublet
ddd	doublet of doublet of doublet
e.g.	for example
eq.	equivalent
ESI	electrospray ionization
Et	ethyl
Et <sub>2</sub> O	diethyl ether
FLP	frustrated Lewis pair
g	gram
h	hour(s)
HD	hydrogen deuteride
HOMO	highest occupied molecular orbital
HRMS	high resolution mass spectrometry
Hz	Hertz, s <sup>-1</sup>

<i>i</i> -Pr	isopropyl
I'Bu	1,3-di- <i>tert</i> -butyl-imidazol-2-ylidene
J	scalar coupling constant
K	Kelvin
kCal	kilocalorie
kJ	kilojoules
LA	Lewis acid
LB	Lewis base
LUMO	lowest unoccupied molecular orbital
<i>m</i>	meta
m	multiplet
m/z	mass to charge ratio
Me	methyl
MeOH	methanol
Mes	mesityl
min	minute(s)
mg	milligram
mL	millilitre
mmol	millimole
mol	mole
MS	mass spectrometry
MHz	megahertz
NHC	N-heterocyclic carbene
NMR	nuclear magnetic resonance
<i>o</i>	ortho
OMe	methoxy
<i>p</i>	para
Ph	phenyl
POV-Ray	Persistence of Vision Raytracer
ppm	parts per million
q	quartet
r.t.	room temperature

s	singlet
t	triplet
<i>t</i> -Bu	tert-butyl
td	triplet of doublet
THF	tetrahydrofuran
Tol	toluene
toluene-d <sub>8</sub>	deuterated toluene
$\alpha$	alpha
$\beta$	beta
$\delta$	chemical shift
$\Delta$	heat

# Chapter 1

## Introduction

### 1.1 Frustrated Lewis Pair Chemistry

In 1923, Gilbert N. Lewis published his seminal work entitled: “Valence and the Structure of Atoms and Molecules” in which he described molecules that behave as electron-pair acceptors as acids, and molecules that behave as electron-pair donors as bases.<sup>1</sup> Donation of electrons from the highest occupied molecular orbital (HOMO) of the base to the lowest unoccupied molecular orbital (LUMO) of the acid would result in the creation of a dative bond to form an adduct (**Figure 1**). For example, the formation of the ammonia-borane coordination complex ( $\text{H}_3\text{B-NH}_3$ ) is a result of the donation of a lone pair of electrons in the  $\text{sp}_3$  hybrid orbital (HOMO) of the nitrogen atom on ammonia to the vacant p-orbital (LUMO) of the boron atom on borane. The formation of an adduct forms a more stable complex with a lower energy HOMO. Since the first description of the Lewis acid/base paradigm, this notion has been essential in our understanding of chemical reactivity.

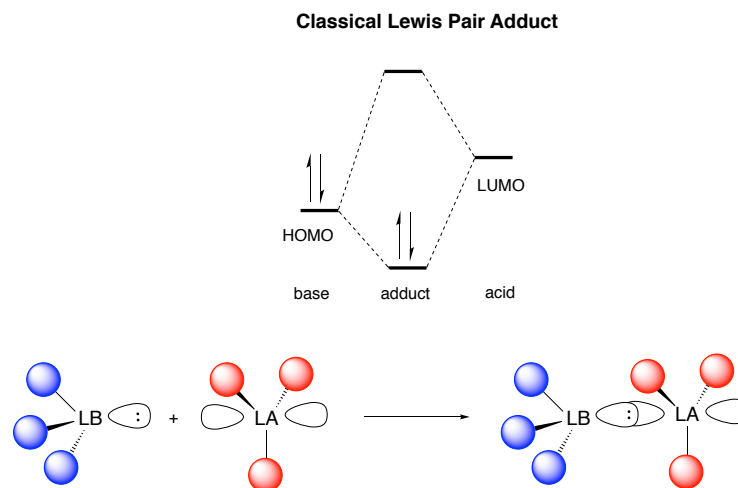
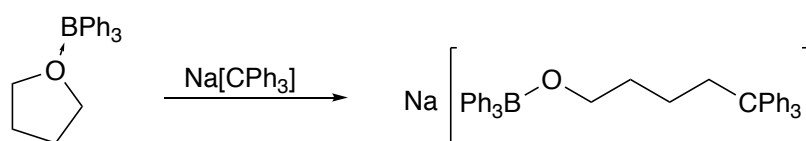


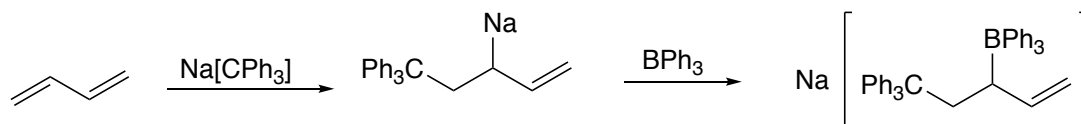
Figure 1: Frontier molecular orbital depiction of a classical Lewis pair reactivity resulting in adduct formation

However, in the years following this work, numerous observations began to collect of systems that did not behave as expected from the acid-base theory proposed by Lewis. In 1942, Brown observed that the reaction of  $\text{BMe}_3$  and 2,6-lutidine did not result in adduct formation.<sup>2</sup> This observation contrasted with the reaction of the less sterically demanding  $\text{BF}_3$  and 2,6-lutidine where the formation of the predicted Lewis acid-base adduct was observed.<sup>2</sup> In 1950, Wittig and Rückert observed that the addition of sodium trityl ( $\text{NaCPh}_3$ ) to the THF adduct of triphenylborane unexpectedly resulted in the ring-opening of THF instead of displacement of THF and adduct formation between triphenylborane and trityl anion (**Scheme 1**).<sup>3</sup>



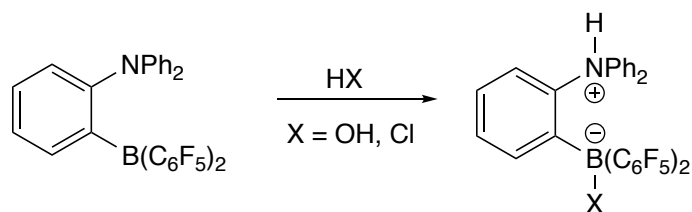
Scheme 1: Non-classical reactivity of sodium trityl and THF-triphenylborane adduct

In 1966, Tochtermann reported that the reaction of  $\text{NaCPh}_3$  and  $\text{BPh}_3$  in the presence of an unsaturated substrate such as 1,3-butadiene gave the 1,2 addition product (**Scheme 2**).<sup>4</sup>



Scheme 2: Non-classical reactivity of sodium trityl and triphenylborane

In a more recent report, Roesler and Piers reported in 2003 the synthesis and characterization of *ortho*-phenylene bridged aminoborane compound.<sup>5</sup> While geometric constraint prevented adduct formation between the Lewis acidic boron centre and the Lewis basic nitrogen centre, it was able to activate small acids such as  $\text{H}_2\text{O}$  and  $\text{HCl}$  to yield the zwitterionic ammonium borate compound (**Scheme 3**).<sup>5</sup>



Scheme 3: Intramolecular reactivity of an aminoborane compound

This and other previous observations marked the beginning of what is now known as frustrated Lewis pair (FLP) chemistry, a term coined by Stephan and co-workers in 2007 to describe systems comprising of Lewis acids and bases in which adduct formation is precluded due to steric and/or electronic reasons.<sup>6</sup> The lack of adduct formation allows the LUMO of the Lewis acid and the HOMO of the Lewis base to effect nonclassical reactivity (**Figure 2**).

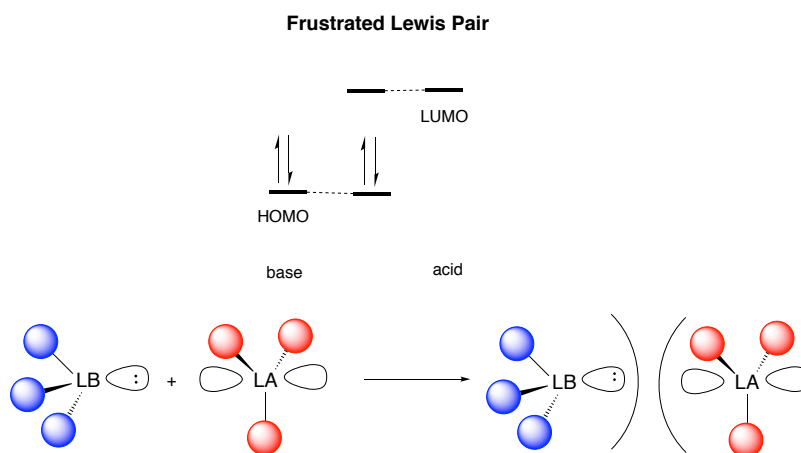
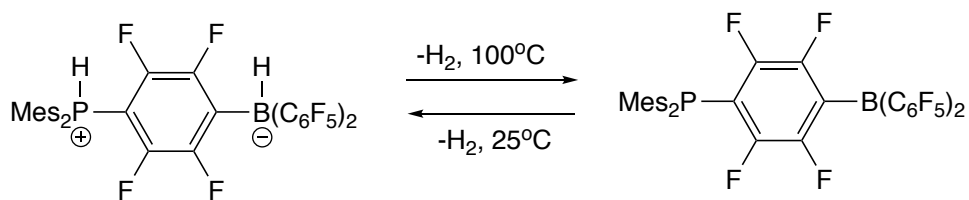


Figure 2: Frontier molecular orbital depiction of a frustrated Lewis pair reactivity resulting in no adduct formation

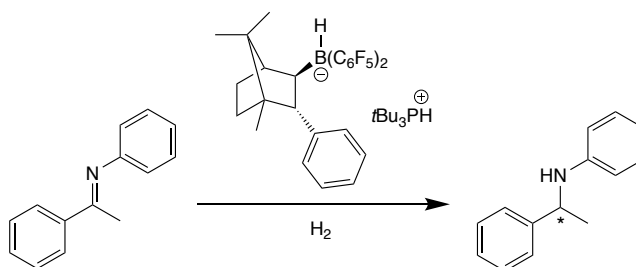
Since then, FLP chemistry has emerged as a strategy for effecting metal-free hydrogenation reactions and small molecule activation or fixation.<sup>7-10</sup> In 2006, Stephan and co-workers reported that a phosphine-borane species  $\text{Mes}_2\text{P}(\text{C}_6\text{F}_4)\text{B}(\text{C}_6\text{F}_5)_2$  was able to heterolytically cleave dihydrogen, giving the zwitterionic phosphonium hydridoborate species  $\text{Mes}_2\text{PH}(\text{C}_6\text{F}_4)\text{BH}(\text{C}_6\text{F}_5)_2$ .<sup>11</sup> Furthermore, upon heating to elevated temperature, the zwitterionic

salt was shown to release dihydrogen, which represents the first example of a reversible metal-free dihydrogen activation (**Scheme 4**).<sup>11</sup>



Scheme 4: Reversible metal-free activation of H<sub>2</sub>

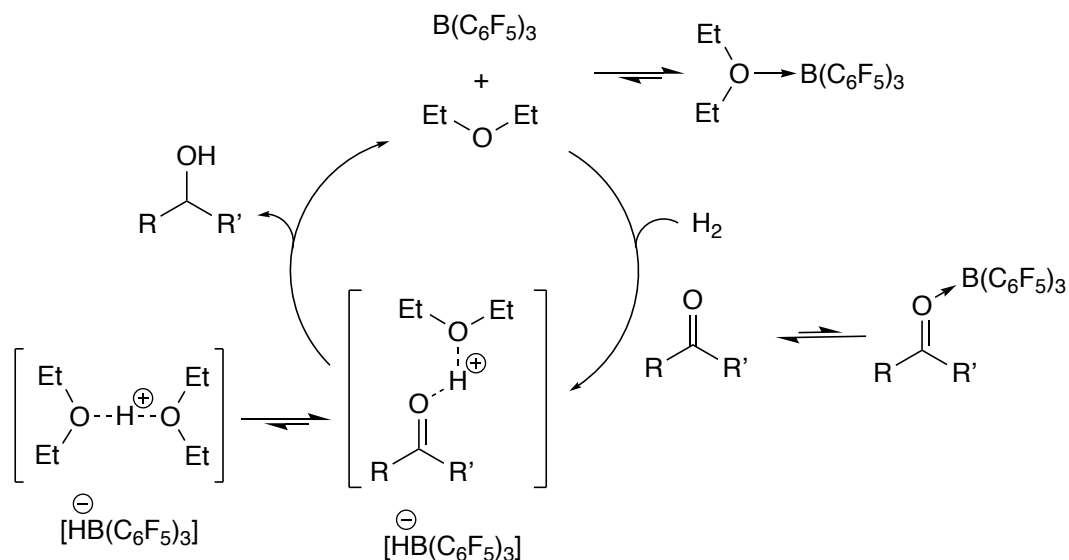
This is a remarkable finding given that, up to this point, it was thought that transition metal species were required for the reversible activation of dihydrogen.<sup>11</sup> Since then, FLP chemistry has been shown to be effective for the hydrogenation of a variety of organic substrates such as imines, enamines, ketones, aldehydes, alkenes, alkynes, aziridines, silyl enol ethers and polycyclic aromatic compounds.<sup>7–10</sup> Particularly noteworthy is the stoichiometric FLP-mediated hydrogenation of the aromatic ring of aniline to cyclohexylammonium derivatives, which is a rare example of a homogeneous metal-free reduction of an aromatic group under relatively mild conditions.<sup>12</sup> It has also been demonstrated that chiral FLP catalysts can be synthesized to effect the highly enantioselective hydrogenation of prochiral substrates such as imines (**Scheme 5**).<sup>13</sup>



Scheme 5: Enantioselective hydrogenation catalyzed by chiral FLP salt

Studies into FLP systems have shown that the Lewis acidity and basicity must be matched in terms of the cumulative strength to effect heterolytic cleavage of H<sub>2</sub>. For example, the use of a weaker Lewis base would necessitate the use of a stronger Lewis acid to effect activation of H<sub>2</sub> and vice-

versa.<sup>14</sup> More recently, it has also been observed that classical Lewis adducts could also exhibit FLP reactivity that can be attributed to reversible adduct formation. For example, it has been shown that the combination of Et<sub>2</sub>O and B(C<sub>6</sub>F<sub>5</sub>)<sub>3</sub> exists in an equilibrium between the classical Lewis adduct and the corresponding FLP. It has been proposed that the FLP is able to effect the heterolytic cleavage of H<sub>2</sub> and catalytically hydrogenate a variety of ketones (**Scheme 6**).

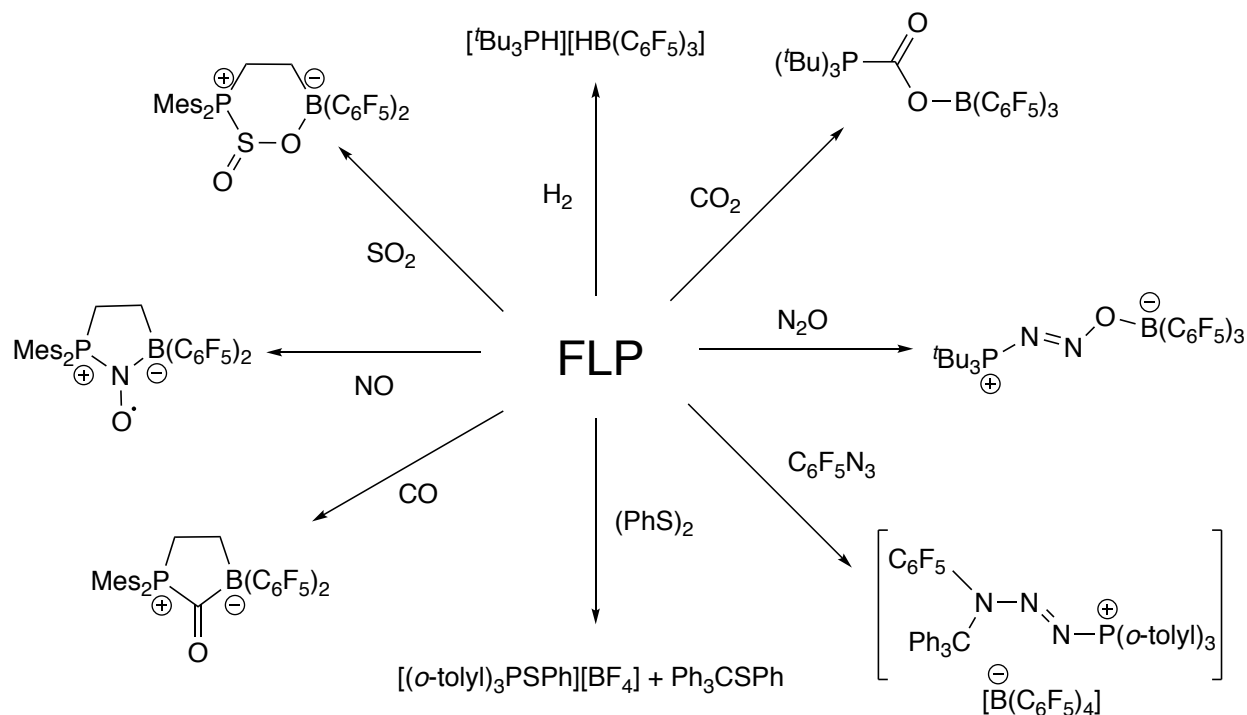


Scheme 6: Proposed mechanism of the catalytic hydrogenation of ketones in ethereal solvent

Computational studies by Pápai<sup>15–18</sup> and Grimme<sup>19</sup> proposed that cleavage of H<sub>2</sub> is driven by initial polarization of the dihydrogen molecule in an “encounter complex” in which steric demands of the Lewis acid and base preclude adduct formation but are stabilized by van der Waals interactions. The complex subsequently reacts with H<sub>2</sub> in a bimolecular fashion.

The field of frustrated Lewis pair chemistry has also helped foster a resurgence of main group small molecule activation chemistry. FLPs have also been shown to be capable of activating a wide range of small molecules other than H<sub>2</sub>. For example, Ashley and coworkers demonstrated the ability of an FLP to mediate the hydrogenation of CO<sub>2</sub> to CH<sub>3</sub>OH.<sup>20</sup> Early efforts have also

shown that FLPs are able to activate organic molecules such as olefins,<sup>6</sup> alkynes,<sup>21</sup> disulfides<sup>22</sup> and cyclopropanes,<sup>23</sup> giving zwitterionic addition products. More recent studies have shown that FLPs can also capture small molecules such as SO<sub>2</sub>,<sup>24</sup> N<sub>2</sub>O,<sup>25,26</sup> NO,<sup>27</sup> CO<sup>28,29</sup>, CO<sub>2</sub><sup>30</sup> and RN<sub>3</sub><sup>31,32</sup> (Scheme 7).

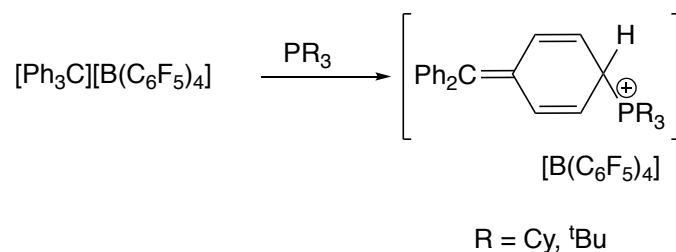


Scheme 7: Small molecule activation by frustrated Lewis pair chemistry

Recently, a study on some well-known FLPs based on boron and aluminum Lewis acids and triarylphosphine Lewis bases has revisited the assumption of a heterolytic, two electron model of FLP-mediated small molecule activation.<sup>33,34</sup> Compelling evidence was provided that, in some instances, a single-electron transfer mechanism is operating.<sup>33,34</sup> This finding goes against the common assumption that FLP chemistry is a two-electron process.

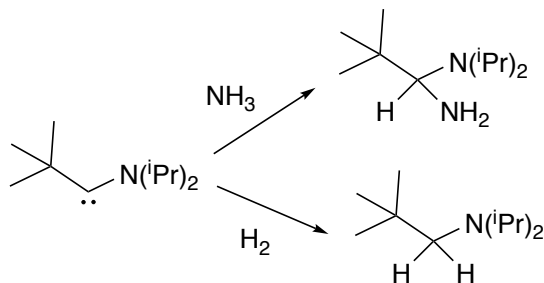
## 1.2 Group 14 Lewis Acids

Since the articulation of the FLP concept in 2006, the Lewis acidic trityl cation  $[\text{Ph}_3\text{C}]^+$  and its derivatives have found limited use in FLP chemistry.<sup>35</sup> In 2006, Stephan and coworkers reported the formation of classical donor-acceptor adducts of trityl cation with small bases such as  $\text{PMe}_3$  and  $\text{PPh}_3$ .<sup>36</sup> However, if bulkier phosphines are present, nucleophilic attack is often observed at the *para* position of a trityl aryl ring to yield cyclohexadienyl-phosphonium cations such as  $[\text{R}_3\text{P}(\text{C}_6\text{H}_5)\text{CPh}_2]^+$  where  $\text{R} = \text{Cy}, \text{}^t\text{Bu}$  (**Scheme 8**).<sup>36</sup>



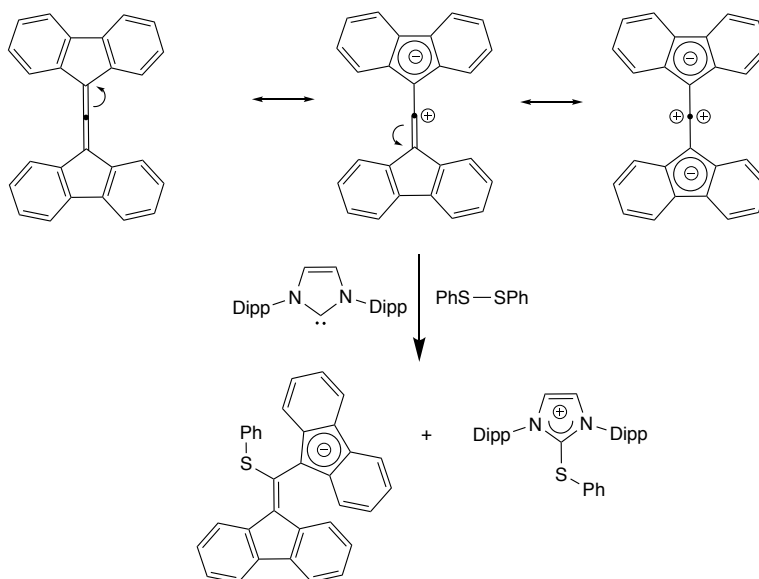
Scheme 8: Nucleophilic aromatic substitution of a trityl cation by a sterically hindered base

In that same year, Bertrand and co-workers showed that an (alkyl)-(amino)-carbene (CAAC) can activate  $\text{H}_2$  and  $\text{NH}_3$ .<sup>37</sup> These carbenes have a vacant orbital and a filled non-bonding orbital and can be viewed as a carbon-based FLP where the Lewis acid and base components reside on the same atom.<sup>37</sup> Computational studies show that cleavage of the  $\text{H-X}$  bond ( $\text{X} = \text{H}, \text{NH}_2$ ) proceeds by nucleophilic activation in which the lone pair on the carbene interacts with the  $\sigma_{\text{H-X}}^*$  orbital to generate a pseudo-amide or hydride fragment followed by transfer of that fragment to the carbon centre (**Scheme 9**).<sup>37</sup>



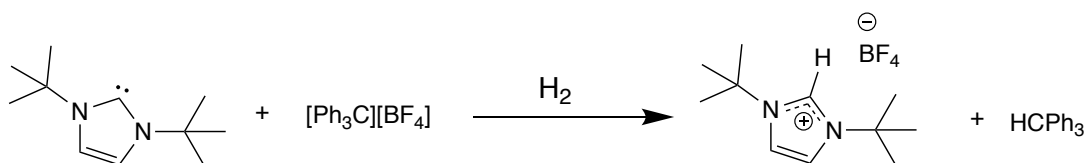
Scheme 9: Activation of H<sub>2</sub> and NH<sub>3</sub> by an (alkyl)(amino)-carbene

In 2010, Alcarazo and co-workers described the reactivity of an electron-poor bis(fluorenyl)allene with Lewis bases.<sup>38</sup> In particular, the combination of the allene with a bulky N-heterocyclic carbene such as 1,3-bis(2',6'-diisopropylphenyl)imidazole-2-ylidene generated an FLP that was shown to heterolytically cleave the S-S bond in disulfides (**Scheme 10**).<sup>38</sup> However, this FLP does not react with H<sub>2</sub> suggesting the limited Lewis acidity of allene.<sup>38</sup>



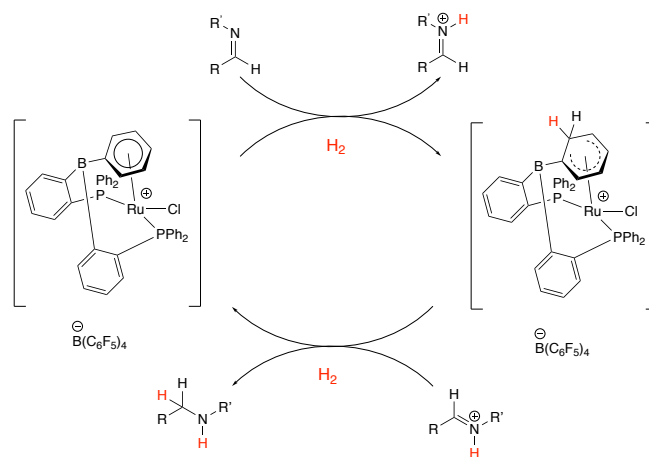
Scheme 10: FLP-mediated heterolytic cleavage of diphenyl disulfide by a carbon-based Lewis acid

In subsequent studies, Alcarazo reported the reactivity of other electron poor allene-bearing electron-withdrawing substituents.<sup>39</sup> When combined with *N*-heterocyclic carbenes, the reaction afforded the corresponding Lewis adduct.<sup>39</sup> However, at -78°C, adduct formation is precluded and the resulting kinetically-induced FLP, in which low temperatures was used to prevent quenching of the Lewis pair components, was shown to effect the heterolytic cleavage of S–S bonds.<sup>39</sup> In 2011, Arduengo and co-workers described an all-carbon FLP that was capable of H<sub>2</sub> activation.<sup>40</sup> By combining the trityl cation and NHC *t*Bu at -60°C, this FLP was able to heterolytically cleave H<sub>2</sub> to generate triphenylmethane and the imidazolium salt (**Scheme 11**).<sup>40</sup>



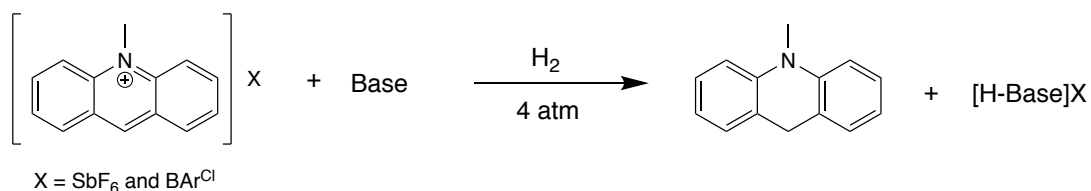
Scheme 11: Activation of H<sub>2</sub> by an all-carbon FLP

Shortly thereafter, Stephan and co-workers reported an unusual carbon-based Lewis acid derived from a cationic Ru-η<sup>6</sup> arene complex.<sup>41</sup> Treatment of this complex with bulky phosphines such as PCy<sub>3</sub> results in the reversible coordination of the phosphine to the phenyl carbon *ortho* to boron.<sup>41</sup> Exposure of this complex to H<sub>2</sub> resulted in heterolytic cleavage of H<sub>2</sub> with hydride addition at either the *ortho* or *para* position of the phenyl group and protonation of phosphine.<sup>41</sup> DFT calculations supports the description of this complex as a carbon-based Lewis acid as it shows the ruthenium metal centre enhancing the Lewis acidity of the aromatic carbons.<sup>41</sup> This FLP is also able to effect the catalytic hydrogenation of aldimines under H<sub>2</sub> at room temperature and is the first example of an FLP hydrogenation using a carbon-based Lewis acid (**Scheme 12**).<sup>41</sup>



Scheme 12: Proposed mechanism of the catalytic hydrogenation of imines using Ru- $\eta^6$ -arene complex as a carbon-based Lewis acid

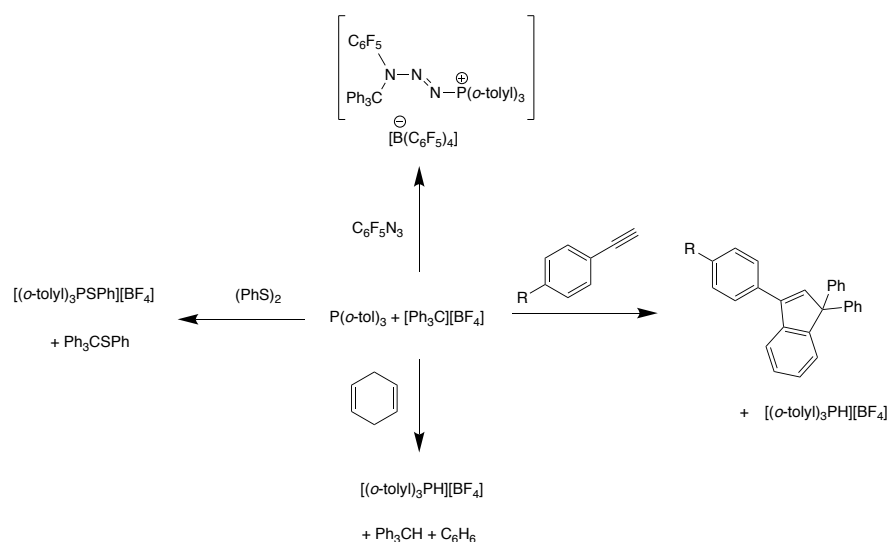
In 2014, Ingelson and co-workers reported that the combination of a methylated acridinium salt with 2,6-lutidine reacted like an FLP to activate  $H_2$  even in the presence of  $H_2O$  (**Scheme 13**).<sup>42</sup>



Scheme 13: FLP activation of  $H_2$  using a methylated acridinium salt

It is able to catalyze the dehydrosilylation of primary, secondary, tertiary and aryl alcohols by silanes with no observable over-reduction to alkanes.<sup>42</sup> As it is less oxophilic than boron, aluminum and silicon-based Lewis acids, it is also air- and moisture-stable and this allows for the possibility of bench-stable FLP-catalyzed reactions and increased functional group tolerance.<sup>42</sup> In 2017, Stephan and co-workers reported that the FLP derived from the trityl cation and  $P(o\text{-tolyl})_3$  is able to dehydrogenate 1,4-cyclohexadiene to benzene and effect the cycloaddition of 1-bromo-

4-ethynylbenzene to the trityl cation to generate an indene derivative.<sup>31</sup> Furthermore, it is also able to heterolytically cleave the S-S bond of diphenyl disulfide and react with pentafluorophenyl azide to trap an intermediate in the Staudinger reaction of (*o*-tolyl)<sub>3</sub>P with azide (**Scheme 14**).<sup>31</sup>



Scheme 14: Reactions of FLP derived from [Ph<sub>3</sub>C]<sup>+</sup> and P(*o*-tolyl)<sub>3</sub>

To our knowledge this is the first reported example of an FLP based on a Lewis basic phosphorus site and a Lewis acidic carbon site. However, this combination of Lewis acid and base is unable to activate hydrogen deuteride.<sup>31</sup>

### 1.3. Scope of Thesis

Over the last decade, research in the area of FLP chemistry have suggested that access to FLP reactivity requires that the donor-acceptor interaction be either sterically or electronically frustrated, which provides observable access to the dissociated acid and base.<sup>7-9</sup> The work presented here describes a classical Lewis acid-base adduct formed from a strong Lewis acid and Lewis base, which shows no spectroscopic evidence of dissociation. However, products of FLP addition reactions are seen with a variety of small molecules. The present findings highlight the importance of experimentally examining the reactions of seemingly stable Lewis adducts even if

initial spectroscopic evidence suggests the lack of a dissociation. This project was performed in collaboration with Dr. Timothy Johnstone, a member of the Stephan research group. Portions of this research has been published at the time of writing this thesis:

T. C. Johnstone, G. N. J. H. Wee, D. W. Stephan, *Angewandte Chemie International Edition* **2018**, *57*, 5881–5884.

The use of carbon-based Lewis acid in FLP chemistry is limited.<sup>35</sup> Recently, in 2017, Stephan and coworkers reported an FLP derived from the trityl cation and (*o*-tolyl)<sub>3</sub>P is able to activate 1,4-cyclohexadiene and 1-bromo-4-ethynylbenzene and heterolytically cleave the S-S bond of diphenyl disulfide.<sup>31</sup> However, this combination of Lewis acid and base is not able to activate hydrogen deuteride.<sup>31</sup> The work presented here describes a family of bench-stable trityl cations that, when combined with proazaphosphatrane and a variety of phosphine Lewis bases, are able to induce the heterolytic splitting of H<sub>2</sub>. In at least one case, reversible activation of H<sub>2</sub> was observed. These recent findings open potential avenues towards the development of bench-stable FLP chemistry and the expansion of the utility of carbon-based Lewis acids in FLP chemistry.

## Chapter 2

### Accessing Frustrated Lewis Pair Chemistry from a Spectroscopically

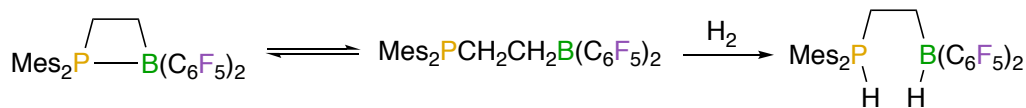
### Stable and Classical Lewis Adduct

This project was performed in collaboration with Dr. Timothy Johnstone, a member of the Stephan research group. Portions of this chapter have been published at the time of writing this thesis:

T. C. Johnstone, G. N. J. H. Wee, D. W. Stephan, *Angewandte Chemie International Edition* **2018**, *57*, 5881–5884.

#### 2.1 Introduction

The concept of frustrated Lewis pairs (FLPs) provides a framework for understanding and developing chemical systems in which distinct Lewis acidic and basic centers act simultaneously on a substrate to effect small molecule activation. Since the initial discovery that H<sub>2</sub> can be reversibly activated by combinations of sterically encumbered Lewis acids and bases, FLPs have led to the discovery of a variety of new reactions such as the development of metal-free catalysts for the hydrogenation of a variety of organic substrates and fostered a resurgence in main group small molecule activation. The first FLP systems inferred that sterically demanding substituents on the Lewis acidic and basic sites preclude adduct formation and provides access to unique FLP reactivity.<sup>14</sup> This notion was later expanded by reports that FLP reactivity can still be accessed by acid-base combinations that exist in equilibrium between the free species and the classical Lewis adduct. For example, Erker and coworkers have shown that the molecule Mes<sub>2</sub>P(CH<sub>2</sub>)<sub>2</sub>B(C<sub>6</sub>F<sub>5</sub>)<sub>2</sub> exists in an equilibrium between its open FLP and closed Lewis adduct forms (**Scheme 15**).<sup>43</sup> In its open FLP form, the molecule is able to engage in a variety of FLP reactions such as H<sub>2</sub> activation.



Scheme 15: H<sub>2</sub> activation by a dynamic intramolecular FLP

This notion was later expanded by demonstrating that mixtures of 2,6-lutidine and B(C<sub>6</sub>F<sub>5</sub>)<sub>3</sub>, which exhibit equilibria between the free species and the classical adducts, also reacts with H<sub>2</sub> to form the salt [Me<sub>2</sub>C<sub>5</sub>H<sub>3</sub>NH][HB(C<sub>6</sub>F<sub>5</sub>)<sub>3</sub>].<sup>44</sup> In addition to steric bulk, electronic effects can also ensure the presence of an equilibrium that provides access to the dissociated acid and base. For example, the adduct between a weak unhindered base Et<sub>2</sub>O and a strong acid B(C<sub>6</sub>F<sub>5</sub>)<sub>3</sub> exists in an equilibrium with the dissociated acid and base in toluene. Upon dissociation, this system activates H<sub>2</sub> and effects the catalytic hydrogenation of alkyl and aryl ketones.<sup>45</sup> While previous examples have employed strong acids and weak bases, similar equilibria can also be accessed using weak acids and strong bases. For example, Fontaine and co-workers have exploited basic N-donors with weakly acidic boron centers to activate C-H bonds of heteroarenes and catalyze the metal-free borylation of heteroarenes.<sup>46</sup> Krempner and co-workers have demonstrated that the combination of BPh<sub>3</sub> and the strong Lewis base P(*i*PrNCH<sub>2</sub>CH<sub>2</sub>)<sub>3</sub>N splits H<sub>2</sub> and catalyzes imine reduction.<sup>47</sup> The results of these and other studies suggest that access to FLP reactivity requires either sterically or electronically induced frustration of the donor-acceptor interaction, which provides access to the dissociated acid and base.

In this study, we describe a classical Lewis adduct comprised of a strong Lewis acid and a strong Lewis base, specifically, the proazaphosphatane base P(MeNCH<sub>2</sub>CH<sub>2</sub>)<sub>3</sub>N and B(C<sub>6</sub>F<sub>5</sub>)<sub>3</sub>. Although the adduct is shown to form a robust dative bond between the strong donor and acceptor and shows no spectroscopic evidence of dissociation, it engages in a range of FLP-type addition reactions with unsaturated substrates. Computational studies show that steric effects preclude the formation

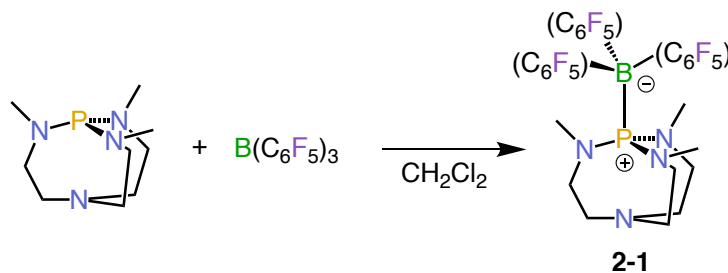
of a stabilizing transannular P-N interaction. The transannulation, which can vary as reflected in the P-N<sub>ta</sub> distance, has previously been identified as one of the main contributors to the strength of the base and results in an overall stabilization in the resulting proazaphosphatrane-electrophile adduct (**Figure 3**).<sup>48</sup>



Figure 3: Transannular distance in a proazaphosphatrane-electrophile adduct

As a result, dissociation into an analogue of the encounter complex described for conventional FLPs and FLP-type reactivity is energetically accessible under ambient conditions. The present finding demonstrates that FLP reactivity can be observed even in cases where steric or electronic frustration does not yield experimentally observable formation of the dissociated acid and base.

## 2.2 Results and Discussion



Scheme 16: Synthesis of **2-1**

Proazaphosphatrane P(MeNCH<sub>2</sub>CH<sub>2</sub>)<sub>3</sub>N reacts with B(C<sub>6</sub>F<sub>5</sub>)<sub>3</sub> to produce a species featuring a doublet in the <sup>11</sup>B{<sup>1</sup>H} NMR spectrum at δ = -12.4 ppm with coupling constant 130 Hz and a quartet in the <sup>31</sup>P NMR spectrum at δ = 80.0 ppm with coupling constant 130 Hz. In the <sup>19</sup>F{<sup>1</sup>H}

NMR spectrum, five distinct signals were observed with multiplicities and intensities consistent with two  $F_{\text{ortho}}$ , two  $F_{\text{meta}}$ , and one  $F_{\text{para}}$  signal. In the  $^{13}\text{C}\{^1\text{H}\}$  NMR spectrum, five distinct signals were also observed. Both the  $^{19}\text{F}$  and  $^{13}\text{C}$  NMR spectra are consistent with a three-fold symmetry of the borane and restricted rotation about the B-C bonds. This gives rise to five inequivalent fluoroarene signals. These data are consistent with the formation of a dative P-B bond. Single-crystal X-ray diffraction studies confirmed the structure of **2-1** (Figure 4).

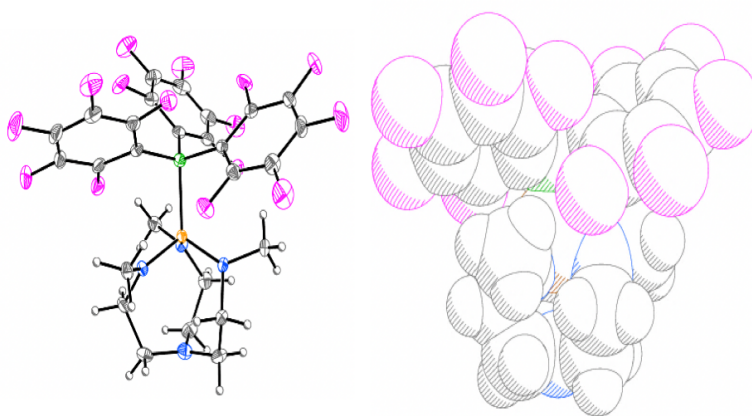


Figure 4: Crystal structure of **2-1**

The P-B distance is 2.096(3) Å, which is typical for phosphine-borane adducts. However, the transannular P-N<sub>ta</sub> distance in **2-1** is 3.289(2) Å, which is substantially longer than in the cation [HP(MeNCH<sub>2</sub>CH<sub>2</sub>)<sub>3</sub>N]<sup>+</sup> and suggests a lack of a transannular interaction in **2-1**. This result stands in contrast to previous reports where the degree of transannulation in P(MeNCH<sub>2</sub>CH<sub>2</sub>)<sub>3</sub>N has been correlated with the strength of the Lewis acid interacting with it. Probing the dissociative stability of **2-1** via standard NMR lineshape analysis at varied temperature was hindered by its low solubility in solvents other than CH<sub>2</sub>Cl<sub>2</sub>. Furthermore, **2-1** decomposes to unidentified products when heated.

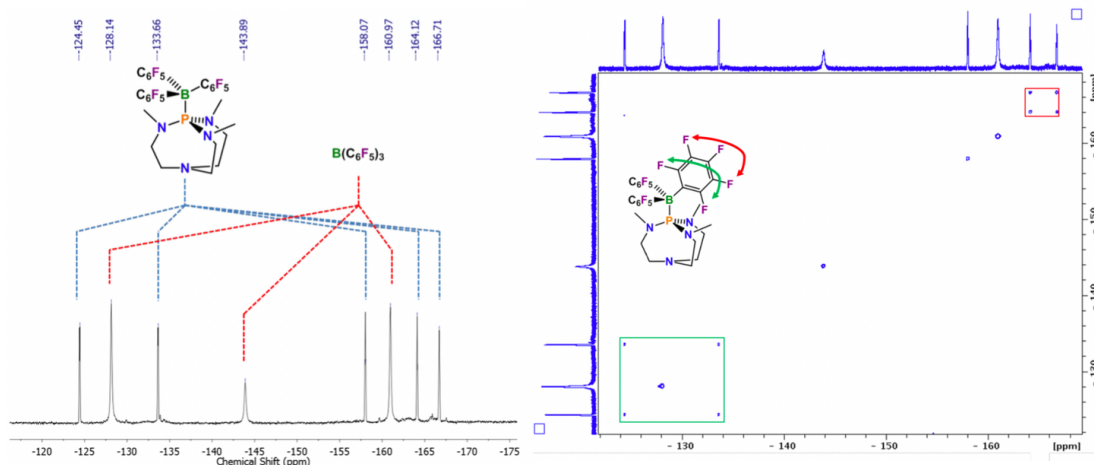
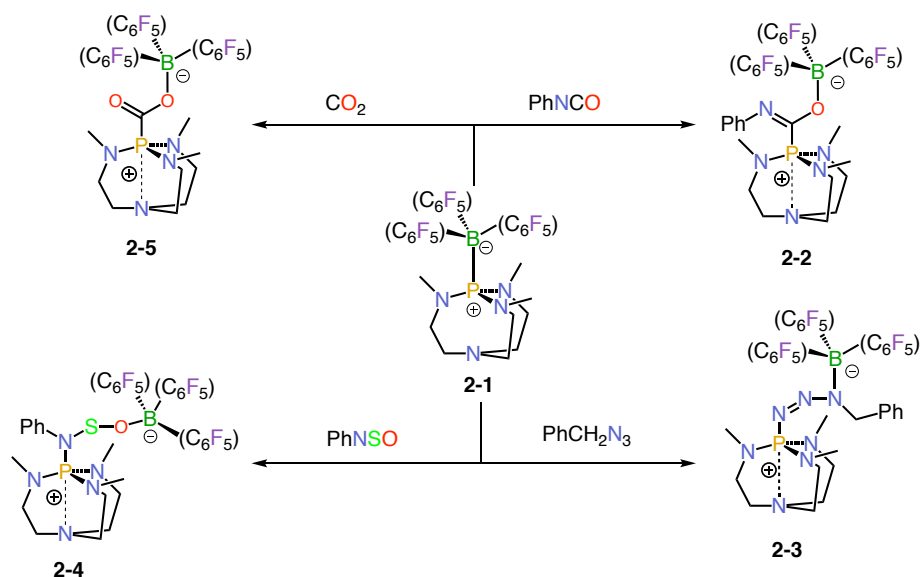


Figure 5:  $^{19}\text{F}\{^1\text{H}\}$  NMR and  $^{19}\text{F}$ - $^{19}\text{F}$  EXSY NMR spectrum of a 1:1 mixture of **2-1** and  $\text{B}(\text{C}_6\text{F}_5)_3$

In order to probe the possible dissociation of the adduct, a  $^{19}\text{F}$  exchange spectroscopy (EXSY) NMR experiment was performed with a 1:1 mixture of  $\text{B}(\text{C}_6\text{F}_5)_3$  and **2-1** (Figure 5). Using mixing times as long as 1500 ms, no evidence of chemical exchange between the  $\text{B}(\text{C}_6\text{F}_5)_3$  bound to  $\text{P}(\text{MeNCH}_2\text{CH}_2)_3\text{N}$  and the  $\text{B}(\text{C}_6\text{F}_5)_3$  free in solution was observed. At these long mixing times, exchange cross-peaks between the inequivalent  $\text{F}_{\text{ortho}}$  and  $\text{F}_{\text{meta}}$  signals of **2-1** are observed, indicating that the adduct exhibits internal rotational dynamics on this timescale. The results illustrates that on the timescale of the experiment performed, **2-1** and  $\text{B}(\text{C}_6\text{F}_5)_3$  combine to quantitatively form a strong, stable adduct that persists in solution.



Scheme 17: Formation of FLP addition products from **2-1**

Compound **2-1** was combined with 1 equivalent of phenyl isocyanate, a known substrate for FLP 1,2-addition reactions.<sup>9</sup> Surprisingly, this combination in either toluene or dichloromethane cleanly affords a single new species within 10 min. NMR and crystallographic characterization of **2-2** revealed it to be the product of 1,2-addition of **2-1** and  $\text{B}(\text{C}_6\text{F}_5)_3$  across the C-O double bond of PhNCO. The  $^{31}\text{P}\{^1\text{H}\}$  NMR spectrum features a new singlet at  $\delta = 26.2$  ppm, indicating scission of the B-P bond. Proton coupling splits the  $^{31}\text{P}$  NMR resonance into a decet, indicating that the P atom is coupled to the three methyl substituents attached to the equatorial N atoms. In the  $^1\text{H}$  NMR spectrum, the methyl resonance is split into a doublet, which collapses into a singlet upon  $^{31}\text{P}$ -decoupling. In the  $^{13}\text{C}\{^1\text{H}\}$  NMR data, signals are observed for the azaphosphatrane backbone, the perfluorophenyl rings from the parent backbone and one additional phenyl ring from an isocyanate. The  $^{11}\text{B}\{^1\text{H}\}$  NMR spectrum features a new singlet resonance at  $\delta = -3.49$  ppm, while the  $^{19}\text{F}\{^1\text{H}\}$  NMR spectrum features three signals at  $\delta = -133.7$ ,  $-161.9$  and  $-166.9$  ppm, both suggesting a four-coordinate B center. These NMR data suggest that compound **2-1** dissociated

and added to the isocyanate. The identity of **2-2** was confirmed by X-ray diffraction. The product resulting from 1,2-addition of B/P across the C=O double bond was observed (**Figure 6**).

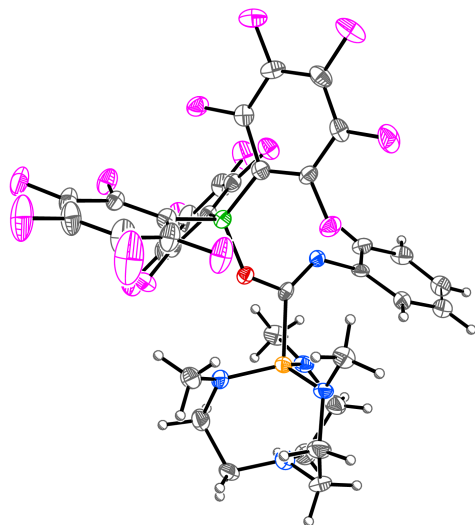


Figure 6: Solid-state structure of **2-2**. C: grey, N: blue, O: red, B: green, F: pink, P: orange, S: yellow, H: white

The formation of **2-2** corresponds to a formal FLP addition reaction, examples of which have been reported for a range of isocyanates and FLPs.<sup>9</sup> In the absence of  $B(C_6F_5)_3$ ,  $P(MeNCH_2CH_2)_3N$  is known to cyclotrimerize isocyanates into isocyanurates.<sup>49</sup> In the presence of a borane, a putative intermediate in the process is trapped and provides an example of a growing application of FLPs as a tool to trap reactive intermediates.

To further probe the ability of compound **2-1** to exhibit FLP reactivity, **2-1** was combined with 1 equivalent of benzyl azide. Within 10 min of addition, this combination in toluene or dichloromethane affords a single new species **2-3** as evidenced by NMR data. The  $^{11}B\{^1H\}$  NMR spectrum reveals an upfield and sharp  $^{11}B$  resonance at  $\delta = -6.33$  ppm and the  $^{19}F\{^1H\}$  NMR spectrum reveals a narrow  $\delta_{para} - \delta_{meta}$  gap of 5.4 ppm, both indicating a four-coordinate boron centre. The product displays a new  $^{31}P\{^1H\}$  NMR signal at 36.9 ppm. The connectivity of **2-3** was

confirmed by X-ray crystallography. The product resulting from 1,3-addition of B/P across azide was observed (**Figure 7**). This isolation of **2-3** can be viewed as a trapped reaction intermediate for the oxidation of the phosphine by the Staudinger reaction.<sup>31</sup>

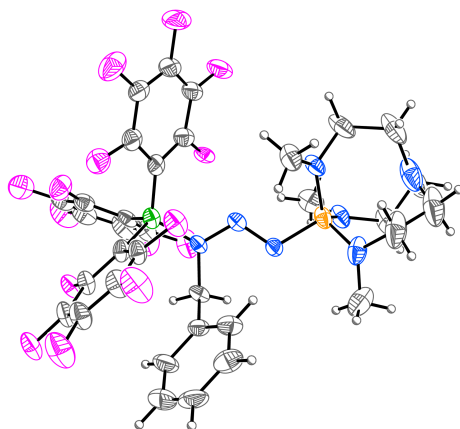


Figure 7: Solid-state structure of **2-3**. C: grey, N: blue, O: red, B: green, F: pink, P: orange, S: yellow, H: white

The analogous reaction of 1 equivalent of PhNSO to **2-1** cleanly affords product **2-4** with a  $^{31}\text{P}\{^1\text{H}\}$  NMR singlet at 36.8 ppm, a  $^{11}\text{B}$  NMR singlet at -1.91 ppm and  $^{19}\text{F}$  NMR signals at -132.57, -162.19 and -166.54 ppm. X-ray diffraction analysis of a single crystal confirmed the structure of **2-4**. The product resulting from 1,3-addition of B/P across the NSO functional group was observed (**Figure 8**).

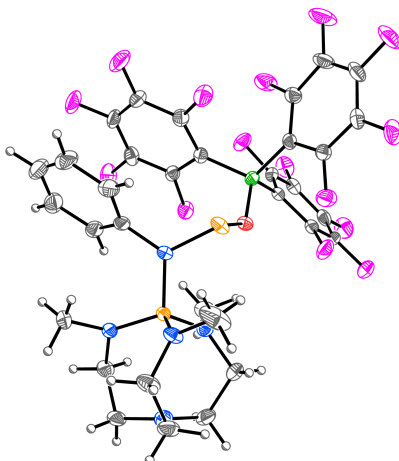


Figure 8: Solid-state structure of **2-4**. C: grey, N: blue, O: red, B: green, F: pink, P: orange, S: yellow, H: white

In the last example, **2-1** was placed under an atmosphere of CO<sub>2</sub>. Again, a single product readily formed. The spectroscopic features of the borane and azaphosphatrane moieties are analogous to those seen in the addition products described above. The <sup>31</sup>P NMR signal at 23.2 ppm along with the <sup>11</sup>B NMR singlet at -3.90 ppm and the <sup>19</sup>F NMR signals at -134.49, -161.32 and -166.58 ppm, are indicative of the formation of a four-coordinate boron and 1,2-addition across the C=O bond. The use of <sup>13</sup>C labelled CO<sub>2</sub> causes the <sup>31</sup>P{<sup>1</sup>H} NMR signal at 23.2 ppm to split into a doublet with <sup>1</sup>J<sub>P-C</sub> = 235 Hz. The corresponding signal in the <sup>13</sup>C{<sup>1</sup>H} NMR spectrum at 137.18 ppm is a doublet with <sup>1</sup>J<sub>P-C</sub> = 235 Hz, confirming P-C bond formation. X-ray diffraction study confirmed the structure of **2-5**. The product resulting from 1,2-addition across the C=O double bond was observed (**Figure 9**).

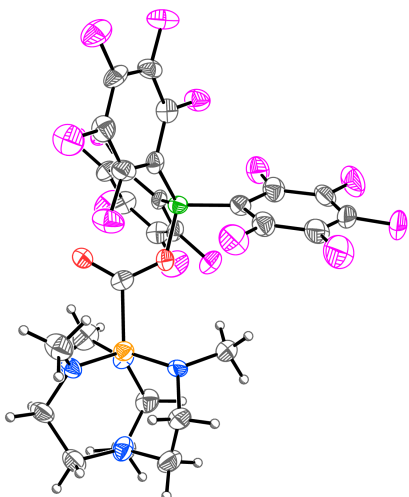


Figure 9: Solid-state structure of **2-5**. C: grey, N: blue, O: red, B: green, F: pink, P: orange, S: yellow, H: white

When probing the origin of the reactivity using natural bond orbital (NBO) and electron density topology analyses, both indicate that compound **2-1** does not contain a transannular P-N<sub>ta</sub> interaction. These findings stand in contrast to the protonated base, where a strong transannular interaction is observed. A relaxed surface scan shows that as the P-N<sub>ta</sub> distance increases, the strength of the donor-acceptor interaction decreases. This result suggests that the lack of transannular interaction does not arise from an energy mismatch between the donor and acceptor orbitals. Instead, it appears that reorientation of the methyl group on the nitrogen atoms of the base, which is induced by the transannular P-N<sub>ta</sub> interaction, enforces an orientation of the methyl group that is upright (e.g. parallel to the P-N<sub>ta</sub> vector). This introduces a steric conflict with the C<sub>6</sub>F<sub>5</sub> rings of the borane, and inhibits a transannular interaction. Thus **2-1** is not so bulky as to prevent formation of the Lewis adduct but is sufficiently bulky enough to prevent formation of the stabilising transannular interaction. This renders the adduct more labile than one might otherwise expect and allows for its unique reactivity, where the classical Lewis adduct has access to FLP reactivity via dissociation, while not exhibiting a dissociative equilibrium on the NMR timescale.

The energetics of dissociation were also probed with a relaxed surface scan of **2** at the B3LYP/def2-SVPP level of theory. It shows the energy rising as the P-B distance increases. However, at a P-B distance of 4.5 Å, there is an additional local minimum (**Figure 10**).

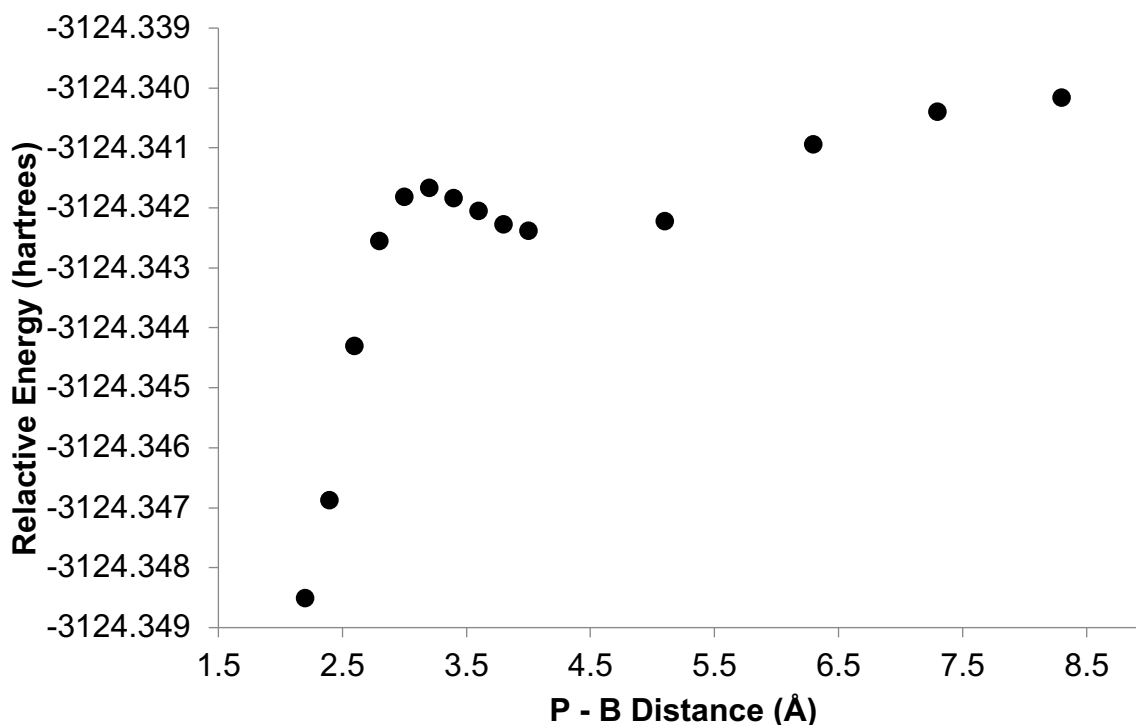


Figure 10: Relaxed potential energy surface scan along the P-B distance of **2-1** (B3LYP/def2-TZVPP).

Applying an empirical dispersion correction (B3LYP-D3/def2-TZVPP) and reoptimizing the minimum resulted in collapse to the stable adduct **2-1**. Full dissociation to the free Lewis acid and base required 8.8 kcal/mol and no transition state could be found. In contrast to typical FLPs such as the <sup>t</sup>Bu<sub>3</sub>P, which require the simultaneous action of the Lewis acid and base, this system appears to react in a stepwise fashion. Dielmann and coworkers recently described a class of imidazoline-2-ylidenamino-substituted phosphines that are able to form thermally stable adducts with CO<sub>2</sub>.<sup>50-</sup>

<sup>53</sup> Although the formation of an adduct between P(MeNCH<sub>2</sub>CH<sub>2</sub>)<sub>3</sub>N and CO<sub>2</sub> is not observed by NMR spectroscopy, the species appears to be trapped by B(C<sub>6</sub>F<sub>5</sub>)<sub>3</sub>.

The results of these studies has broader implications for the field of FLP chemistry. Previously, FLP reactivity was observed with fully frustrated systems and subsequent studies showed that FLP reactivity is still accessible if an equilibrium with the dissociated acid and base was observable. The present system is the first seemingly robust classical Lewis adduct to exhibit FLP reactivity, where an equilibrium with the dissociated acid and base is yet to be observed. It also highlights the importance of more carefully examining seemingly stable Lewis adducts for FLP reactivity even if initial spectroscopic evidence suggests a lack of dissociative equilibrium.

## 2.3 Conclusion

We have reported the preparation for **2-1** a Lewis adduct of the electrophilic borane B(C<sub>6</sub>F<sub>5</sub>)<sub>3</sub> and proazaphosphatrane P(MeNCH<sub>2</sub>CH<sub>2</sub>)<sub>3</sub>N. Although it demonstrates no evidence of dissociative equilibrium by NMR spectroscopy, it readily affords products of FLP addition reactions upon mixing with unsaturated substrates. The lability of **2-1** can be attributed to the steric bulk, which, although not sufficient to preclude adduct formation, inhibits the transannular interaction characteristic of azaphosphatranes. These results highlight the importance of investigating apparently stable Lewis adducts for FLP chemistry.

## 2.4 Experimental Section

### 2.4.1 General Consideration

#### **Materials and Methods**

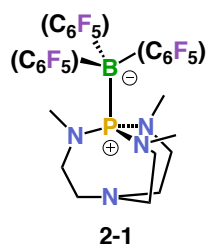
All manipulations were performed under an atmosphere of N<sub>2</sub> in a Vacuum Atmospheres glovebox or on a dual-manifold Schlenk line. Non-deuterated solvents were dried on a Grubbs-type solvent

purification system and stored under N<sub>2</sub> over 3 Å molecular sieves. CD<sub>2</sub>Cl<sub>2</sub> was distilled from CaH under a N<sub>2</sub> atmosphere and stored under over 3 Å molecular sieves. C<sub>6</sub>D<sub>5</sub>Br was dried over 3 Å molecular sieves, degassed with 3 freeze-pump-thaw cycles, and stored over 3 Å molecular sieves. Unless otherwise stated, chemicals were purchased from Alfa Aesar or Sigma-Aldrich and used as received without further purification. B(C<sub>6</sub>F<sub>5</sub>)<sub>3</sub> was purchased from Boulder Scientific and recrystallized from pentane at -35 °C. NMR spectra were recorded on a Bruker Avance III 400 MHz NMR spectrometer and an Agilent DD2-500 MHz NMR spectrometer. NMR resonances are reported as chemical shifts (ppm) from established standards: (CH<sub>3</sub>)<sub>4</sub>Si for <sup>1</sup>H and <sup>13</sup>C, 15% BF<sub>3</sub>·Et<sub>2</sub>O in CDCl<sub>3</sub> for <sup>11</sup>B, and 85% H<sub>3</sub>PO<sub>4</sub> in H<sub>2</sub>O for <sup>31</sup>P. <sup>1</sup>H and <sup>13</sup>C NMR spectra were referenced to residual solvent signals and <sup>11</sup>B, <sup>31</sup>P, and <sup>19</sup>F NMR spectra were externally referenced to standard solutions. Elemental analyses were performed with a Flash 2000 CHNS Analyzer.

### Computational details

Electronic structure calculations were performed using Gaussian 09.<sup>54</sup> Full geometry optimizations were carried out at the B3LYP-GD3/def2-TZVPP//B3LYP/def2-TZVPP level of theory.<sup>55–58</sup> Fully optimized geometries were confirmed to be minima via the absence of imaginary frequencies from a frequency calculation (positive definite Hessian). Relaxed surface scans were performed along the P–N<sub>ta</sub> internal coordinate for **2-1** at the B3LYP/def2-SVPP level of theory. Natural Bond Orbital Analyses were performed using NBO 6.0.<sup>59</sup> Topological analysis of electron density was performed with MultiWFN 3.3.8.<sup>60</sup>

## 2.4.2 Synthesis of Starting Materials



### Synthesis of **2-1**·CH<sub>2</sub>Cl<sub>2</sub>

Solutions of B(C<sub>6</sub>F<sub>5</sub>)<sub>3</sub> (92 mg, 0.18 mmol) and P(MeNCH<sub>2</sub>CH<sub>2</sub>)<sub>3</sub>N (39 mg, 0.18 mmol) in 2 mL of CH<sub>2</sub>Cl<sub>2</sub> each were prepared and cooled to -30 °C. The B(C<sub>6</sub>F<sub>5</sub>)<sub>3</sub> solution was allowed to warm slightly to ensure that any precipitated material fully entered into solution. The two solutions were combined cold and

allowed to warm to room temperature over the course of 30 min. The reaction mixture was then stored at -30 °C for 2 d, affording colorless crystals of **2-1**·CH<sub>2</sub>Cl<sub>2</sub>, which were washed with cold CH<sub>2</sub>Cl<sub>2</sub> and pentane and dried under vacuum. Yield 127 mg, 97%.

<sup>1</sup>H NMR (400 MHz, CD<sub>2</sub>Cl<sub>2</sub>) δ 2.25 (d, <sup>3</sup>J<sub>HP</sub> = 7.9 Hz, 9H, CH<sub>3</sub>), 2.61 (ddd, <sup>3</sup>J<sub>HP</sub> = 21.5 Hz, <sup>2</sup>J<sub>HH</sub> = 15 Hz, <sup>3</sup>J<sub>HH</sub> = 2.7 Hz, 3H, CHH), 2.80 (td, <sup>2</sup>J<sub>HH</sub> = 15 Hz, <sup>3</sup>J<sub>HH</sub> = 3.6 Hz, 3H, CHH), 2.86 (td, <sup>2</sup>J<sub>HH</sub> = 15 Hz, <sup>3</sup>J<sub>HH</sub> = 3 Hz, 3H, CHH), 3.03 (tdd, <sup>2</sup>J<sub>HH</sub> = 13.7 Hz, <sup>3</sup>J<sub>HH</sub> = 3.5 Hz, <sup>2</sup>J<sub>HP</sub> = 2.8 Hz, 3H, CHH), 5.33 (s, 2H, CH<sub>2</sub>Cl<sub>2</sub>).

<sup>1</sup>H{<sup>31</sup>P} NMR(400 MHz, CD<sub>2</sub>Cl<sub>2</sub>) δ 2.25 (s, 9H, CH<sub>3</sub>), 2.62 (d, *J* = 15 Hz, 3H, CHH), 2.80 (td, <sup>2</sup>J<sub>HH</sub> = 15 Hz, <sup>3</sup>J<sub>HH</sub> = 3.6 Hz, 3H, CHH), 2.86 (td, <sup>2</sup>J<sub>HH</sub> = 15 Hz, <sup>3</sup>J<sub>HH</sub> = 3 Hz, 3H, CHH), 3.03 (td, <sup>2</sup>J<sub>HH</sub> = 12.5 Hz, <sup>3</sup>J<sub>HH</sub> = 3.5 Hz, 3H, CHH), 5.33 (s, 2H, CH<sub>2</sub>Cl<sub>2</sub>).

<sup>19</sup>F{<sup>1</sup>H} NMR (377 MHz, CD<sub>2</sub>Cl<sub>2</sub>) δ -166.73 (td, *J* = 22 Hz, *J* = 8.6 Hz, 1F), -164.13 (tdd, *J* = 22 Hz, *J* = 7 Hz, *J* = 3 Hz, 1F), -158.01 (tdt, *J* = 21 Hz, *J* = 4.6 Hz, *J* = 2.5 Hz, 1F), -133.66 (dd, *J* = 22.3 Hz, *J* = 8.3 Hz, 1F), -124.45 (dd, *J* = 24 Hz, *J* = 5.3 Hz, 1F).

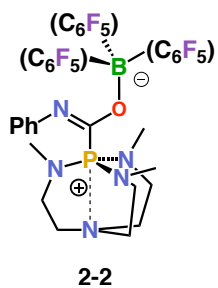
<sup>31</sup>P NMR (162 MHz, CD<sub>2</sub>Cl<sub>2</sub>) δ 79.97 (br q, <sup>1</sup>J<sub>PB</sub> = 130 Hz, FWHM = 130 Hz).

<sup>31</sup>P{<sup>1</sup>H} NMR (162 MHz, CD<sub>2</sub>Cl<sub>2</sub>) δ 79.98 (br q, <sup>1</sup>J<sub>PB</sub> = 130 Hz, FWHM = 79 Hz).

<sup>11</sup>B{<sup>1</sup>H} NMR (128 MHz, CD<sub>2</sub>Cl<sub>2</sub>) δ -12.43 (br d, <sup>1</sup>J<sub>BP</sub> = 133 Hz).

<sup>13</sup>C{<sup>1</sup>H} NMR (126 MHz, CD<sub>2</sub>Cl<sub>2</sub>) δ 36.01 (dd, <sup>2</sup>J<sub>CP</sub> = 20 Hz, *J* = 4.7 Hz, CH<sub>3</sub>), 49.18 (d, <sup>3</sup>J<sub>CP</sub> = 0.5 Hz), 53.97 (d, <sup>2</sup>J<sub>CP</sub> = 2 Hz), 137.22 (d, <sup>1</sup>J<sub>CF</sub> = 262 Hz, CF<sub>Ar</sub>), 138.22 (d, <sup>1</sup>J<sub>CF</sub> = 293 Hz, CF<sub>Ar</sub>), 140.19 (d, <sup>1</sup>J<sub>CF</sub> = 299 Hz, CF<sub>Ar</sub>), 149.42 (d, <sup>1</sup>J<sub>CF</sub> = 249 Hz, CF<sub>Ar</sub>), 150.49 (d, <sup>1</sup>J<sub>CF</sub> = 240 Hz, CF<sub>Ar</sub>).

Elemental analysis: calcd for C<sub>27</sub>H<sub>21</sub>BF<sub>15</sub>N<sub>4</sub>P·CH<sub>2</sub>Cl<sub>2</sub> (found) C 41.36 (41.66), H 2.85 (2.81), N 6.89 (6.85).



### Synthesis of 2-2·C<sub>7</sub>H<sub>8</sub>

Solutions of B(C<sub>6</sub>F<sub>5</sub>)<sub>3</sub> (43 mg, 0.084 mmol), P(MeNCH<sub>2</sub>CH<sub>2</sub>)<sub>3</sub>N (18 mg, 0.084 mmol), and PhNCO (10 mg, 0.084 mmol) in 1 mL toluene each were prepared and cooled to -30 °C. The B(C<sub>6</sub>F<sub>5</sub>)<sub>3</sub> solution was added to the solution of P(MeNCH<sub>2</sub>CH<sub>2</sub>)<sub>3</sub>N followed by the PhNCO solution. A similar result was obtained if a solution of isolated **2-1** was combined with PhNCO. The reaction

mixture was then layered under pentane (15 mL). Over the course of 3 d, colorless blades formed, which were washed with cold CH<sub>2</sub>Cl<sub>2</sub> and pentane and dried under vacuum. Yield 55 mg, 70%.

<sup>1</sup>H NMR (400 MHz, CD<sub>2</sub>Cl<sub>2</sub>) δ 2.70 (d, <sup>3</sup>J<sub>HP</sub> = 11.3 Hz, 9H, CH<sub>3</sub>), 2.74-2.82 (m, 12H, CH<sub>2</sub>), 6.47 (d, *J* = 7.5 Hz, 2H, CH<sub>Ar</sub>), 6.95 (t, *J* = 7.4 Hz, 1H, CH<sub>Ar</sub>), 7.14 (t, *J* = 7.8 Hz, 2H, CH<sub>Ar</sub>).

<sup>1</sup>H{<sup>31</sup>P} NMR(400 MHz, CD<sub>2</sub>Cl<sub>2</sub>) δ 2.69 (s, 9H, CH<sub>3</sub>) 2.75 (A<sub>2</sub>B<sub>2</sub>, Δδ<sub>AB</sub> = 0.05 ppm, *J*<sub>AB</sub> = 4.1 Hz, 12H, CH<sub>2</sub>), 6.46 (d, *J* = 7.7 Hz, 2H, CH<sub>Ar</sub>), 6.94 (t, *J* = 7.4 Hz, 1H, CH<sub>Ar</sub>), 7.12 (t, *J* = 7.8 Hz, 2H, CH<sub>Ar</sub>).

<sup>19</sup>F{<sup>1</sup>H} NMR (377 MHz, CD<sub>2</sub>Cl<sub>2</sub>) δ -133.7 (d, *J* = 22.0 Hz, 2F), -161.93 (t, *J* = 20.3 Hz, 1F), -166.92 (t, *J* = 18.8 Hz, 2F).

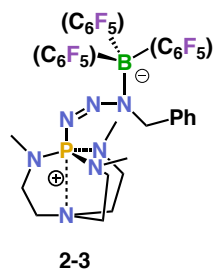
<sup>31</sup>P NMR (162 MHz, CD<sub>2</sub>Cl<sub>2</sub>) δ 26.1 (dec, <sup>3</sup>J<sub>HP</sub> = 11.4 Hz).

<sup>31</sup>P{<sup>1</sup>H} NMR (162 MHz, CD<sub>2</sub>Cl<sub>2</sub>) δ 26.2 (s, *J*<sub>CP</sub> = 201 Hz).

<sup>11</sup>B{<sup>1</sup>H} NMR (128 MHz, CD<sub>2</sub>Cl<sub>2</sub>) δ -3.49 (s).

<sup>13</sup>C{<sup>1</sup>H} NMR (126 MHz, CD<sub>2</sub>Cl<sub>2</sub>, partial, *C*<sub>ipso</sub> of C<sub>6</sub>F<sub>5</sub> rings not observed) δ 21.72 (s, CH<sub>3</sub>(tol)), 36.43 (d, <sup>2</sup>*J* = 5.2 Hz, CH<sub>3</sub>), 50.22 (d, *J* = 1.7 Hz, CH<sub>3</sub>NCH<sub>2</sub>CH<sub>2</sub>N), 50.96 (s, CH<sub>3</sub>NCH<sub>2</sub>CH<sub>2</sub>N), 120.06 (s, CH<sub>Ar</sub>), 123.21 (s, CH<sub>Ar</sub>), 125.83 (s, CH<sub>Ar</sub>(tol)), 128.54 (s, CH<sub>Ar</sub>(tol)), 128.76 (s, CH<sub>Ar</sub>), 129.57 (s, CH<sub>Ar</sub>(tol)), 137.06 (br d, *J*<sub>CF</sub> = 235 Hz, CF<sub>Ar</sub>(2 overlapping signals)), 138.57 (s, *C*<sub>ipso</sub>(tol)), 145.96 (d, *J*<sub>CP</sub> = 10.7 Hz, *C*<sub>ipso</sub>), 148.17 (d, *J*<sub>CP</sub> = 198 Hz, PC(O)NPh), 148.50 (br d, *J*<sub>CF</sub> = 243 Hz, CF<sub>Ar</sub>).

Elemental analysis: calcd for C<sub>34</sub>H<sub>26</sub>BF<sub>15</sub>N<sub>5</sub>PO·C<sub>7</sub>H<sub>8</sub> (found) C 52.42 (52.73), H 3.65 (3.50), N 7.45 (7.38).



### Synthesis of 2-3·C<sub>7</sub>H<sub>8</sub>

Solutions of B(C<sub>6</sub>F<sub>5</sub>)<sub>3</sub> (39 mg, 0.075 mmol), P(MeNCH<sub>2</sub>CH<sub>2</sub>)<sub>3</sub>N (16 mg, 0.075 mmol), and PhCH<sub>2</sub>N<sub>3</sub> (10 mg, 0.075 mmol) in 1 mL toluene each were prepared and cooled to -30 °C. The B(C<sub>6</sub>F<sub>5</sub>)<sub>3</sub> solution was added to the solution of P(MeNCH<sub>2</sub>CH<sub>2</sub>)<sub>3</sub>N followed by the PhCH<sub>2</sub>N<sub>3</sub> solution. A similar result was obtained if a solution of isolated **2-1** was combined with PhCH<sub>2</sub>N<sub>3</sub>. The reaction

mixture was then layered under pentane (15 mL). Over the course of 2 d, colorless blocks formed, which were washed with pentane and dried under vacuum. Yield 40 mg, 55%.

<sup>1</sup>H NMR (400 MHz, CD<sub>2</sub>Cl<sub>2</sub>) δ 2.34 (s, 3H, CH<sub>3</sub>(tol)), 2.56 (d, <sup>3</sup>J<sub>HP</sub> = 8.9 Hz, 9H, CH<sub>3</sub>), 2.77 (t, *J* = 5.2 Hz, 6H, CH<sub>2</sub>), 2.90 (dt, *J*<sub>HP</sub> = 14 Hz, *J*<sub>HH</sub> = 5.2 Hz, 6H, CH<sub>2</sub>), 4.97 (s, 2H, CH<sub>2</sub>(benzyl)), 6.82-6.83 (m, 2H, CH<sub>Ar</sub>), 7.02-7.06 (m, 3H, CH<sub>Ar</sub>), 7.12-7.26 (m, 5H, CH<sub>Ar</sub>(tol)).

<sup>1</sup>H{<sup>31</sup>P} NMR(400 MHz, CD<sub>2</sub>Cl<sub>2</sub>) δ 2.39 (s, 3H, CH<sub>3</sub>(tol)), 2.61 (s, 9H, CH<sub>3</sub>), 2.82 (t, *J* = 5.2 Hz, 6H, CH<sub>2</sub>), 2.95 (t, *J* = 5.2 Hz, 6H, CH<sub>2</sub>), 5.02 (s, 2H, CH<sub>2</sub>(benzyl)), 6.81-6.95 (m, 2H, CH<sub>Ar</sub>), 7.07-7.08 (m, 3H, CH<sub>Ar</sub>), 7.19-7.31 (m, 5H, CH<sub>Ar</sub>(tol)).

<sup>19</sup>F{<sup>1</sup>H} NMR (377 MHz, CD<sub>2</sub>Cl<sub>2</sub>) δ -166.76 (t, *J* = 18 Hz, 2F), -161.37 (t, *J* = 20 Hz, 1F), -132.27 (br s, 2F).

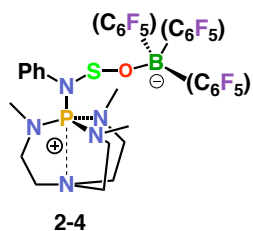
<sup>31</sup>P NMR (162 MHz, CD<sub>2</sub>Cl<sub>2</sub>) δ NMR: 36.9 (s, FWHM = 4 Hz).

<sup>31</sup>P{<sup>1</sup>H} NMR (162 MHz, CD<sub>2</sub>Cl<sub>2</sub>) δ 36.9 (s, FWHM = 54Hz).

<sup>11</sup>B{<sup>1</sup>H} NMR (128 MHz, CD<sub>2</sub>Cl<sub>2</sub>) δ -6.33 (s).

<sup>13</sup>C{<sup>1</sup>H} NMR (126 MHz, CD<sub>2</sub>Cl<sub>2</sub>, *C*<sub>ipso</sub> of C<sub>6</sub>F<sub>5</sub> rings not observed) δ 21.71 (s, CH<sub>3</sub>(tol)), 35.54 (d, *J*<sub>CP</sub> = 35.5 Hz, CH<sub>2</sub>), 51.38 (d, *J*<sub>CP</sub> = 1.3 Hz, CH<sub>2</sub>), 52.61 (s, CH<sub>2</sub>(benzyl)), 125.82 (s, CH<sub>Ar</sub>(tol)), 126.35 (s, CH<sub>Ar</sub>), 127.73 (s, CH<sub>Ar</sub>), 127.79 (s, CH<sub>Ar</sub>), 128.74 (s, CH<sub>Ar</sub>(tol)), 129.55 (s, CH<sub>Ar</sub>(tol)), 138.44 (s, *C*<sub>ipso</sub>(tol)), 139.55 (d, *J*<sub>CF</sub> = 235 Hz, CF<sub>Ar</sub>(2 overlapping signals)), 141.61 (s, *C*<sub>ipso</sub>), 148.74 (d, *J*<sub>CF</sub> = 251 Hz, CF<sub>Ar</sub>).

Elemental analysis: calcd for C<sub>34</sub>H<sub>28</sub>BF<sub>15</sub>N<sub>7</sub>P·1.5C<sub>7</sub>H<sub>8</sub> (found) C 53.47 (52.93), H 4.03 (4.06), N 9.81 (9.70).



### Synthesis of 2-4·0.5(C<sub>7</sub>H<sub>8</sub>)

Solutions of B(C<sub>6</sub>F<sub>5</sub>)<sub>3</sub> (37 mg, 0.072 mmol), P(MeNCH<sub>2</sub>CH<sub>2</sub>)<sub>3</sub>N (16 mg, 0.072 mmol), and PhNSO (10 mg, 0.072 mmol) in 1 mL toluene each were prepared and cooled to -30 °C. The B(C<sub>6</sub>F<sub>5</sub>)<sub>3</sub> solution was added to the solution of P(MeNCH<sub>2</sub>CH<sub>2</sub>)<sub>3</sub>N followed by the PhNSO solution. A similar result was obtained if a solution of isolated **2-1** was combined with PhNSO. The reaction mixture was then layered under pentane (15 mL). Over the course of 1 d, colorless solid precipitated, which was washed with pentane and dried under vacuum. Yield 29 mg, 47%.

<sup>1</sup>H NMR (400 MHz, CD<sub>2</sub>Cl<sub>2</sub>) δ 2.59 (d, *J* = 9.6 Hz, 9H, CH<sub>3</sub>), 2.78 (t, *J* = 5.1 Hz, 6H, CH<sub>2</sub>), 2.91 (dt, *J*<sub>HH</sub> = 5.1 Hz, *J*<sub>HP</sub> = 15 Hz, 6H, CH<sub>2</sub>), 6.96 (d, *J* = 8.3 Hz, 2H, CH<sub>Ar</sub>), 7.23-7.18 (m, 3H, CH<sub>Ar</sub>).

<sup>1</sup>H{<sup>31</sup>P} NMR (400 MHz, CD<sub>2</sub>Cl<sub>2</sub>) δ 2.51 (s, 9H, CH<sub>3</sub>), 2.70 (t, *J* = 5.1 Hz, 6H, CH<sub>2</sub>), 2.83 (t, *J* = 5.2 Hz, 6H, CH<sub>2</sub>), 6.88 (d, *J* = 6.4 Hz, 2H, CH<sub>Ar</sub>), 7.10-7.16 (m, 3H, CH<sub>Ar</sub>).

<sup>19</sup>F{<sup>1</sup>H} NMR (377 MHz, CD<sub>2</sub>Cl<sub>2</sub>) δ -166.54 (t, *J* = 20 Hz, 2F), -162.19 (t, *J* = 20 Hz, 1F), -132.57 (d, *J* = 24 Hz, 1F).

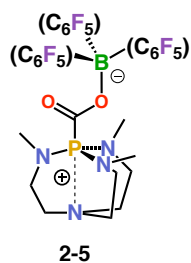
<sup>31</sup>P NMR (162 MHz, CD<sub>2</sub>Cl<sub>2</sub>) δ 36.8 (s, FWHM = 5 Hz).

<sup>31</sup>P{<sup>1</sup>H} NMR (162 MHz, CD<sub>2</sub>Cl<sub>2</sub>) δ 36.8 (s, FWHM = 66 Hz).

<sup>11</sup>B{<sup>1</sup>H} NMR (128 MHz, CD<sub>2</sub>Cl<sub>2</sub>) δ -1.91 (s).

<sup>13</sup>C{<sup>1</sup>H} NMR (126 MHz, CD<sub>2</sub>Cl<sub>2</sub>, partial, *C*<sub>ipso</sub> of C<sub>6</sub>F<sub>5</sub> rings not observed) δ 36.80 (d, <sup>2</sup>*J*<sub>CP</sub> = 2.9 Hz, CH<sub>3</sub>), 50.11 (s, CH<sub>2</sub>), 52.75 (d, *J*<sub>CP</sub> = 2.3 Hz, CH<sub>2</sub>), 127.92 (s, CH<sub>Ar</sub>), 128.81 (d, *J*<sub>CP</sub> = 1.6 Hz, CH<sub>Ar</sub>), 129.69 (s, CH<sub>Ar</sub>), 137.01 (d, *J*<sub>CF</sub> = 250 Hz, CF<sub>Ar</sub>), 139.27 (d, *J*<sub>CF</sub> = 235 Hz, CF<sub>Ar</sub>), 144.77 (d, *J*<sub>CP</sub> = 9.7 Hz, *C*<sub>ipso</sub>), 148.31 (d, *J*<sub>CF</sub> = 248 Hz, CF<sub>Ar</sub>).

Elemental analysis: calcd for C<sub>33</sub>H<sub>26</sub>BF<sub>15</sub>N<sub>5</sub>POS·0.5C<sub>7</sub>H<sub>8</sub> (found) C 47.99 (47.30), H 3.31 (3.26), N 7.67 (7.65).



### Synthesis of 2-5

Solutions of  $B(C_6F_5)_3$  (43 mg, 0.084 mmol) and  $P(MeNCH_2CH_2)_3N$  (18 mg, 0.083 mmol) in 2 mL  $CH_2Cl_2$  each were prepared and cooled to  $-30\text{ }^\circ\text{C}$ . The  $B(C_6F_5)_3$  solution was added to the solution of  $P(MeNCH_2CH_2)_3N$  in a Teflon-tap-sealed reaction flask and removed from the glovebox. A similar result was obtained if isolated **2-1** was dissolved in  $CH_2Cl_2$  and transferred into the reaction vessel. The reaction mixture was degassed with three freeze-pump-thaw cycles and the vessel was then filled with 1 atm  $CO_2$ . The reaction mixture was immediately returned to the glovebox and concentrated to 3 mL. Pentane was added until the solution clouded and it was placed in a  $-30\text{ }^\circ\text{C}$  freezer. Over the course of 2 d, colorless solid precipitated, which was washed with pentane and dried under vacuum. Yield 42 mg, 65%. The experiment was also performed on a 0.03 mmol scale in a J. Young NMR tube with  $^{13}\text{C}$ -enriched  $CO_2$ .

### 2-5 (natural abundance)

$^1\text{H}$  NMR (400 MHz,  $CD_2Cl_2$ )  $\delta$  2.71 (t,  $J = 5.2$  Hz, 6H,  $CH_2$ ), 2.75 (d,  $^2J_{HP} = 11$  Hz, 9H,  $CH_3$ ), 2.88 (dt,  $^1J_{HP} = 15$  Hz,  $^3J_{HH} = 5.4$  Hz, 6H,  $CH_2$ ).

$^1\text{H}\{^{31}\text{P}\}$  NMR(400 MHz,  $CD_2Cl_2$ )  $\delta$  2.74 (t,  $J = 5$  Hz, 6H,  $CH_2$ ), 2.76 (s, 15H,  $CH_3$ ), 2.90 (t,  $J = 5.2$  Hz).

$^{19}\text{F}\{^1\text{H}\}$  NMR (377 MHz,  $CD_2Cl_2$ )  $\delta$  -166.55 (td,  $J = 19$  Hz, 2F), -161.32 (t,  $J = 20.3$  Hz, 1F), -134.49 (d,  $J = 19$  Hz).

$^{31}\text{P}$  NMR (162 MHz,  $CD_2Cl_2$ )  $\delta$  23.15 (m,  $^3J_{PH} = 12$  Hz, FWHM = 49 Hz).

$^{31}\text{P}\{^1\text{H}\}$  NMR (162 MHz,  $CD_2Cl_2$ )  $\delta$  23.15 (s).

$^{11}\text{B}\{^1\text{H}\}$  NMR (128 MHz,  $CD_2Cl_2$ )  $\delta$  -3.82 (s).

Elemental analysis: calcd for  $C_{28}H_{21}BF_{15}N_4PO_2$  (found) C 43.55 (43.09), H 2.74 (2.71), N 7.26 (6.91).

### 2-5 ( $^{13}\text{C}$ -enriched)

$^1\text{H}$  NMR (400 MHz,  $CD_2Cl_2$ )  $\delta$  2.73 (t,  $J = 5.2$  Hz, 6H,  $CH_2$ ), 2.75 (d,  $^2J_{HP} = 11$  Hz, 9H,  $CH_3$ ), 2.88 (dt,  $^1J_{HP} = 15$  Hz,  $^3J_{HH} = 5.4$  Hz, 6H,  $CH_2$ ).

$^1\text{H}\{^{31}\text{P}\}$  NMR(400 MHz,  $CD_2Cl_2$ )  $\delta$  2.72 (t,  $J = 5$  Hz, 6H,  $CH_2$ ), 2.75 (s, 15H,  $CH_3$ ), 2.88 (t,  $J = 5.2$  Hz).

$^{19}\text{F}\{\text{H}\}$  NMR (377 MHz,  $\text{CD}_2\text{Cl}_2$ )  $\delta$  -166.58 (td,  $J = 23.8$  Hz,  $J = 7.3$  Hz, 2F), -161.32 (t,  $J = 20.3$  Hz, 1F), -134.49 (d,  $J = 18.5$  Hz).

$^{31}\text{P}$  NMR (162 MHz,  $\text{CD}_2\text{Cl}_2$ )  $\delta$  23.16 (dm,  $^1J_{\text{PC}} = 235$  Hz,  $^3J_{\text{PH}} = 12$  Hz).

$^{31}\text{P}\{\text{H}\}$  NMR (162 MHz,  $\text{CD}_2\text{Cl}_2$ )  $\delta$  23.16 (d,  $^1J_{\text{PC}} = 234$  Hz).

$^{11}\text{B}\{\text{H}\}$  NMR (128 MHz,  $\text{CD}_2\text{Cl}_2$ )  $\delta$  -3.90 (s).

$^{13}\text{C}\{\text{H}\}$  NMR (126 MHz,  $\text{CD}_2\text{Cl}_2$ , partial,  $C_{\text{ipso}}$  of  $\text{C}_6\text{F}_5$  rings not observed)  $\delta$  35.24 (d,  $^2J_{\text{CP}} = 4.2$  Hz,  $\text{CH}_3$ ), 50.38 (d,  $^2J_{\text{CP}} = 3.4$  Hz,  $\text{CH}_2$ ), 50.51 (s,  $\text{CH}_2$ ), 137.18 (d,  $^1J_{\text{CF}} = 237$  Hz,  $\text{CF}_{\text{Ar}}$ ), 148.39 (d,  $^1J_{\text{CF}} = 231$  Hz), 158.03 (d,  $^1J_{\text{CF}} = 168$  Hz,  $\text{CF}_{\text{Ar}}$ ).

### 2.4.3 X-ray crystallography

Single crystals were obtained as follows: **2-1** from a solution of  $\text{CH}_2\text{Cl}_2$  at  $-30^\circ\text{C}$  over 2 days ; **2-2**· $\text{CH}_2\text{Cl}_2$ , **2-3**· $\text{CH}_2\text{Cl}_2$ , **2-4**, **2-5**, from layering pentane onto a  $\text{CH}_2\text{Cl}_2$  solution of the compound. Suitable crystals were mounted on a MiTeGen polyimide loop and cooled to 150(2) K under a stream of  $\text{N}_2$  on a Bruker Apex II diffractometer using an Oxford Cryosystems cryoprobe. Diffraction was carried out using graphite monochromated Mo  $K\alpha$  radiation ( $\lambda = 0.71073$  Å). Diffraction data were integrated and reduced using SAINT. Absorption corrections were applied using SADABS or TWINABS. Space group assignment was initially performed by analysis of Laue symmetry, systematic absences, and intensity statistics using XPREP. Space group selection was confirmed with SHELXT following structure solution by intrinsic phasing. Full-matrix least-squares refinement on  $F^2$  was carried out using standard methods with SHELXL. All non-H atoms were refined anisotropically. H atoms were placed at geometrically calculated positions and refined using an appropriate riding model with coupled displacement parameters. For **2-2**· $\text{CH}_2\text{Cl}_2$ , the final model was refined against both domains of a twinned dataset. For **2-2**· $\text{CH}_2\text{Cl}_2$ , the unit cell parameters, space group type, and number of molecules in the asymmetric unit suggest the presence of missed higher symmetry, but validation with PLATON reveals no such higher symmetry. Moreover, visual inspection of pseudo-projection images confirms that the Laue symmetry is indeed  $2/m$ . All other structures were also checked for missed higher symmetry and

twinning using PLATON. The data collection and refinement parameters are collected in Tables 1 and 2.

Table 1: X-ray crystallographic data for **2-1** – **2-5**.

	<b>2-1</b> ·CH <sub>2</sub> Cl <sub>2</sub> <sup>a</sup>	<b>2-2</b> ·CH <sub>2</sub> Cl <sub>2</sub> <sup>b</sup>	<b>2-3</b>	<b>2-4</b>	<b>2-5</b>
Formula	C <sub>28</sub> H <sub>23</sub> BCl <sub>2</sub> F <sub>15</sub> N <sub>4</sub> P	C <sub>35</sub> H <sub>28</sub> BCl <sub>2</sub> F <sub>15</sub> N <sub>5</sub> OP	C <sub>34</sub> H <sub>28</sub> BF <sub>15</sub> N <sub>7</sub> P	C <sub>33</sub> H <sub>26</sub> BF <sub>15</sub> N <sub>5</sub> OPS	C <sub>28</sub> H <sub>21</sub> BF <sub>15</sub> N <sub>4</sub> O <sub>2</sub> P
FW	813.18	932.30	861.41	867.43	772.27
Size (mm <sup>3</sup> )	0.30×0.20×0.12	0.41×0.07×0.05	0.15×0.14×0.05	0.20×0.18×0.03	0.20×0.10×0.10
Color	colorless	colorless	colorless	colorless	colorless
T (K)	150(2)	150(2)	150(2)	150(2)	150(2)
λ (Å)	0.71073	0.71073	0.71073	0.71073	0.71073
Crystal system	Triclinic	Monoclinic	Monoclinic	Orthorhombic	Monoclinic
Space group	<i>P</i> $\bar{1}$	<i>Cc</i>	<i>P2</i> <sub>1</sub> / <i>n</i>	<i>Pbca</i>	<i>P2</i> <sub>1</sub> / <i>n</i>
a (Å)	10.7251(7)	12.4340(11)	11.9738(15)	18.806(10)	14.246(8)
b (Å)	10.9736(8)	57.735(5)	13.1246(14)	18.700(9)	13.660(7)
c (Å)	14.7218(10)	12.4544(10)	24.205(3)	20.005(11)	16.168(9)
α (°)	78.150(4)				
β (°)	73.557(3)	119.226(2)	90.203(4)		98.912(15)
γ (°)	72.536(3)				
Volume (Å <sup>3</sup> )	1571.40(19)	7802.6(12)	3803.8(8)	7035(6)	3108(3)
Z	2	8	4	8	4
θ range (°)	2.049–29.687	2.002–27.295	2.289–25.047	1.842–26.372	1.962–23.525
Total Reflections	60101	86024	22821	102258	16038
Unique data	39908	17064	6671	7192	4481
R <sub>int</sub>	0.0358	0.0658	0.0604	0.0707	0.1409
Completeness (%)	100	99.9	99.0	100	97.3
GoF	1.027	1.039	1.032	1.020	0.968
R <sub>1</sub> (I > 2σ)	0.0441	0.0561	0.0647	0.0372	0.0629
wR <sub>2</sub> (I > 2σ)	0.0947	0.1191	0.1154	0.0796	0.1027
Peak, hole (e Å <sup>-3</sup> )	1.109, -1.002	0.688, -0.637	0.215, -0.249	0.425, -0.338	0.287, -0.310

<sup>a</sup> Non-merohedric twin. Twin ratio: 56:44. Twin law: 180° rotation about *c*\*. Unit cell parameters were refined on the primary domain data. Data collection parameters reflect all data from both domains. Refinement parameters correspond to those from final model refined against the full twinned dataset.

<sup>b</sup> Flack *x* parameter = 0.01(9)

## Chapter 3

### Bench-Stable Carbon-Based Lewis Acids in Frustrated Lewis Pair

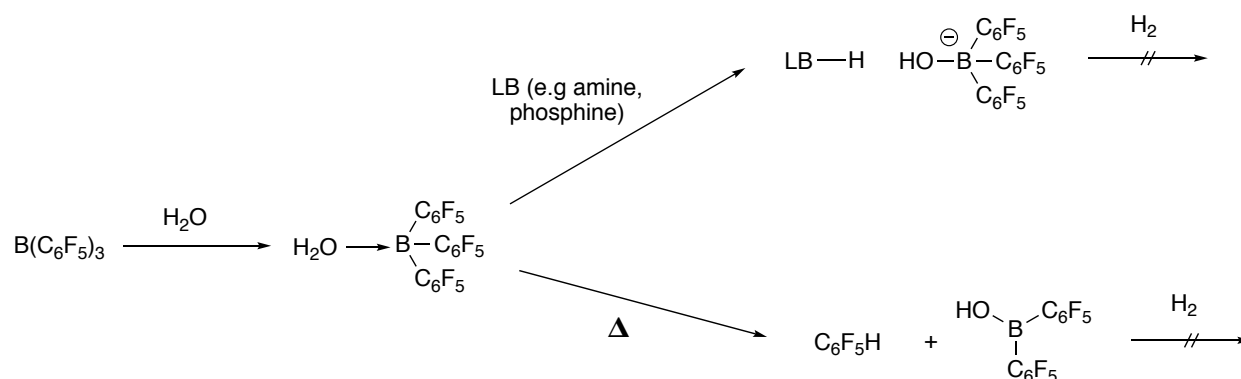
### Chemistry

#### 3.1 Introduction

As discussed in Chapter 1, the articulation of the frustrated Lewis pair (FLP) paradigm has spurred the development of new methods for small molecule activation. In 2006, Stephan and coworkers reported the discovery of the first reversible activation of H<sub>2</sub> by a main group compound, namely *p*-(Mes<sub>2</sub>P)C<sub>6</sub>F<sub>4</sub>[B(C<sub>6</sub>F<sub>5</sub>)<sub>2</sub>].<sup>11</sup> Subsequent studies showed that this initial finding can be generalized to many combinations of Lewis acids and bases for which steric demands preclude classical adduct formation.<sup>7-9,35</sup> This led to the formulation of a new mode of chemical reactivity that is FLP chemistry.

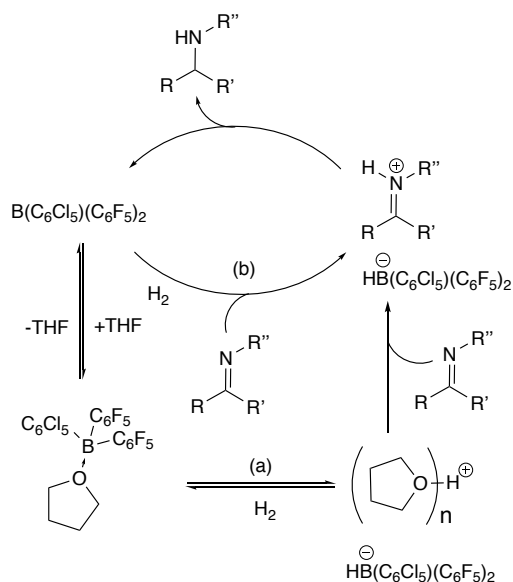
Since this early work, the reactivity of FLPs with H<sub>2</sub> has led to the development of metal-free hydrogenation catalysts for the reduction of unsaturated substrates.<sup>7-9,12,13,35</sup> It has also been applied for the activation of small molecules.<sup>61</sup> This has led to metal-free strategies for CO<sup>28,29</sup> and CO<sub>2</sub> reduction.<sup>20,62</sup> The scope of Lewis acids and bases that generate FLPs has also been expanded. Many Lewis bases have been used in FLP chemistry including phosphines,<sup>11</sup> amines,<sup>63</sup> carbenes<sup>64</sup> and ethers.<sup>65</sup> However, the breadth of Lewis acids has been more limited. The majority of FLP chemistry has utilized perfluorinated group 13 Lewis acids, most notably the commercially available B(C<sub>6</sub>F<sub>5</sub>)<sub>3</sub> and its derivatives.<sup>35</sup> While its high Lewis acidity is necessary for certain FLP reactivity, its high oxophilicity limits its utility in wet solvents and tolerance to functional groups.<sup>66</sup> The Brønsted acid H<sub>2</sub>O-B(C<sub>6</sub>F<sub>5</sub>)<sub>3</sub> was examined by Parkin and coworkers, who determined it to have a p*K*<sub>a</sub> = 8.4 in MeCN, which is comparable to that of HCl.<sup>67</sup> As a result, this limits the water tolerance of polyfluorinated arylboranes in the presence of Brønsted bases. In FLP chemistry,

moderately strong bases such as amines and phosphines can effect the irreversible deprotonation of the borane-water adduct to yield an inactive hydroxytriarylborate anion and enhances the strength of the water binding to the boron center (Scheme 19).<sup>68</sup> Under forcing conditions, the  $\text{H}_2\text{O}-\text{B}(\text{C}_6\text{F}_5)_3$  adduct is also prone to decomposition via B-C bond protonolysis (**Scheme 18**).<sup>68</sup> As a result, these reagents need to be handled under rigorously inert conditions and this represents a practical barrier to the uptake of FLP catalysis by the broader chemical community.<sup>68</sup> Therefore, there is a demand for cheaper and less oxophilic Lewis acids for FLP applications. As a result, in the last few years, numerous efforts have been made to develop bench-stable FLP systems to address air and moisture sensitivity.



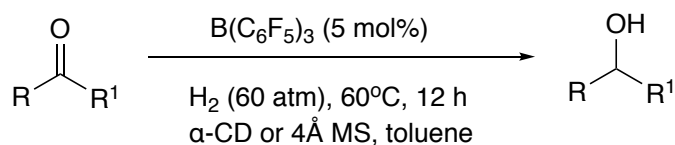
Scheme 18: Deactivation pathways of  $\text{B}(\text{C}_6\text{F}_5)_3$  by  $\text{H}_2\text{O}$

In 2011, Ashley and coworkers reported the use of  $\text{B}(\text{C}_6\text{Cl}_5)(\text{C}_6\text{F}_5)_2$  as a bench-stable Lewis acid for FLP chemistry.<sup>69</sup> Subsequent studies in 2014 showed that when combined with a strong-donor solvent such as THF, metal-free catalytic hydrogenation reactions can be performed under mild conditions (**Scheme 19**).<sup>70</sup> This includes the first examples of metal-free catalytic hydrogenation of furan heterocycles.<sup>70</sup> However, the system still requires rigorously dry reaction conditions.<sup>70</sup>



Scheme 19: Proposed mechanism for hydrogenation of imines by activation of H<sub>2</sub> using either a) THF solvent or b) substrate as a frustrated Lewis base

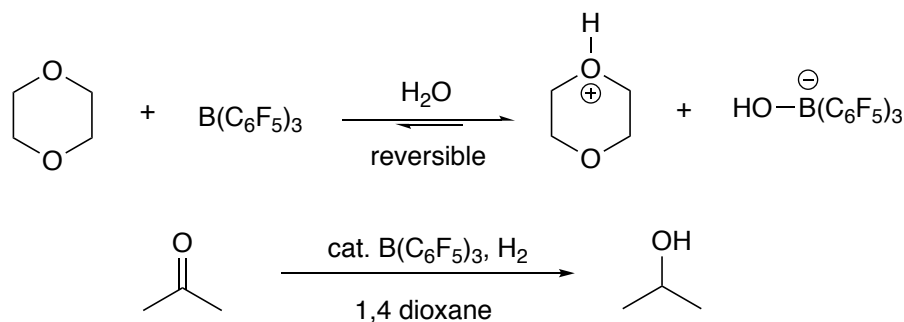
A year later, Stephan and coworkers reported an FLP-catalyzed hydrogenation of aryl ketones and aldehydes (**Scheme 20**).<sup>71</sup> While the reaction produces H<sub>2</sub>O, the use of molecular sieves as a reagent ensures that the reaction mixture remains anhydrous.<sup>71</sup>



Scheme 20: Catalytic hydrogenation of ketones and aldehydes in toluene

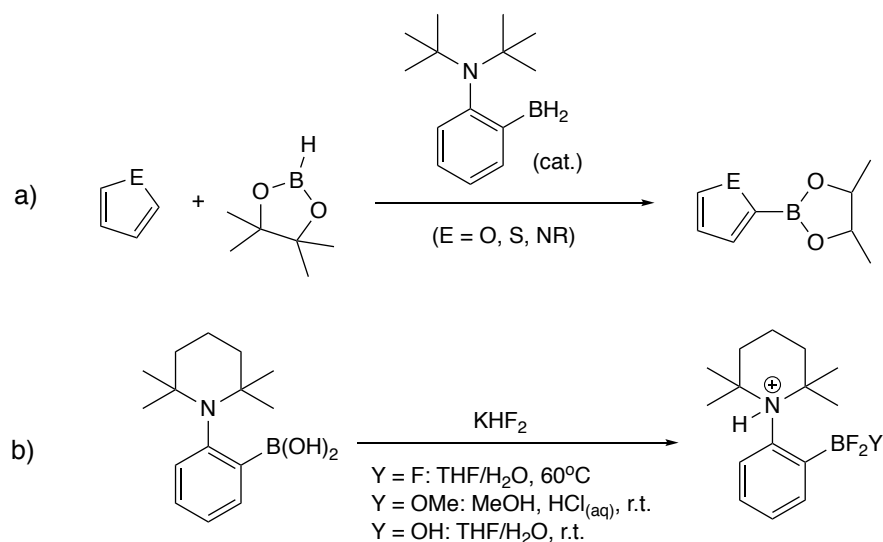
Ingleson and coworkers also reported the use of N-methylacridinium salts as carbon Lewis acids.<sup>42</sup> They were able to catalytically hydrosilylate several imines and effect the dehydrocoupling of alcohols with silanes.<sup>42</sup> In a remarkable finding, it was reported that performing H<sub>2</sub> activation in wet *o*-dichlorobenzene with *N*-alkyl acridinium salt still resulted in H<sub>2</sub> activation. However, heterolytic O–H cleavage of H<sub>2</sub>O was also observed to give a minor product.<sup>42</sup> Shortly after, Soós and coworkers synthesized a family of bench-stable boranes consisting of chlorine and fluorine

atoms at the *ortho* positions of the aromatic rings.<sup>72</sup> These Lewis acids were able to effect the catalytic reduction of aldehydes in THF without the need for an inert atmosphere.<sup>72</sup> Reaction mixtures can be prepared in an open flask using technical grade solvents.<sup>72</sup> As water inhibition of the catalyst is reversible, this represents the first example of an FLP catalyst that is moisture tolerant.<sup>72</sup> In that same year, Ashley and coworkers reported that the 1,4-dioxane solution of  $B(C_6F_5)_3$  shows appreciable moisture tolerance and can catalyze the hydrogenation of a range of weakly basic substrates such as ketones and aldehydes without the need for rigorously inert conditions (**Scheme 21**).<sup>68</sup> Most reactions can be performed in non-anhydrous solvents under open bench conditions to afford clean catalytic reduction products.<sup>68</sup>



Scheme 21: Moisture-tolerant hydrogenation of acetone

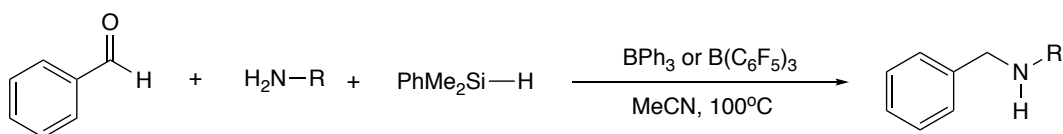
In 2015, Fontaine and coworkers reported that the borane (1-TMP-2-BH<sub>2</sub>-C<sub>6</sub>H<sub>4</sub>)<sub>2</sub> (TMP, 2,2,6,6-tetramethylpiperidine) is able to activate C-H bonds of heteroarenes.<sup>46</sup> This allows for the catalytic borylation of furans, pyrroles and electron-rich thiophenes.<sup>46</sup> In a follow-up study, they reported the active borane catalyst can be protected as its fluoroborate analogue (**Scheme 22**).<sup>73</sup> In this form, it is easy to handle and store in a benchtop setting without the need for a glovebox and Schlenk techniques because the precatalyst is air and moisture stable.<sup>73</sup> *In situ* deprotection can catalyze the borylation of heteroarenes with an efficiency that is similar to the unprotected catalyst.<sup>73</sup>



Scheme 22: a) Previously reported FLP-catalyzed borylation of heteroarenes b) Synthesis of bench-stable fluoroborate precatalysts

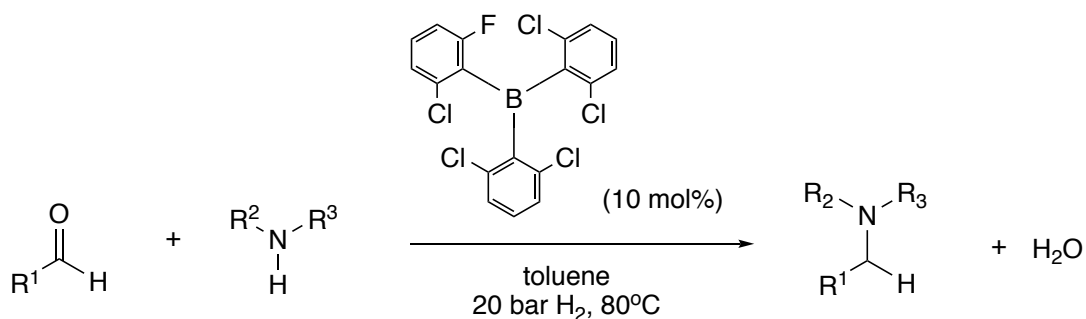
In 2016, Ashley and coworkers reported the FLP-mediated H<sub>2</sub> activation and catalytic hydrogenation activity of the Lewis acid *i*PrSnOTf, which acts as a surrogate for the trialkylstannyl cation *i*Pr<sub>3</sub>Sn<sup>+</sup>.<sup>74</sup> The Lewis acid can be readily prepared from inexpensive starting materials and is found to be a suitable catalyst for the hydrogenation of a variety of substrates including aldehydes, ketones and imines.<sup>74</sup> Furthermore, it also displays a remarkable tolerance to moisture.<sup>74</sup> When the hydrogenation of acetone was performed on the open bench in non-anhydrous reagents and solvents using *i*PrSnOTf that had been exposed to air for one week, the reaction proceeded without any observable reduction in reaction rate.<sup>74</sup> This is unique in FLP catalysis where even previously reported reaction of moisture tolerant FLP systems have been slowed by trace presence of H<sub>2</sub>O. This demonstrates the value of pursuing Sn-based Lewis acids.<sup>74</sup> In 2017, Ingleson and coworkers reported that BPh<sub>3</sub> has improved water tolerance in the presence of alkylamines as the Brønsted acidic adduct H<sub>2</sub>O-BPh<sub>3</sub> does not undergo irreversible deprotonation with aliphatic amines in contrast to H<sub>2</sub>O-B(C<sub>6</sub>F<sub>5</sub>)<sub>3</sub>.<sup>66</sup> Therefore, they reported that

BPh<sub>3</sub> can serve as a catalyst for reductive amination of aldehydes and ketones with alkylamines using silanes as reductants.<sup>66</sup> However, it is not an effective catalyst for the reductive amination of arylamines.<sup>66</sup> It turns out that it has a complementary reductive amination scope to B(C<sub>6</sub>F<sub>5</sub>)<sub>3</sub>, which is able to catalyze the reduction amination of arylamines but not alkylamines.<sup>66</sup> It appears that BPh<sub>3</sub> is limited by the protodeboronation of the adduct H<sub>2</sub>O-BPh<sub>3</sub> in the presence of weaker amine bases, while B(C<sub>6</sub>F<sub>5</sub>)<sub>3</sub> is limited by the adduct H<sub>2</sub>O-B(C<sub>6</sub>F<sub>5</sub>)<sub>3</sub> undergoing irreversible deprotonation by stronger amine bases such as alkylamines.<sup>66</sup> The methodology presented is operationally simple and requires no additional purification of materials and solvents.<sup>66</sup> Reactions can be performed under air and are suited to gram-scale synthesis (**Scheme 23**).<sup>66</sup>



Scheme 23: Reductive amination catalyzed by BPh<sub>3</sub> or B(C<sub>6</sub>F<sub>5</sub>)<sub>3</sub>

In the same year, Soós and coworkers reported the development of a boron/nitrogen-centered FLP with high water tolerance. It is able to effect the reductive amination of carbonyls.<sup>75</sup> Systematic steric tuning of the boron-based Lewis acid by stepwise exchange of fluorine for chlorine atoms reveals that enhanced back strain makes water binding increasingly reversible in the presence of a relatively strong base.<sup>75</sup> As a result, they were able to maintain a preference for hydrogen activation while minimizing the interference of water.<sup>75</sup> Experiments have shown that a fully optimized system can show tolerance of up to 10 equivalents of water in FLP-promoted reductive amination (**Scheme 24**).<sup>75</sup>



Scheme 24: FLP reductive amination of carbonyl compounds using water-tolerant borane as catalyst

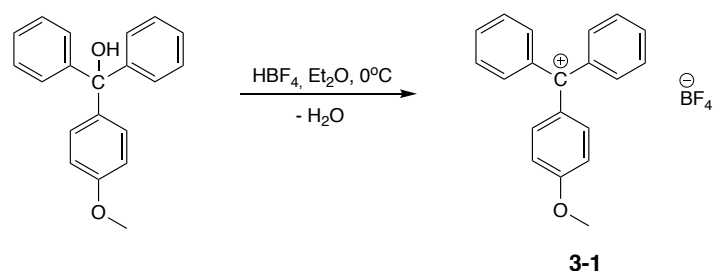
Despite numerous reports on bench stable FLP systems, they have primarily focused on the use of boron Lewis acids. Other main group Lewis acids such as aluminum and silicon have been exploited in FLP systems but they often remain oxophilic. Therefore there is a demand for readily accessible and less oxophilic Lewis acids for FLP applications. However, reports on bench-stable FLP systems based on other elements such as carbon continue to be relatively rare.

## 3.2 Results and Discussion

### 3.2.1 Reactivity of Bench-Stable Trityl Cations with Proazaphosphatrane

In an effort to broaden the utility of carbon-based Lewis acids in bench stable FLP chemistry, this chapter describes a new family of bench stable trityl cations that, when combined with  $\text{P}(\text{MeNCH}_2\text{CH}_2)_3\text{N}$  and a variety of phosphine Lewis bases, are able to induce the heterolytic splitting of  $\text{H}_2$ . This project was partially inspired by a recent report by Stephan and coworkers in 2016, which describes Markovnikov hydrothiolation of 1,1-disubstituted and trisubstituted olefins using alkyl and aryl thiols.<sup>76</sup> This reaction is catalyzed by the air stable trityl-cation salt [ $(p\text{-MeOC}_6\text{H}_4)\text{CPh}_2$ ][ $\text{BF}_4$ ] (**3-1**) under mild conditions without the use of dried or degassed solvents or reagents.<sup>76</sup>

To explore the application of these bench-stable carbon-based Lewis acids towards FLP chemistry, **3-1** was synthesized from the corresponding commercially available trityl alcohol. Treatment of the trityl alcohol with ethereal tetrafluoroboric acid generated **3-1** as an orange solid (**Scheme 25**).

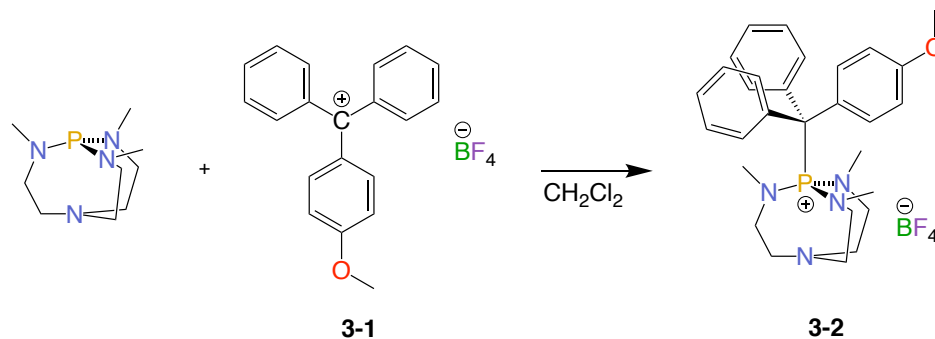


Scheme 25: Synthesis of **3-1**

The  $^1\text{H}$  NMR spectrum reveals a downfield singlet at 4.3 ppm, which is characteristic of the methoxy substituent in **3-1**. Signals corresponding to the three phenyl rings are also observed in the aromatic region of the spectrum between 7.5 and 8.0 ppm. The  $^{11}\text{B}\{^1\text{H}\}$  NMR spectrum reveals a singlet at -1.0 ppm and the  $^{19}\text{F}\{^1\text{H}\}$  NMR spectrum reveals a singlet at -153.4 ppm, both of which correspond to signals of the tetrafluoroborate anion. The  $^{13}\text{C}\{^1\text{H}\}$  NMR spectrum reveals a downfield signal at 198.4 ppm, which is characteristic of the central carbon of **3-1**. An upfield signal at 58.9 ppm is also observed, which corresponds to the methoxy substituent. Ten distinct carbon signals are also observed in the spectrum. Results from ESI-MS reveal a mass of 273.13 Da, which matches the expected mass of the cation of **3-1**. Taken together, the NMR and ESI-MS data are consistent with the formulation of **3-1** as  $[(p\text{-MeOC}_6\text{H}_4)\text{CPh}_2][\text{BF}_4]$ .

As discussed in the previous chapter, we reported that the adduct formed by combining  $\text{B}(\text{C}_6\text{F}_5)_3$  and proazaphosphatane  $\text{P}(\text{MeNCH}_2\text{CH}_2)_3\text{N}$  was able to generate products of FLP addition reactions despite not exhibiting spectroscopic evidence of dissociation. Initial investigation of **3-1** was geared towards exploring its chemistry in combination with  $\text{P}(\text{MeNCH}_2\text{CH}_2)_3\text{N}$ . A stoichiometric reaction of  $\text{P}(\text{MeNCH}_2\text{CH}_2)_3\text{N}$  with **3-1** was conducted at room temperature and

resulted in the formation of **3-2** within 10 min. Purification by recrystallization of **3-2** from a solution of CH<sub>2</sub>Cl<sub>2</sub> layered under toluene at -45°C resulted in the isolation of light red crystals. The <sup>31</sup>P{<sup>1</sup>H} NMR spectrum reveals a signal at 45.0 ppm. This peak is proposed to be the Lewis adduct resulting from the reaction of P(MeNCH<sub>2</sub>CH<sub>2</sub>)<sub>3</sub>N and **3-1** (Scheme 26).



Scheme 26: Reaction of P(MeNCH<sub>2</sub>CH<sub>2</sub>)<sub>3</sub>N with **3-1**

Previous reports have indicated a correlation between the degree of P-N<sub>ta</sub> transannular interaction and the <sup>31</sup>P NMR chemical shift. It has been observed that as the degree of P-N<sub>ta</sub> transannular interaction decreases, the <sup>31</sup>P NMR resonance shifts downfield and vice versa.<sup>77</sup> The decrease in the P-N<sub>ta</sub> transannular interaction has been reported to render the Lewis adduct more labile.<sup>32</sup> Given that the <sup>31</sup>P{<sup>1</sup>H} NMR chemical shift of **2-1** is 80.0 ppm, the chemical shifts would suggest that adduct **3-2** has a greater degree of transannular interaction than **2-1** and would therefore be a more robust adduct. This would later be confirmed by single crystal X-ray diffraction studies and further experimental work. The <sup>11</sup>B{<sup>1</sup>H} and <sup>19</sup>F{<sup>1</sup>H} of **3-2** reveals a singlet at -1.0 ppm and -152.9 ppm, respectively, both of which correspond to signals of the tetrafluoroborate anion. Single-crystal x-ray diffraction study confirmed the formulation of **3-2**, where addition to the central carbon was observed (Figure 11).

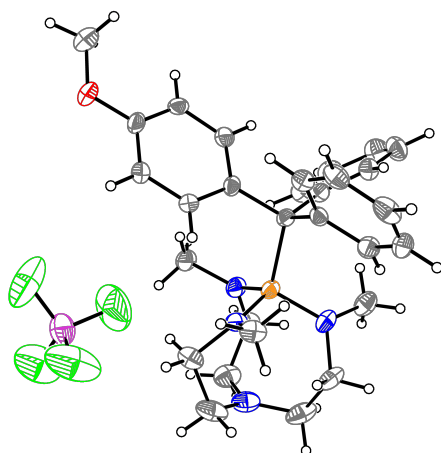


Figure 11: Solid-state structure of **3-2**. C: grey, N: blue, O: red, B: pink, F: yellow, P: orange

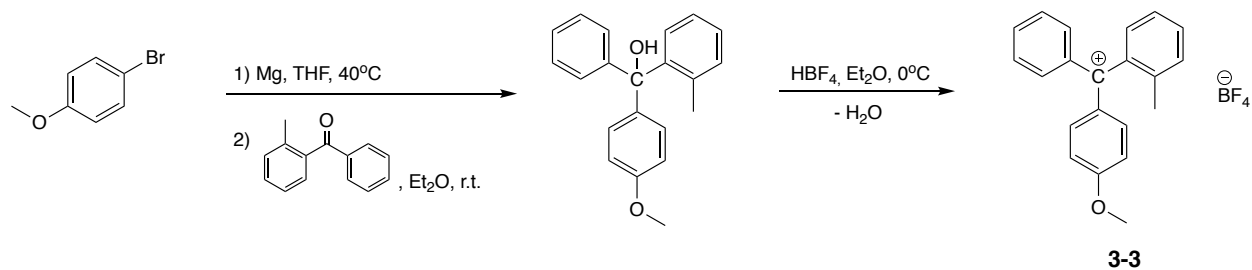
The P-C distance in **3-2** is 1.902(3) Å. The P-N<sub>ta</sub> distance is 3.097(3) Å, which is longer than that seen in the cation [HP(CH<sub>3</sub>NCH<sub>2</sub>CH<sub>2</sub>)<sub>3</sub>N]<sup>+</sup>. It is interesting to note that the P-N<sub>ta</sub> distance for **3-2** is shorter than that of **2-1**. The shorter P-N<sub>ta</sub> distance confirms that **3-2** experiences a greater degree of transannular interactions as compared to **2-1**. This parameter suggests that **3-2** is a more robust adduct than **2-1**.

We were interested in exploring whether analogous FLP reactivity as seen in **2-1** can be observed with the newly synthesized **3-2** despite it being a more robust adduct. A stoichiometric reaction of **3-2** with PhNCO was conducted at room temperature over the course of 1 h. The <sup>31</sup>P{<sup>1</sup>H} NMR spectrum before and after PhNCO was added revealed a singlet at 45.1 ppm. The result indicates that **3-2** persists in solution even after addition of PhNCO and does not generate the corresponding FLP addition product as seen in **2-1**. A stoichiometric reaction of adduct **3-2** with approximately 4 atm of H<sub>2</sub> at room temperature was also conducted to determine if it would activate H<sub>2</sub>. The <sup>31</sup>P{<sup>1</sup>H} NMR spectrum before and after H<sub>2</sub> addition revealed a single peak at 45.0 ppm suggesting

no reactivity in the presence of H<sub>2</sub>. The lack of FLP reactivity with either PhNCO or H<sub>2</sub> suggests that the behavior of **3-2** is consistent with that of a classical Lewis adduct.

As previously discussed, computational studies of **2-1** to rationalize its unexpected FLP reactivity suggest that the lack of a stabilizing transannular interaction can be attributed to steric effects. We hypothesized that introducing a substituent on the *ortho* position of an aromatic ring of the trityl cation could give the resulting proazaphosphatrane-trityl adduct access to FLP reactivity as seen with **2-1**. The transannular interaction in the resulting proazaphosphatrane-trityl adduct could be sufficiently precluded due to the increased steric bulk around the central carbon of the trityl cation, which would make the adduct weaker than expected.

Initial investigation focused on the synthesis of **3-3**, which contains a methyl group in the *ortho* position (**Scheme 27**). Compound **3-3** was synthesized from the corresponding aryl bromide and diaryl ketone via a Grignard reaction to generate the trityl alcohol. The trityl alcohol was then allowed to react with ethereal tetrafluoroboric acid to generate **3-3** as an orange solid.



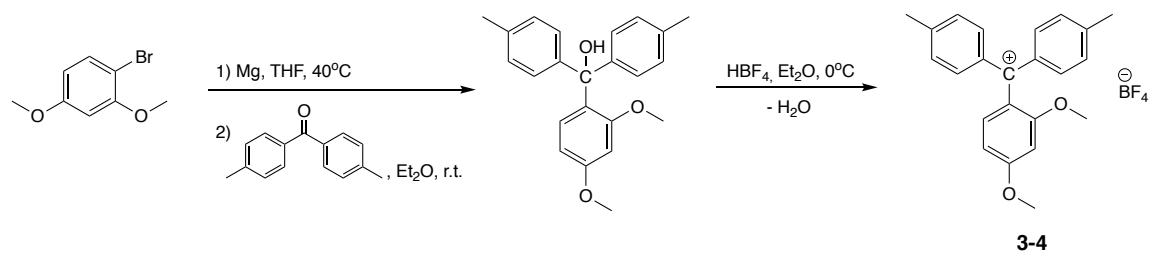
Scheme 27: Synthesis of **3-3**

The <sup>1</sup>H NMR spectrum reveals an upfield singlet at 1.92 ppm, which is characteristic of the methyl substituent. A more downfield singlet at 4.34 ppm is observed and this corresponds to the methoxy substituent. Signals corresponding to the three distinct phenyl rings are also observed in the aromatic region of the spectrum between 7.2 and 8.0 ppm. The <sup>11</sup>B{<sup>1</sup>H} NMR spectrum reveals a singlet at -1.0 ppm and the <sup>19</sup>F{<sup>1</sup>H} NMR spectrum reveals a singlet at -153.3 ppm, both of which

correspond to signals of the tetrafluoroborate anion. Taken together, the NMR data are consistent with the formulation of **3-3** as [(*p*-MeOC<sub>6</sub>H<sub>4</sub>)(*o*-MeC<sub>6</sub>H<sub>4</sub>)CPh][BF<sub>4</sub>].

A stoichiometric reaction of P(MeNCH<sub>2</sub>CH<sub>2</sub>)<sub>3</sub>N and **3-3** was conducted at room temperature. The <sup>31</sup>P{<sup>1</sup>H} NMR spectrum revealed two distinct signals at 46.3 ppm and 46.7 ppm. The <sup>11</sup>B{<sup>1</sup>H} and <sup>19</sup>F{<sup>1</sup>H} NMR spectrum revealed signals at -1.1 ppm and -152.6 ppm, which are both consistent with the presence of the tetrafluoroborate anion. We suspect that the presence of two signals in the <sup>31</sup>P{<sup>1</sup>H} NMR spectrum can be attributed to nucleophilic attacks at the two unsubstituted *para* positions of the inequivalent aryl rings to yield cyclohexadienyl-phosphonium cations. Such mode of reactivity has been reported in the literature.<sup>36</sup> Sterically cumbersome phosphines are known to undergo nucleophilic attack at the *para* position of the aryl ring of the trityl cation.<sup>36</sup> No further characterization of these products were performed.

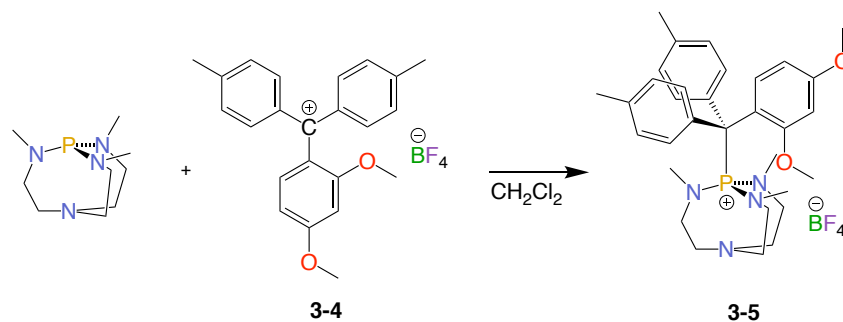
In an effort to address the propensity for bulky Lewis bases to undergo *para* attack, it was proposed that introducing substituents such as methyl or methoxy groups at all three *para* positions of the trityl cation would preclude the possibility of nucleophilic attack at that position. The presence of at least one methoxy group would also confer some bench stability to the trityl cation as seen with **3-1**. With these considerations in mind, efforts were directed towards the synthesis of **3-4** (Scheme 28). As in the previous case, **3-4** was synthesized from the corresponding aryl halide and diaryl ketone. Treatment of the trityl alcohol with ethereal tetrafluoroboric acid generated **3-4**, which was washed with diethyl ether to yield a dark red solid.



Scheme 28: Synthesis of **3-4**

The  $^1\text{H}$  NMR spectrum reveals a singlet at 2.6 ppm, which is indicative of the two methyl groups in **3-4**. Two singlets further downfield at 3.8 ppm and 4.3 ppm can be attributed to the *ortho* and *para* methoxy substituents in **3-4**, respectively. The  $^{11}\text{B}\{^1\text{H}\}$  NMR and  $^{19}\text{F}$  NMR  $\{^1\text{H}\}$  spectrum reveal a singlet at 0.9 ppm and 152.90 ppm, respectively, both of which are indicative of the tetrafluoroborate anion. The  $^{13}\text{C}\{^1\text{H}\}$  NMR spectrum reveals a downfield signal at 193.15 ppm, which is characteristic of the central carbon of **3-4**. Upfield signals at 22.47 ppm, 57.29 ppm and 58.9 ppm are also observed, which correspond to the methyl, *p*-methoxy and *o*-methoxy substituents, respectively. Fourteen distinct carbon signals are also observed in the  $^{13}\text{C}\{^1\text{H}\}$  NMR spectrum. Results from ESI-MS reveal a mass of 331.17 Da, which matches the expected mass of the cation of **3-4**. Taken together, the NMR and ESI-MS data are consistent with the formulation of **3-4** as  $[(p\text{-MeC}_6\text{H}_4)_2((o\text{-OMe})(p\text{-OMe})\text{C}_6\text{H}_3)\text{C}][\text{BF}_4]$ .

With **3-4** in hand, its reactivity with  $\text{P}(\text{MeNCH}_2\text{CH}_2)_3\text{N}$  was explored. A stoichiometric reaction of  $\text{P}(\text{MeNCH}_2\text{CH}_2)_3\text{N}$  and **3-4** was performed at room temperature. The  $^{31}\text{P}\{^1\text{H}\}$  NMR spectrum reveals a singlet at 61.9 ppm. This signal is proposed to be the Lewis adduct **3-5** (Scheme 29).

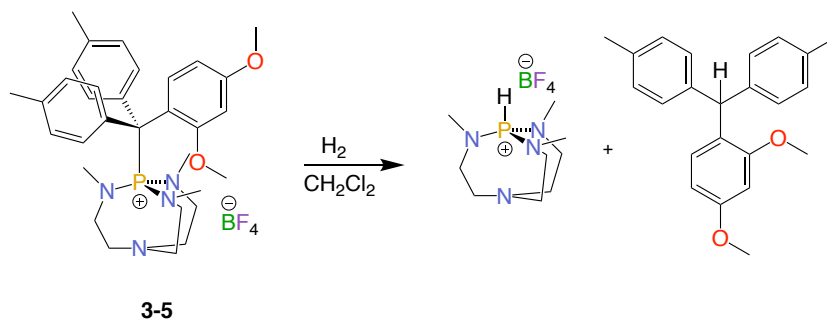


Scheme 29: Reaction of  $\text{P}(\text{MeNCH}_2\text{CH}_2)_3\text{N}$  with **3-4**

The  $^{31}\text{P}\{^1\text{H}\}$  NMR shift of **3-5** is further downfield than that of **3-2**, which suggests that the transannular interaction in **3-5** is weaker than that of **3-2**. This would be consistent with our previous hypothesis, which predicts that the resulting adduct **3-5** would experience less

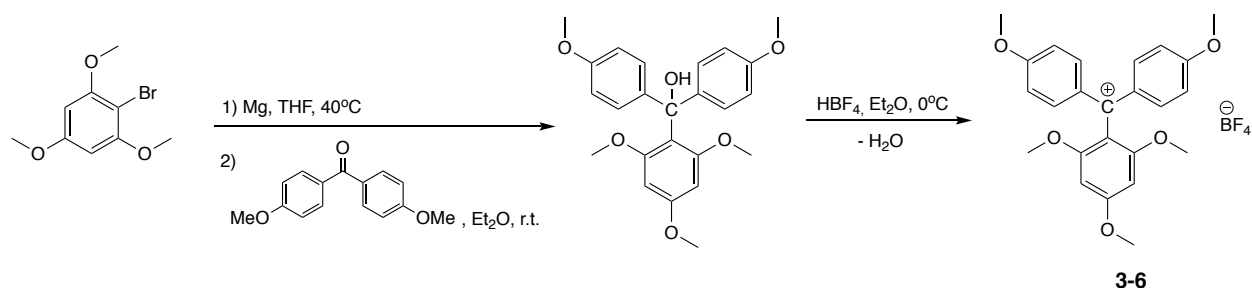
transannular interaction than **3-2** due to steric effects. Numerous attempts have been made to obtain a crystal of **3-5** suitable for X-ray diffraction studies, but these have been unsuccessful thus far.

A stoichiometric reaction of **3-5** and PhNCO was performed at room temperature. The  $^{31}\text{P}\{^1\text{H}\}$  NMR spectrum before and after addition of PhNCO reveal a singlet at 62.0 ppm. This indicates that adduct **3-5** does not exhibit FLP reactivity in the presence of PhNCO. Given that the  $^{31}\text{P}\{^1\text{H}\}$  NMR shift of **3-5** appears further upfield than that of **2-1**, we can infer that **3-5** is a more robust adduct than **2-1** due to the greater degree of transannular interaction and it is perhaps unsurprising that no reactivity was observed in this initial experiment. The analogous reaction was also performed with 4 atm of  $\text{H}_2$ , after which adduct **3-5** was observed to engage in the heterolytic cleavage of  $\text{H}_2$ . The  $^{31}\text{P}\{^1\text{H}\}$  NMR spectrum before  $\text{H}_2$  addition reveals a singlet at 62.0 ppm and over the course of approximately 2 h after  $\text{H}_2$  addition, that peak gradually decreases in intensity and a peak at 10.6 ppm, which corresponds to the  $[\text{HP}(\text{CH}_3\text{NCH}_2\text{CH}_2)_3\text{N}]^+$  cation, increases in intensity. The reaction mixture was passed through a plug of silica and a  $^1\text{H}$  NMR spectrum in  $\text{CDCl}_3$  of the resulting solution revealed the presence of the corresponding triphenylmethane derivative of **3-4**. In particular, the growth of a new peak at 5.09 ppm in the  $^1\text{H}$  NMR spectrum is consistent with the chemical shift of a proton on the central carbon of the corresponding triphenylmethane derivative. Furthermore, the possibility that this reactivity is a product of water activation can also be discounted since the chemical shift of a proton on the hydroxyl group of triphenylmethanol and other similar derivatives appear around 2.8 ppm in  $\text{CDCl}_3$ .<sup>78</sup> It is also important to note that the corresponding  $^1\text{H}$  NMR chemical shifts of the methyl and methoxy groups have shifted considerably upfield from that observed in **3-4**, which is consistent with the formation of a triphenylmethane species. Taken together, the data provide strong evidence of  $\text{H}_2$  activation by **3-5** (Scheme 30).



Scheme 30: Heterolytic cleavage of H<sub>2</sub> by FLP **3-5**

To determine whether analogous reactivity can be observed with trityl cations that are more sterically bulky than **3-4**, efforts were made to synthesize **3-6**. It was proposed that the addition of two methoxy groups in the *ortho* positions would render **3-6** more sterically demanding and therefore provide an opportunity to determine whether similar reactivity with P(MeNCH<sub>2</sub>CH<sub>2</sub>)<sub>3</sub>N can be observed. Compound **3-6** was synthesized from the corresponding aryl halide and diaryl ketone (Scheme 31). Treatment of the trityl alcohol with ethereal tetrafluoroboric acid generated **3-6**, which was washed with diethyl ether to yield a dark red solid.

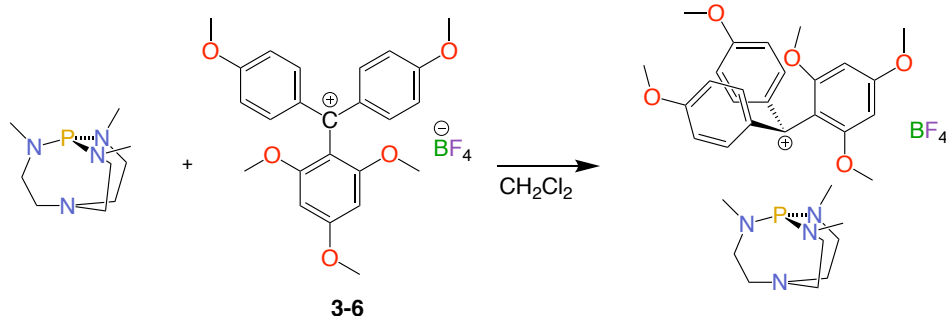


Scheme 31: Synthesis of **3-6**

The <sup>1</sup>H NMR spectrum reveals a singlet at 4.07 ppm, which is indicative of the two *ortho* methoxy substituents in **3-6**. Two singlets further upfield at 3.77 ppm and 3.55 ppm is indicative of the three *para* methoxy group. The <sup>11</sup>B{<sup>1</sup>H} NMR and <sup>19</sup>F{<sup>1</sup>H} NMR spectrum reveal a singlet at 0.9 ppm and 152.90 ppm, respectively, which is consistent with the presence of the tetrafluoroborate anion.

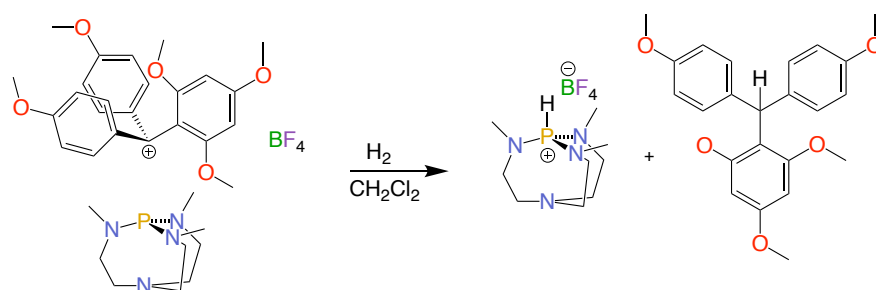
Results from ESI-MS reveal a mass of 393.1697 Da, matching the expected mass of the cation of **3-6**. Taken together, the NMR and ESI-MS data are consistent with the formulation of **3-6** as  $[(p\text{-OMeC}_6\text{H}_4)_2(o\text{-OMe})_2(p\text{-OMe})\text{C}_6\text{H}_3\text{C}][\text{BF}_4]$ .

A stoichiometric reaction of  $\text{P}(\text{MeNCH}_2\text{CH}_2)_3\text{N}$  and **3-6** was performed at room temperature. In contrast to previous examples, no adduct formation was observed. Instead, the  $^{31}\text{P}\{^1\text{H}\}$  NMR spectrum reveals a signal at 118.5 ppm, which indicates the presence of free  $\text{P}(\text{MeNCH}_2\text{CH}_2)_3\text{N}$ . This suggests that the combination of  $\text{P}(\text{MeNCH}_2\text{CH}_2)_3\text{N}$  and **3-6** generates a classical FLP where adduct formation is not observed (**Scheme 32**).



Scheme 32: Reaction of  $\text{P}(\text{MeNCH}_2\text{CH}_2)_3\text{N}$  and **3-6**

The reaction solution was then exposed to 4 atm of  $\text{H}_2$ . The  $^{31}\text{P}\{^1\text{H}\}$  NMR spectrum taken within 15 and 30 min of exposure to  $\text{H}_2$  both reveal growth in the peak at 10.6 ppm, which confirms that free  $\text{P}(\text{MeNCH}_2\text{CH}_2)_3\text{N}$  is being converted to the  $[\text{HP}(\text{CH}_3\text{NCH}_2\text{CH}_2)_3\text{N}]^+$  cation. Full conversion to the  $[\text{HP}(\text{CH}_3\text{NCH}_2\text{CH}_2)_3\text{N}]^+$  cation is observed 3 h after addition. These results suggest that the combination of  $\text{P}(\text{MeNCH}_2\text{CH}_2)_3\text{N}$  and **3-6** is capable of mimicking classical FLP behavior by heterolytically cleaving  $\text{H}_2$  (**Scheme 33**).



Scheme 33: Heterolytic cleavage of H<sub>2</sub> by P(MeNCH<sub>2</sub>CH<sub>2</sub>)<sub>3</sub>N and 3-6 FLP

This contrasts with previous results with **2-1**, **3-1** and **3-4**. In the cases of **2-1** and **3-4**, the resulting species generated from combination with P(MeNCH<sub>2</sub>CH<sub>2</sub>)<sub>3</sub>N gives an adduct that behaves like an FLP. In the case of **3-1**, an adduct is also produced but it does not exhibit FLP reactivity (**Figure 12**)

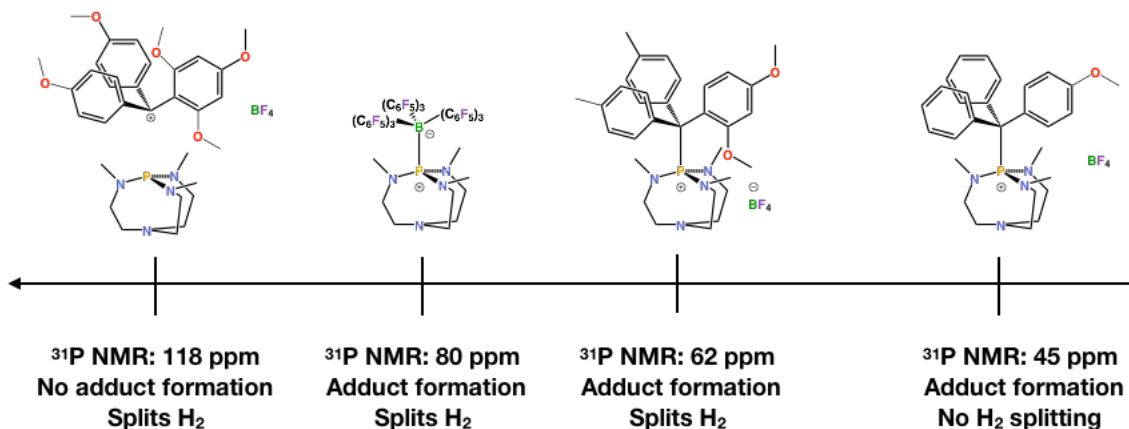


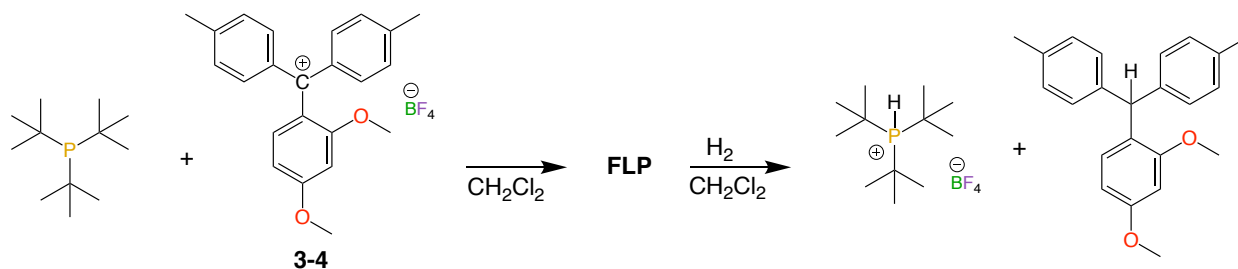
Figure 12: A comparison of the reactivity and <sup>31</sup>P NMR shifts of various trityl cations and B(C<sub>6</sub>F<sub>5</sub>)<sub>3</sub> with P(MeNCH<sub>2</sub>CH<sub>2</sub>)<sub>3</sub>N

### 3.2.2 Reactivity of Bench-Stable Trityl Cations with Phosphines

Up to this point, our investigation of bench-stable trityl cations has centered on the reactivity of several trityl cations with the highly Lewis basic P(MeNCH<sub>2</sub>CH<sub>2</sub>)<sub>3</sub>N. In an effort to expand its utility in FLP chemistry, the reactivity of these trityl cations with more conventional and weaker phosphine bases are also explored. Bulky phosphines often engage in nucleophilic attack at the

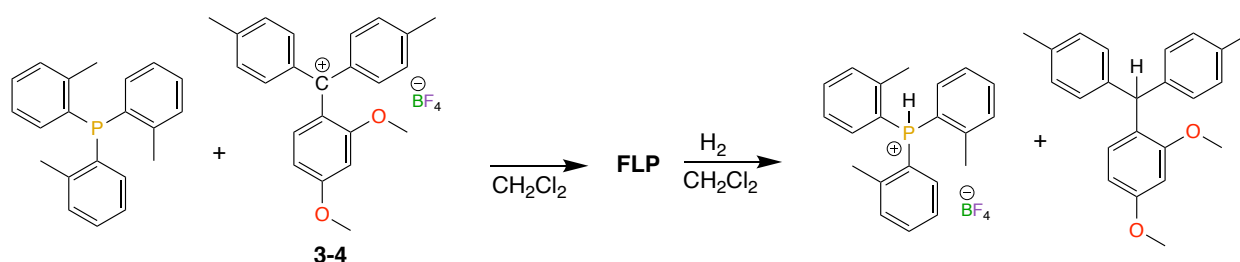
*para* position of the trityl cation. This often precludes the formation of an FLP and is presumably one reason why there are very few reports of FLP systems based on phosphines and trityl cations. Stephan and coworkers recently reported a notable exception where the FLP derived from P(*o*-tolyl)<sub>3</sub> and the parent trityl cation is able to effect the activation of 1,4-cyclohexadiene, 1-bromo-4-ethynylbenzene and heterolytically cleaves the S-S bond of diphenyl disulfide.<sup>31</sup> However, this FLP is not able to activate H<sub>2</sub>.<sup>31</sup> Given that we have a family of trityl cations with its *para* positions inaccessible to nucleophilic attack due to the presence of substituents, it would be of interest to investigate its potential towards FLP reactivity particularly for H<sub>2</sub> activation.

A stoichiometric reaction of **3-4** with P(*t*-Bu)<sub>3</sub> was performed at room temperature. The <sup>31</sup>P{<sup>1</sup>H} NMR spectrum taken within 10 min of addition reveals a singlet at 62.5 ppm, which is consistent with the presence of free P(*t*-Bu)<sub>3</sub> and suggests an FLP between **3-4** and P(*t*-Bu)<sub>3</sub>. The <sup>11</sup>B{<sup>1</sup>H} and <sup>19</sup>F{<sup>1</sup>H} NMR spectrum reveal a signal at -1.1 ppm and -150.7 ppm, respectively, both of which are indicative of the tetrafluoroborate anion. Upon exposure to 4 atm of H<sub>2</sub>, the dark red solution quickly turns colorless. Within 10 min of addition, the <sup>31</sup>P{<sup>1</sup>H} NMR spectrum reveals a growth of a singlet at 53.3 ppm. Upon proton coupling, this signal splits into a doublet with a coupling constant of approximately 480 Hz. This confirms the formation of the [HP(*t*-Bu)<sub>3</sub>]<sup>+</sup> cation, resulting from the heterolytic cleavage of H<sub>2</sub> (**Scheme 34**).



Scheme 34: Heterolytic cleavage of H<sub>2</sub> by P(*t*-Bu)<sub>3</sub> and **3-4** FLP

The analogous experiment was performed with  $P(o\text{-tolyl})_3$ . Like the previous example, the combination of  $P(o\text{-tolyl})_3$  and **3-4** generates an FLP. The  $^{31}\text{P}\{^1\text{H}\}$  NMR spectrum reveals a singlet at -30.2 ppm, indicating the presence of free  $P(o\text{-tolyl})_3$ . The  $^{11}\text{B}\{^1\text{H}\}$  and  $^{19}\text{F}\{^1\text{H}\}$  NMR confirm the presence of the tetrafluoroborate anion. Approximately 4 atm of  $\text{H}_2$  was added and within 10 min, the  $^{31}\text{P}\{^1\text{H}\}$  NMR spectrum reveals the growth of a singlet at -13.7 ppm. Upon proton coupling, this signal splits into a doublet with a coupling constant of approximately 486 Hz. This confirms the formation of the  $[\text{HP}(o\text{-tolyl})_3]^+$  cation, resulting from the heterolytic cleavage of  $\text{H}_2$  (Scheme 35).

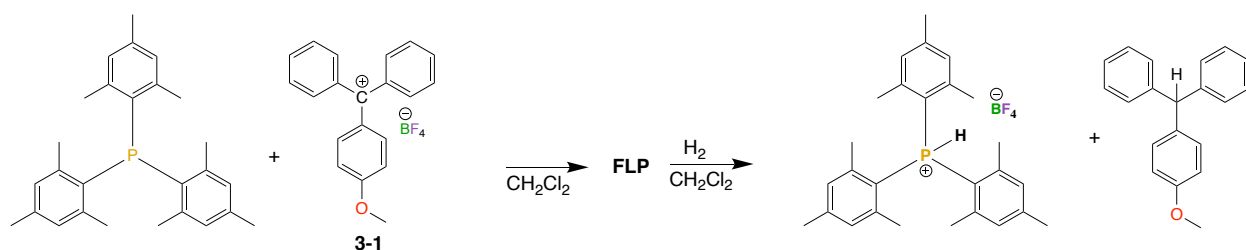


Scheme 35: Heterolytic cleavage of  $\text{H}_2$  by  $P(o\text{-tolyl})_3$  and **3-4** FLP

In summary, the combinations of **3-4** with  $P(\text{MeNCH}_2\text{CH}_2)_3\text{N}$ ,  $P(t\text{-Bu})_3$  or  $P(o\text{-tolyl})_3$  form an FLP, which is then able to effect the heterolytic cleavage of  $\text{H}_2$ . To our knowledge, this represents the first example of  $\text{H}_2$  activation by an FLP system based on phosphines and trityl cations.

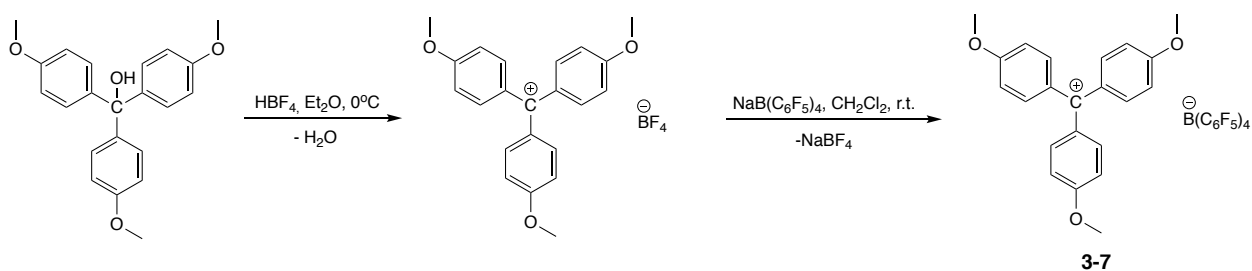
In an effort to demonstrate that these FLP reactivities are not only limited to **3-4** and can be generalized to other trityl cations, analogous experiments with  $P(t\text{-Bu})_3$  and  $\text{PMes}_3$  were performed with **3-1**. A stoichiometric reaction of the  $\text{B}(\text{C}_6\text{F}_5)_4$  salt of **3-1** and  $P(t\text{-Bu})_3$  was performed at room temperature. The  $^{31}\text{P}\{^1\text{H}\}$  NMR spectrum reveals what appeared to be an unidentifiable mixture of decomposition products. As **3-1** is susceptible to nucleophilic attack at the *para* position, it was initially proposed that one of the products is the corresponding cyclohexyldienyl-phosphonium cation. However, the expected peak at 50.2 ppm is not observed. A stoichiometric reaction of

PMes<sub>3</sub> and **3-1** generated the expected FLP as indicated by the free PMes<sub>3</sub> signal at -36.5 ppm in the <sup>31</sup>P{<sup>1</sup>H} NMR spectrum. The reaction mixture was subsequently exposed to 4 atm of H<sub>2</sub>. The <sup>31</sup>P{<sup>1</sup>H} NMR spectrum taken within 10 min after H<sub>2</sub> addition revealed two signals, one at -36.5 ppm and another at -28.0 ppm. Upon proton coupling, the latter peak was observed to split into a doublet with coupling constant of about 480 Hz. This is consistent with the formation of the [HPMes<sub>3</sub>]<sup>+</sup> cation, resulting from the heterolytic cleavage of H<sub>2</sub> (**Scheme 36**).



Scheme 36: Heterolytic cleavage of H<sub>2</sub> by PMes<sub>3</sub> and **3-1** FLP

Similar experiments were also performed with a related trityl cation **3-7** [(*p*-OMeC<sub>6</sub>H<sub>4</sub>)<sub>3</sub>C][B(C<sub>6</sub>F<sub>5</sub>)<sub>4</sub>], which is synthesized by treating the corresponding commercially available trityl alcohol with tetrafluoroboric acid in diethyl ether and subsequently exchanging the BF<sub>4</sub><sup>-</sup> anion for the B(C<sub>6</sub>F<sub>5</sub>)<sub>4</sub><sup>-</sup> anion (**Scheme 37**).

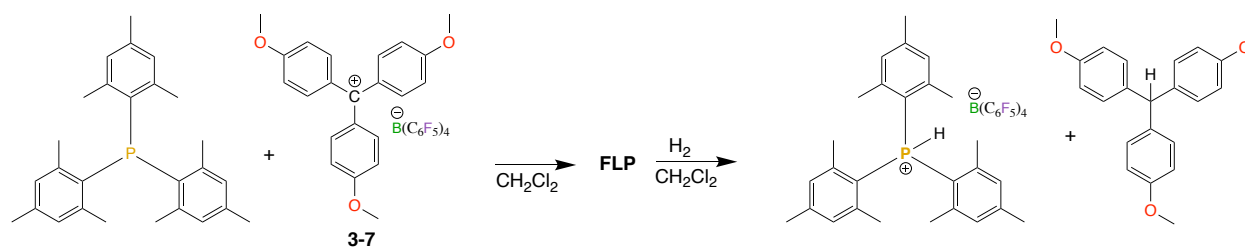


Scheme 37: Synthesis of **3-7**

The <sup>1</sup>H NMR spectrum of the orange solid reveals a singlet at 4.05 ppm corresponding to the three *para* methoxy substituents. Signals corresponding to the aromatic protons on the three phenyl rings are also observed between 7.2 ppm and 7.5 ppm. The <sup>11</sup>B{<sup>1</sup>H} NMR spectrum reveals a singlet at

-16.7 ppm and the  $^{19}\text{F}\{^1\text{H}\}$  NMR spectrum reveals singlets at -132.6 ppm, -163.1 ppm and -166.8 ppm, which correspond to signals of the  $\text{B}(\text{C}_6\text{F}_5)_4$  anion. The  $^{13}\text{C}\{^1\text{H}\}$  NMR spectrum reveals a downfield signal at 192.5 ppm, which is characteristic of the central carbon of **3-7**. An upfield signal at 56.9 ppm is also observed, which corresponds to the three *para* methoxy substituents. Six distinct carbon signals are also observed in the spectrum. Results from ESI-MS reveal a mass of 331.1491 Da, which matches the expected mass of **3-7**. Taken together, the NMR and ESI-MS data are consistent with the formulation of **3-7** as  $[(p\text{-OMeC}_6\text{H}_4)_3\text{C}][\text{B}(\text{C}_6\text{F}_5)_4]$ .

A stoichiometric reaction of  $\text{P}(t\text{-Bu})_3$  and **3-7** was performed at room temperature. The  $^{31}\text{P}\{^1\text{H}\}$  NMR spectrum taken within 10 min of addition reveals what appeared to be an unidentifiable mixture of decomposition products. The analogous reaction was performed with  $\text{PMes}_3$ . A stoichiometric reaction of  $\text{PMes}_3$  and **3-7** generated the expected FLP as indicated by the free  $\text{PMes}_3$  signal at -36.5 ppm in the  $^{31}\text{P}\{^1\text{H}\}$  NMR spectrum. The reaction solution was exposed to 4 atm of  $\text{H}_2$  and a  $^{31}\text{P}\{^1\text{H}\}$  NMR spectrum taken within 10 min of this addition reveals an additional peak at -28.0 ppm, which upon proton coupling, splits into a doublet with coupling of about 495.7 Hz. This is consistent with the presence of the  $[\text{HPMes}_3]^+$  cation resulting from the heterolytic cleavage of  $\text{H}_2$  (**Scheme 38**).



Scheme 38: Heterolytic cleavage of  $\text{H}_2$  by  $\text{PMes}_3$  and **3-7** FLP

The same experiments were also performed with **3-6**. However, the resulting FLPs generated from  $\text{P}(t\text{-Bu})_3$  and  $\text{PMes}_3$  were found to be inactive towards  $\text{H}_2$  activation. This is probably a result of the insufficient cumulative strength of the Lewis acid and base to effect  $\text{H}_2$  activation. In summary,

we have demonstrated that combinations of various trityl cations with common phosphine bases generate FLPs, which are shown to be capable of activating H<sub>2</sub>.

In an effort to explore the potential application of these FLPs as catalysts for hydrogenation, hydrogen deuteride scrambling experiments were performed to determine if the FLPs are able to reversibly activate H<sub>2</sub>. A stoichiometric reaction of P(*o*-tolyl)<sub>3</sub> and the B(C<sub>6</sub>F<sub>5</sub>)<sub>4</sub> salt of **3-4** was performed at room temperature in toluene-*d*<sub>8</sub>. The reaction solution was exposed to 1 atm of HD and monitored over time using <sup>1</sup>H NMR spectroscopy to determine if H<sub>2</sub> was generated. The <sup>1</sup>H NMR spectrum taken within 15 min of HD addition did not reveal any noticeable increase in the H<sub>2</sub> signal. The reaction solution was heated to 110 °C in an effort to increase the reaction rate and <sup>1</sup>H NMR spectra were taken at regular intervals. No noticeable growth in the H<sub>2</sub> signal was observed even at elevated temperatures over approximately 2 days.

In an effort to address this problem, it was proposed that a more electron-rich trityl cation may confer increased hydricity to the corresponding triphenylmethane and allow for the reformation of the FLP and H<sub>2</sub>. As a result, the analogous experiment was performed with the more electron-rich trityl cation **3-7**. A stoichiometric reaction of PMe<sub>3</sub> and **3-7** was performed at room temperature in toluene-*d*<sub>8</sub>. The reaction solution was exposed to 1 atm of HD and monitored at regular intervals using <sup>1</sup>H NMR spectroscopy to determine if H<sub>2</sub> is generated over time. Over the course of about 15 h at 110 °C, an increase in the signal indicative of H<sub>2</sub> is observed, suggesting that the combination of PMe<sub>3</sub> and **3-7** is able to activate H<sub>2</sub> in a reversible manner (**Figure 12**).

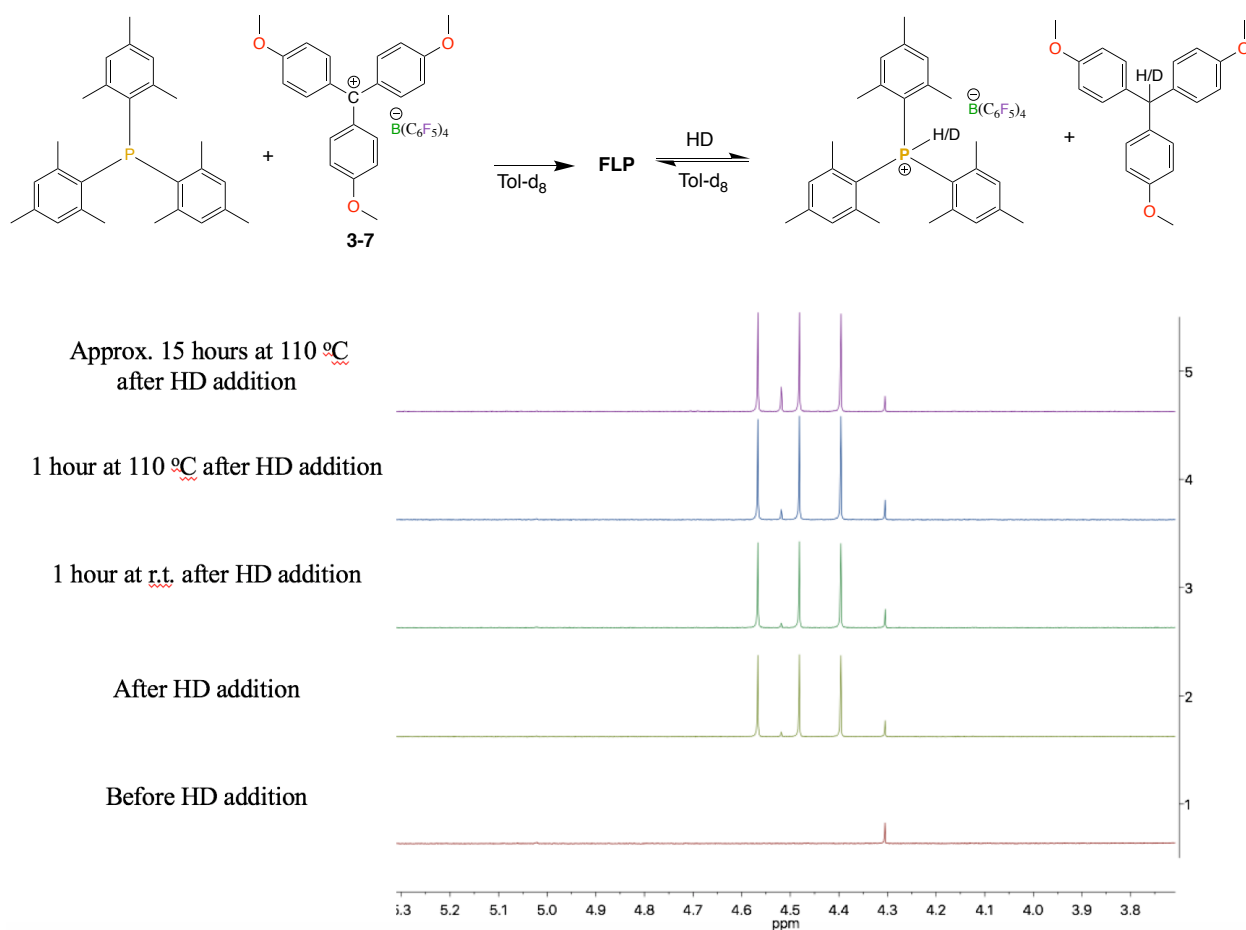


Figure 13: HD scrambling experiment with  $\text{PMes}_3$  and **3-7** FLP

These results suggest that the trityl cation **3-7** could provide an FLP approach to catalytic hydrogenation.

### 3.3 Conclusion

We have described the synthesis and reactivity of a new family of bench-stable trityl cations for FLP chemistry. When combined with  $\text{P}(\text{MeNCH}_2\text{CH}_2)_3\text{N}$  and a variety of phosphine bases, these trityl cations were able to induce the heterolytic splitting of  $\text{H}_2$ . For example, the combination of  $\text{P}(\text{MeNCH}_2\text{CH}_2)_3\text{N}$  and **3-4** generates a stable adduct, which then goes on to activate  $\text{H}_2$ . The reactivity of this adduct is reminiscent of that seen with **2-1**. Furthermore, combinations of **3-4**

with weaker bases such  $P(t\text{-Bu})_3$  and  $P(o\text{-tolyl})_3/\text{PMes}_3$  are still able to effect the heterolytic cleavage of  $\text{H}_2$ . This reactivity can be extended to other trityl cations such as **3-1** and **3-7**. In particular, the combination of  $\text{PMes}_3$  and **3-7** is found to be able to activate  $\text{H}_2$  in a reversible manner as evidenced by a HD scrambling experiment. Efforts designed to conduct analogous reactions in wet solvents and further probe the catalytic applications and FLP reactivity of these bench-stable trityl cations are the subject of ongoing efforts.

## 3.4 Experimental Section

### 3.4.1 General Consideration

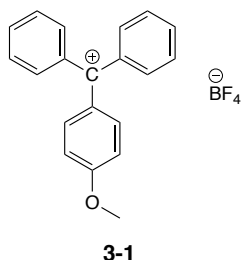
#### **Materials and Methods**

All manipulations were performed under an atmosphere of  $\text{N}_2$  in a Vacuum Atmosphere glovebox equipped with a  $-45^\circ\text{C}$  freezer, or on a dual-manifold Schlenk line. Non-deuterated solvents were dried on a Grubbs-type solvent purification system and stored under  $\text{N}_2$  over 3 Å molecular sieves. Unless otherwise stated, chemicals were purchased from Alfa Aesar, Sigma-Aldrich or Oakwood Chemicals and used as received without further purification.  $\text{CDCl}_3$  was used as received without further drying or purification.  $^1\text{H}$ ,  $^{11}\text{B}$ ,  $^{31}\text{P}$  and  $^{19}\text{F}$  NMR spectra were recorded on a Bruker Avance III 400 MHz NMR spectrometer or an Agilent DD2-500 MHz NMR spectrometer. NMR resonances are reported as chemical shifts (ppm) and referenced to residual solvent signal. Chemical shifts ( $\delta$ ) are reported in ppm and the absolute value of the coupling constants ( $J$ ) are reported in Hz. Hydrogen gas was obtained from Linde and purified through a Matheson Model 450B or Matheson Nanochem WeldAssure TM gas purifier. High-resolution mass spectra (HRMS) were obtained on an Agilent 6538 Q-TOF (ESI) or a JMS-T100LC JOEL (DART).

### 3.4.2 Synthesis of Starting Materials

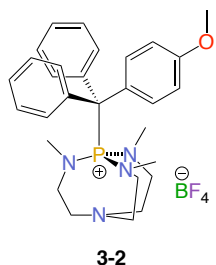
#### Synthetic Procedures

##### Preparation of trityl tetrafluoroborate salt **3-1**



In a 100 mL round-bottom flask equipped with a magnetic stirring bar, 4-methoxytrityl alcohol was dissolved in diethyl ether and stirred at 0°C for 20 min. 5 equivalents of tetrafluoroboric acid (50-55% w/w in diethyl ether) was added dropwise to the solution over a period of 15 min under vigorous stirring. The resulting mixture turned to a bright orange suspension and was allowed to continue stirring at 0°C for 1 h. The mixture was evaporated to dryness to afford an orange red oil and was dissolved in dichloromethane. Diethyl ether was added to precipitate the product as a dark orange solid. The product was filtered over a fine-pore frit and washed with pentane and dried under vacuum overnight to afford the desired product as a dark orange solid. **<sup>1</sup>H NMR (400 MHz, CDCl<sub>3</sub>):** δ 4.29 (s, 3H, OCH<sub>3</sub>), 7.50-7.52 (m, 6H, ArH), 7.73-7.76 (m, 4H, ArH), 7.83-7.85 (m, 2H, ArH), 7.98-8.01 (m, 2H, ArH). **<sup>13</sup>C{<sup>1</sup>H} NMR (500 MHz, CDCl<sub>3</sub>):** δ 58.94 (s, OCH<sub>3</sub>), 119.34 (s, *m*-C<sub>6</sub>H<sub>4</sub>), 129.88 (s, *m*-C<sub>6</sub>H<sub>5</sub>), 133.52 (s, *ipso*-C<sub>6</sub>H<sub>4</sub>), 138.90 (s, *ipso*-C<sub>6</sub>H<sub>5</sub>), 139.06 (s, *o*-C<sub>6</sub>H<sub>5</sub>), 139.30 (s, *o*-C<sub>6</sub>H<sub>4</sub>), 147.98 (s, *p*-C<sub>6</sub>H<sub>5</sub>), 177.01 (s, C(OMe)), 198.43 (s, CPh<sub>2</sub>(MeO(C<sub>6</sub>H<sub>4</sub>))). **<sup>11</sup>B{<sup>1</sup>H} NMR (400 MHz, CDCl<sub>3</sub>)** δ -1.02 (BF<sub>4</sub>). **<sup>19</sup>F{<sup>1</sup>H} NMR (400 MHz, CDCl<sub>3</sub>):** δ 153.38 (s, BF<sub>4</sub>). ESI-MS exact mass calculated for (C<sub>23</sub>H<sub>23</sub>O<sub>2</sub>)<sup>+</sup> require m/z 273.13, found m/z 273.13.

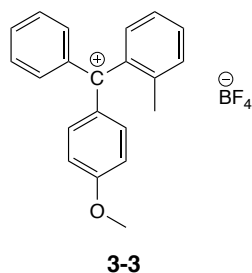
##### Preparation of P(MeNCH<sub>2</sub>CH<sub>2</sub>)<sub>3</sub>N and trityl tetrafluoroborate salt adduct **3-2**



Solutions of **3-1** and P(MeNCH<sub>2</sub>CH<sub>2</sub>)<sub>3</sub>N in dichloromethane were prepared and cooled to approximately -45°C. The two solutions were combined cold and allowed to warm to room temperature over 20 min. The reaction mixture was then layered under toluene and stored at -45°C. Over the course of 3 days, light red blocks formed, which were dried under vacuum. **<sup>1</sup>H NMR (500 MHz, CD<sub>2</sub>Cl<sub>2</sub>):** δ 2.22 (d, <sup>3</sup>J<sub>HP</sub> = 7.65 Hz, 3H, CH<sub>3</sub>), 2.24 (d, <sup>3</sup>J<sub>HP</sub> = 7.89 Hz, 3H, CH<sub>3</sub>), 2.28 (d, <sup>3</sup>J<sub>HP</sub> = 7.65 Hz, 3H, CH<sub>3</sub>), 2.82-2.96 (m, 12H, CH<sub>2</sub>), 6.95-7.44 (m, 14H, ArH). **<sup>31</sup>P{<sup>1</sup>H} NMR (400 MHz, CD<sub>2</sub>Cl<sub>2</sub>):** δ 45.00. **<sup>11</sup>B{<sup>1</sup>H} NMR (400 MHz, CD<sub>2</sub>Cl<sub>2</sub>)** δ -1.14 (BF<sub>4</sub>). **<sup>19</sup>F{<sup>1</sup>H} NMR (400 MHz,**

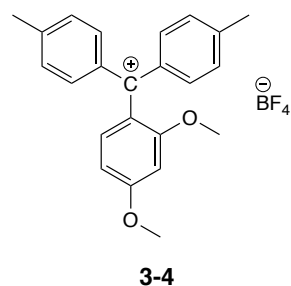
**CD<sub>2</sub>Cl<sub>2</sub>**):  $\delta$  152.92 (s, BF<sub>4</sub>). ESI-MS exact mass calculated for (C<sub>23</sub>H<sub>23</sub>O<sub>2</sub>)<sup>+</sup> require m/z 489.28, found m/z 489.28.

### Preparation of trityl tetrafluoroborate salt **3-3**



4-bromoanisole was dissolved in diethyl ether and charged in a 100 mL round-bottom flask equipped with a magnetic stirring bar. Mg turnings and a crystal of iodine was suspended inside the solution and left to stir vigorously for 12 h at ambient temperature. 2-methylbenzophenone was then dissolved in diethyl ether and added dropwise to the reaction mixture. The reaction mixture was left to stir for 12 h at ambient temperature. Water was then added to the reaction mixture and the combined mixture was left to stir for 30 min at ambient temperature. The organic layer was separated from the aqueous layer and the resulting aqueous layer was extracted twice with diethyl ether. The combined organic layer was washed with brine, dried over magnesium sulfate and evaporated to dryness to yield a yellow oil. The oil was dissolved in diethyl ether and stirred at 0°C for 15 min. 2 equivalents of tetrafluoroboric acid (50-55% w/w in diethyl ether) was added dropwise to the solution over a period of 15 min. The mixture turned into a bright orange suspension. The product was filtered over a fine-pore frit and washed with pentane and dried under vacuum overnight to afford the desired product as an orange solid. <sup>1</sup>H NMR (400 MHz, CDCl<sub>3</sub>):  $\delta$  1.92 (s, 3H, *o*-CH<sub>3</sub>), 4.34 (m, 3H, *p*-OCH<sub>3</sub>), 7.15-7.17 (m, 1H, ArH), 7.39-7.52 (m, 5H, ArH), 7.61-7.64 (m, 1H, ArH), 7.69-7.74 (m, 4H, ArH), 7.95-7.98 (m, 1H, ArH), 8.03-8.06 (m, 1H, ArH). <sup>11</sup>B NMR (400 MHz, CDCl<sub>3</sub>):  $\delta$  -1.00 (s, BF<sub>4</sub>). <sup>19</sup>F NMR (400 MHz, CDCl<sub>3</sub>):  $\delta$  -153.27 (s, BF<sub>4</sub>).

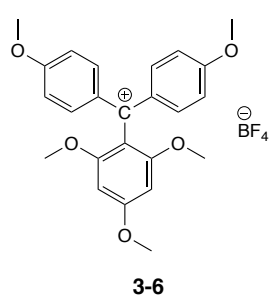
### Preparation of trityl tetrafluoroborate salt **3-4**



1-bromo-2,4-dimethoxybenzene was dissolved in THF and charged in a 100 mL round-bottom flask equipped with a magnetic stirring bar. Mg turnings was suspended inside the solution and left to stir vigorously for 12 h at approximately 40°C. 4,4'-dimethylbenzophenone was then dissolved in diethyl ether and added dropwise to the reaction mixture. The reaction mixture was left to stir for 12 h at ambient temperature. Water was then added to the reaction mixture and the combined mixture was left to stir for 30 min at ambient temperature. The organic layer was separated from the aqueous layer and the resulting aqueous

layer was extracted twice with diethyl ether. The combined organic layer was washed with brine, dried over magnesium sulfate and evaporated to dryness to yield a pale-yellow oil. The oil was dissolved in diethyl ether and stirred at 0°C for 15 min. 1 equivalent of tetrafluoroboric acid (50-55% w/w in diethyl ether) was added dropwise to the solution over a period of 15 min. The mixture turned into a dark red suspension. The mixture was evaporated to dryness and dissolved in dichloromethane. Pentane was added to the solution to precipitate the product as a dark red solid. The product was filtered over a fine-pore frit and washed with pentane and dried under vacuum overnight to afford the desired product as a dark red solid. **<sup>1</sup>H NMR (400 MHz, CDCl<sub>3</sub>):** δ 2.55 (s, CH<sub>3</sub>), 3.73 (s, *o*-OCH<sub>3</sub>), 4.21 (s, *p*-OCH<sub>3</sub>), 6.77-6.79 (m, 1H, ArH), 6.83 (m, 1H, ArH), 7.13-7.15 (m, 1H, ArH), 7.30-7.45 (m, 8H, ArH). **<sup>13</sup>C NMR (500 MHz, CDCl<sub>3</sub>):** δ 22.47 (s, CH<sub>3</sub>), 57.29 (s, *p*-OCH<sub>3</sub>), 58.50 (s, *o*-OCH<sub>3</sub>), 98.91 (s, *m*-C<sub>6</sub>H<sub>3</sub>), 113.73 (s, *m*-C<sub>6</sub>H<sub>3</sub>), 124.94 (s, *ipso*-C<sub>6</sub>H<sub>3</sub>), 130.16 (s, *m*-C<sub>6</sub>H<sub>4</sub>), 130.51 (s, *ipso*-C<sub>6</sub>H<sub>4</sub>), 136.64 (s, *o*-C<sub>6</sub>H<sub>4</sub>), 138.49 (s, *o*-C<sub>6</sub>H<sub>3</sub>), 144.59 (s, *p*-C(OMe)), 170.57 (s, *o*-C(OMe)), 177.04 (s, *p*-CH<sub>3</sub>) 193.15 (s, C(C<sub>6</sub>H<sub>4</sub>CH<sub>3</sub>)<sub>2</sub>(C<sub>6</sub>H<sub>3</sub>(OCH<sub>3</sub>)<sub>2</sub>)). **<sup>11</sup>B NMR (400 MHz, CDCl<sub>3</sub>):** δ -0.96 (s, BF<sub>4</sub>). **<sup>19</sup>F NMR (400 MHz, CDCl<sub>3</sub>):** δ -153.16 (s, BF<sub>4</sub>). ESI-MS exact mass calculated for (C<sub>23</sub>H<sub>23</sub>O<sub>2</sub>)<sup>+</sup> require m/z 331.43, found m/z 331.17.

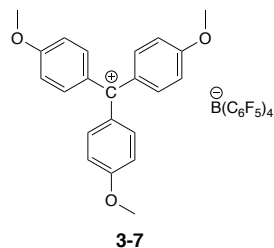
### Preparation of trityl tetrafluoroborate salt **3-6**



1-bromo-2,4,6-trimethoxybenzene was dissolved in THF and charged in a 100 mL round-bottom flask equipped with a magnetic stirring bar. Mg turnings was suspended inside the solution and left to stir vigorously for 12 h at approximately 40°C. 4,4'-dimethoxybenzophenone was then dissolved in diethyl ether and added dropwise to the reaction mixture. The reaction mixture was left to stir for 12 h at ambient temperature. Water was then added to the reaction mixture and the combined mixture was left to stir for 30 min at ambient temperature. The organic layer was separated from the aqueous layer and the resulting aqueous layer was extracted twice with diethyl ether. The combined organic layer was washed with brine, dried over magnesium sulfate and evaporated to dryness to yield a pale-yellow oil. The oil was dissolved in diethyl ether and stirred at 0°C for 15 min. 1 equivalent of tetrafluoroboric acid (50-55% w/w in diethyl ether) was added dropwise to the solution over a period of 15 min. The mixture turned into a dark red suspension. The mixture was evaporated to dryness and dissolved in dichloromethane. Pentane was added to the solution to precipitate the product as a dark red solid. The product was filtered over a fine-pore frit and washed with pentane and dried under vacuum

overnight to afford the desired product as a dark red solid. **<sup>1</sup>H NMR (400 MHz, CDCl<sub>3</sub>):** δ 3.55 (s, CH<sub>3</sub>), 3.77 (s, *o*-OCH<sub>3</sub>), 4.07 (s, *p*-OCH<sub>3</sub>), 6.27 (m, 2H, ArH), 7.14-7.16 (m, 4H, ArH), 7.52-7.54 (m, 4H, ArH). **<sup>11</sup>B NMR (400 MHz, CDCl<sub>3</sub>):** δ -0.86 (s, BF<sub>4</sub>). **<sup>19</sup>F NMR (400 MHz, CDCl<sub>3</sub>):** δ -153.69 (s, BF<sub>4</sub>). ESI-MS exact mass calculated for (C<sub>23</sub>H<sub>23</sub>O<sub>2</sub>)<sup>+</sup> require m/z 393.17, found m/z 393.17.

### Preparation of trityl tetrafluoroborate salt 3-7



In a 100 mL round-bottom flask equipped with a magnetic stirring bar, 4,4',4''-trimethoxytrityl alcohol was dissolved in diethyl ether and stirred at 0°C for 20 min. 5 equivalents of tetrafluoroboric acid (50-55% w/w in diethyl ether) was added dropwise to the solution over a period of 15 min under vigorous stirring. The resulting mixture turned to a bright orange suspension and was allowed to continue stirring at 0°C for 1 h. The mixture was evaporated to dryness to afford an orange red oil and was dissolved in dichloromethane. Diethyl ether was added to precipitate the product as a dark orange solid. The product was filtered over a fine-pore frit and washed with pentane and dried under vacuum overnight to afford the desired product as a dark orange solid. **<sup>1</sup>H NMR (400 MHz, CDCl<sub>3</sub>):** δ 4.05 (s, 3H, OCH<sub>3</sub>), 7.17-7.19 (m, 2H, ArH), 7.47-7.49 (m, 2H, ArH). **<sup>13</sup>C{<sup>1</sup>H} NMR (500 MHz, CDCl<sub>3</sub>):** δ 56.90 (s, OCH<sub>3</sub>), 116.44 (s, *m*-C<sub>6</sub>H<sub>4</sub>), 132.01 (s, *ipso*-C<sub>6</sub>H<sub>4</sub>), 142.69 (s, *o*-C<sub>6</sub>H<sub>4</sub>), 170.64 (s, C(OCH<sub>3</sub>)), 192.52 (s, C(C<sub>6</sub>H<sub>4</sub>(OCH<sub>3</sub>))). **<sup>11</sup>B{<sup>1</sup>H} NMR (400 MHz, CDCl<sub>3</sub>)** δ -16.72 (s, B(C<sub>6</sub>F<sub>5</sub>)<sub>4</sub>). **<sup>19</sup>F{<sup>1</sup>H} NMR (400 MHz, CDCl<sub>3</sub>):** δ 132.58 (s, 2 *o*-F, (B(C<sub>6</sub>F<sub>5</sub>)<sub>4</sub>), 163.06 (s, 1 *p*-F, (B(C<sub>6</sub>F<sub>5</sub>)<sub>4</sub>), 166.84 (s, 2 *m*-F, B(C<sub>6</sub>F<sub>5</sub>)<sub>4</sub>). ESI-MS exact mass calculated for (C<sub>23</sub>H<sub>23</sub>O<sub>2</sub>)<sup>+</sup> require m/z 331.15, found m/z 331.15.

### 3.4.3 X-ray crystallography

Suitable crystals were coated in Paratone-N-oil in an N<sub>2</sub> filled glovebox, mounted on a MiTeGen polyimide loop and cooled to 150(2) K under a stream of N<sub>2</sub> on a Bruker Apex diffractometer using an Oxford Cryosystems cryoprobe. Diffraction was carried out using graphite monochromated Mo K $\alpha$  radiation (( $\lambda$  = 0.71073 Å). Diffraction data were integrated and reduced using Bruker SAINT. Absorption corrections were applied using SADABS or TWINABS. The structures were solved by direct methods using SHELXS and subjected to full-matrix least squares

refinement on  $F^2$  using SHELX. All non-H atoms were refined anisotropically. H atoms were placed at geometrically calculated positions and refined using an appropriate riding model with coupled displacement parameters. Structures were validated using PLATON and CheckCIF. Selected crystallographic parameters for the structure **3-1** are collected in Table 2.

Table 2. X-ray crystallographic data for **3-1**

	<b>3-1</b> ·1.5(C <sub>6</sub> H <sub>6</sub> )
Empirical formula	C <sub>38</sub> H <sub>47</sub> BF <sub>4</sub> N <sub>4</sub> OP
Formula weight	693.60
Crystal system	monoclinic
Space group	<i>P</i> 2 <sub>1</sub> / <i>n</i>
<i>a</i> (Å)	10.2978(9)
<i>b</i> (Å)	21.148(2)
<i>c</i> (Å)	16.621(1)
$\alpha$ (°)	90
$\beta$ (°)	99.009(3)
$\gamma$ (°)	90
Volume (Å <sup>3</sup> )	3575.1(5)
<i>Z</i>	4
Completeness (%)	99.7
$\mu$ (mm <sup>-1</sup> )	0.134
<i>T</i> (K)	150(2)
<i>F</i> (000)	1468.0
GoF	0.962
<i>R</i> <sub>1</sub> ( <i>I</i> > 2 $\sigma$ )	0.0747
w <i>R</i> <sub>2</sub> ( <i>I</i> > 2 $\sigma$ )	0.2449
Reflections collected	30464
Unique reflections	7816 [R(int) = 0.1070]
Largest diff. peak and hole	0.472 and -0.476 e.Å <sup>-3</sup>

## References

- (1) Lewis, G. N.; Jolly, W. L. *Valence and the Structure of Atoms and Molecules*; American chemical society. Monograph series; The Chemical Catalog Company, inc.: New York, 1923.
- (2) Brown, H. C.; Schlesinger, H. I.; Cardon, S. Z. Studies in Stereochemistry. I. Steric Strains as a Factor in the Relative Stability of Some Coördination Compounds of Boron. *J. Am. Chem. Soc.* **1942**, *64* (2), 325–329. <https://doi.org/10.1021/ja01254a031>.
- (3) Wittig, G.; Rückert, A. Über Komplexbildung Mit Triphenylbor (II. Mitt.). *Liebigs Ann.* **1950**, *566* (2), 101–113. <https://doi.org/10.1002/jlac.19505660202>.
- (4) Tochtermann, W. Structures and Reactions of Organic ate-Complexes. *Angew. Chem. Int. Ed.* **1966**, *5* (4), 351–371. <https://doi.org/10.1002/anie.196603511>.
- (5) Roesler, R.; Piers, W. E.; Parvez, M. Synthesis, Structural Characterization and Reactivity of the Amino Borane 1-(NPh<sub>2</sub>)-2-[B(C<sub>6</sub>F<sub>5</sub>)<sub>2</sub>]C<sub>6</sub>H<sub>4</sub>. *J. Organomet. Chem.* **2003**, *680* (1), 218–222. [https://doi.org/10.1016/S0022-328X\(03\)00384-X](https://doi.org/10.1016/S0022-328X(03)00384-X).
- (6) McCahill, J. S. J.; Welch, G. C.; Stephan, D. W. Reactivity of “Frustrated Lewis Pairs”: Three-Component Reactions of Phosphines, a Borane, and Olefins. *Angew. Chem. Int. Ed.* **2007**, *46* (26), 4968–4971. <https://doi.org/10.1002/anie.200701215>.
- (7) Stephan, D. W. The Broadening Reach of Frustrated Lewis Pair Chemistry. *Science* **2016**, *354* (6317), aaf7229. <https://doi.org/10.1126/science.aaf7229>.
- (8) Stephan, D. W. Frustrated Lewis Pairs. *J. Am. Chem. Soc.* **2015**, *137* (32), 10018–10032. <https://doi.org/10.1021/jacs.5b06794>.
- (9) Stephan, D. W.; Erker, G. Frustrated Lewis Pair Chemistry: Development and Perspectives. *Angew. Chem. Int. Ed.* **2015**, *54* (22), 6400–6441. <https://doi.org/10.1002/anie.201409800>.
- (10) Frustrated Lewis Pairs: Metal-free Hydrogen Activation and More - Stephan - 2010 - *Angewandte Chemie International Edition* - Wiley Online Library <https://onlinelibrary.wiley.com/doi/abs/10.1002/anie.200903708> (accessed Oct 9, 2018).
- (11) Welch, G. C.; Juan, R. R. S.; Masuda, J. D.; Stephan, D. W. Reversible, Metal-Free Hydrogen Activation. *Science* **2006**, *314* (5802), 1124–1126. <https://doi.org/10.1126/science.1134230>.
- (12) Mahdi, T.; Heiden, Z. M.; Grimme, S.; Stephan, D. W. Metal-Free Aromatic Hydrogenation: Aniline to Cyclohexyl-Amine Derivatives. *J. Am. Chem. Soc.* **2012**, *134* (9), 4088–4091. <https://doi.org/10.1021/ja300228a>.

- (13) Chen, D.; Wang, Y.; Klankermayer, J. Enantioselective Hydrogenation with Chiral Frustrated Lewis Pairs. *Angew. Chem. Int. Ed.* **2010**, *49* (49), 9475–9478. <https://doi.org/10.1002/anie.201004525>.
- (14) Welch, G. C.; Stephan, D. W. Facile Heterolytic Cleavage of Dihydrogen by Phosphines and Boranes. *J. Am. Chem. Soc.* **2007**, *129* (7), 1880–1881. <https://doi.org/10.1021/ja067961j>.
- (15) Hamza, A.; Stirling, A.; Rokob, T. A.; Pápai, I. Mechanism of Hydrogen Activation by Frustrated Lewis Pairs: A Molecular Orbital Approach. *Int. J. Quantum Chem.* **2009**, *109* (11), 2416–2425. <https://doi.org/10.1002/qua.22203>.
- (16) Rokob, T. A.; Hamza, A.; Stirling, A.; Pápai, I. On the Mechanism of B(C<sub>6</sub>F<sub>5</sub>)<sub>3</sub>-Catalyzed Direct Hydrogenation of Imines: Inherent and Thermally Induced Frustration. *J. Am. Chem. Soc.* **2009**, *131* (5), 2029–2036. <https://doi.org/10.1021/ja809125r>.
- (17) Rokob, T. A.; Hamza, A.; Pápai, I. Rationalizing the Reactivity of Frustrated Lewis Pairs: Thermodynamics of H<sub>2</sub> Activation and the Role of Acid–Base Properties. *J. Am. Chem. Soc.* **2009**, *131* (30), 10701–10710. <https://doi.org/10.1021/ja903878z>.
- (18) Rokob, T. A.; Hamza, A.; Stirling, A.; Soós, T.; Pápai, I. Turning Frustration into Bond Activation: A Theoretical Mechanistic Study on Heterolytic Hydrogen Splitting by Frustrated Lewis Pairs. *Angew. Chem. Int. Ed.* **2008**, *47* (13), 2435–2438. <https://doi.org/10.1002/anie.200705586>.
- (19) Grimme, S.; Kruse, H.; Goerigk, L.; Erker, G. The Mechanism of Dihydrogen Activation by Frustrated Lewis Pairs Revisited. *Angew. Chem. Int. Ed.* **2010**, *49* (8), 1402–1405. <https://doi.org/10.1002/anie.200905484>.
- (20) Ashley, A. E.; Thompson, A. L.; O’Hare, D. Non-Metal-Mediated Homogeneous Hydrogenation of CO<sub>2</sub> to CH<sub>3</sub>OH. *Angew. Chem. Int. Ed.* **2009**, *48* (52), 9839–9843. <https://doi.org/10.1002/anie.200905466>.
- (21) Dureen, M. A.; Stephan, D. W. Terminal Alkyne Activation by Frustrated and Classical Lewis Acid/Phosphine Pairs. *J. Am. Chem. Soc.* **2009**, *131* (24), 8396–8397. <https://doi.org/10.1021/ja903650w>.
- (22) Dureen, M. A.; Welch, G. C.; Gilbert, T. M.; Stephan, D. W. Heterolytic Cleavage of Disulfides by Frustrated Lewis Pairs. *Inorg. Chem.* **2009**, *48* (20), 9910–9917. <https://doi.org/10.1021/ic901590s>.
- (23) Morton, J. G. M.; Dureen, M. A.; Stephan, D. W. Ring-Opening of Cyclopropanes by “Frustrated Lewis Pairs.” *Chem. Commun.* **2010**, *46* (47), 8947–8949. <https://doi.org/10.1039/C0CC02862B>.

- (24) Ye, K.-Y.; Bursch, M.; Qu, Z.-W.; Daniliuc, C. G.; Grimme, S.; Kehr, G.; Erker, G. Reversible Formylborane/SO<sub>2</sub> Coupling at a Frustrated Lewis Pair Framework. *Chem. Commun.* **2017**, 53 (3), 633–635. <https://doi.org/10.1039/C6CC07071J>.
- (25) Otten, E.; Neu, R. C.; Stephan, D. W. Complexation of Nitrous Oxide by Frustrated Lewis Pairs. *J. Am. Chem. Soc.* **2009**, 131 (29), 9918–9919. <https://doi.org/10.1021/ja904377v>.
- (26) Neu, R. C.; Otten, E.; Stephan, D. W. Bridging Binding Modes of Phosphine-Stabilized Nitrous Oxide to Zn(C<sub>6</sub>F<sub>5</sub>)<sub>2</sub>. *Angew. Chem. Int. Ed.* **2009**, 48 (51), 9709–9712. <https://doi.org/10.1002/anie.200905650>.
- (27) Sajid, M.; Stute, A.; Cardenas, A. J. P.; Culotta, B. J.; Hepperle, J. A. M.; Warren, T. H.; Schirmer, B.; Grimme, S.; Studer, A.; Daniliuc, C. G.; et al. N,N-Addition of Frustrated Lewis Pairs to Nitric Oxide: An Easy Entry to a Unique Family of Aminoxyl Radicals. *J. Am. Chem. Soc.* **2012**, 134 (24), 10156–10168. <https://doi.org/10.1021/ja302652a>.
- (28) Sajid, M.; Elmer, L.-M.; Rosorius, C.; Daniliuc, C. G.; Grimme, S.; Kehr, G.; Erker, G. Facile Carbon Monoxide Reduction at Intramolecular Frustrated Phosphane/Borane Lewis Pair Templates. *Angew. Chem. Int. Ed.* **2013**, 52 (8), 2243–2246. <https://doi.org/10.1002/anie.201208750>.
- (29) Dobrovetsky, R.; Stephan, D. W. Stoichiometric Metal-Free Reduction of CO in Syn-Gas. *J. Am. Chem. Soc.* **2013**, 135 (13), 4974–4977. <https://doi.org/10.1021/ja401492s>.
- (30) Mömmling, C. M.; Otten, E.; Kehr, G.; Fröhlich, R.; Grimme, S.; Stephan, D. W.; Erker, G. Reversible Metal-Free Carbon Dioxide Binding by Frustrated Lewis Pairs. *Angew. Chem. Int. Ed.* **2009**, 48 (36), 6643–6646. <https://doi.org/10.1002/anie.200901636>.
- (31) Zhou, J.; Cao, L. L.; Liu, L. (Leo); Stephan, D. W. FLP Reactivity of [Ph<sub>3</sub>C]<sup>+</sup> and (o-Tolyl)<sub>3</sub>P and the Capture of a Staudinger Reaction Intermediate. *Dalton Trans.* **2017**, 46 (29), 9334–9338. <https://doi.org/10.1039/C7DT01726J>.
- (32) Johnstone, T. C.; Wee, G. N. J. H.; Stephan, D. W. Accessing Frustrated Lewis Pair Chemistry from a Spectroscopically Stable and Classical Lewis Acid-Base Adduct. *Angew. Chem. Int. Ed.* **2018**, 57 (20), 5881–5884. <https://doi.org/10.1002/anie.201802385>.
- (33) Liu, L. (Leo); Cao, L. L.; Shao, Y.; Ménard, G.; Stephan, D. W. A Radical Mechanism for Frustrated Lewis Pair Reactivity. *Chem* **2017**, 3 (2), 259–267. <https://doi.org/10.1016/j.chempr.2017.05.022>.
- (34) Hamilton, H. B.; Wass, D. F. How Important Are Radical Mechanisms in Frustrated Lewis Pair Chemistry? *Chem* **2017**, 3 (2), 198–199. <https://doi.org/10.1016/j.chempr.2017.07.003>.

- (35) Weicker, S. A.; Stephan, D. W. Main Group Lewis Acids in Frustrated Lewis Pair Chemistry: Beyond Electrophilic Boranes. *Bull. Chem. Soc. Jpn.* **2015**, *88* (8), 1003–1016. <https://doi.org/10.1246/bcsj.20150131>.
- (36) Cabrera, L.; Welch, G. C.; Masuda, J. D.; Wei, P.; Stephan, D. W. Pyridine and Phosphine Reactions with [CPh<sub>3</sub>][B(C<sub>6</sub>F<sub>5</sub>)<sub>4</sub>]. *Inorganica Chim. Acta* **2006**, *359* (9), 3066–3071. <https://doi.org/10.1016/j.ica.2006.02.006>.
- (37) Frey, G. D.; Lavallo, V.; Donnadieu, B.; Schoeller, W. W.; Bertrand, G. Facile Splitting of Hydrogen and Ammonia by Nucleophilic Activation at a Single Carbon Center. *Science* **2007**, *316* (5823), 439–441. <https://doi.org/10.1126/science.1141474>.
- (38) Inés, B.; Holle, S.; Goddard, R.; Alcarazo, M. Heterolytic S-S Bond Cleavage by a Purely Carbogenic Frustrated Lewis Pair. *Angew. Chem. Int. Ed.* **2010**, *49* (45), 8389–8391. <https://doi.org/10.1002/anie.201004149>.
- (39) Palomas, D.; Holle, S.; Inés, B.; Bruns, H.; Goddard, R.; Alcarazo, M. Synthesis and Reactivity of Electron Poor Allenes: Formation of Completely Organic Frustrated Lewis Pairs. *Dalton Trans.* **2012**, *41* (30), 9073–9082. <https://doi.org/10.1039/C2DT30195D>.
- (40) Runyon, J. W.; Steinhof, O.; Dias, H. V. R.; Calabrese, J. C.; Marshall, W. J.; Arduengo, A. J. Carbene-Based Lewis Pairs for Hydrogen Activation. *Aust. J. Chem.* **2011**, *64* (8), 1165–1172. <https://doi.org/10.1071/CH11246>.
- (41) Boone, M. P.; Stephan, D. W. A Ru- $\eta^6$ -Arene Complex as a C-Based Lewis Acid in the Activation of Hydrogen and Hydrogenation Catalysis. *J. Am. Chem. Soc.* **2013**, *135* (23), 8508–8511. <https://doi.org/10.1021/ja403912n>.
- (42) Clark, E. R.; Ingleson, M. J. N-Methylacridinium Salts: Carbon Lewis Acids in Frustrated Lewis Pairs for  $\sigma$ -Bond Activation and Catalytic Reductions. *Angew. Chem. Int. Ed.* **2014**, *53* (42), 11306–11309. <https://doi.org/10.1002/anie.201406122>.
- (43) Spies, P.; Kehr, G.; Bergander, K.; Wibbeling, B.; Fröhlich, R.; Erker, G. Metal-Free Dihydrogen Activation Chemistry: Structural and Dynamic Features of Intramolecular P / B Pairs. *Dalton Trans.* **2009**, *0* (9), 1534–1541. <https://doi.org/10.1039/B815832K>.
- (44) Geier, S. J.; Stephan, D. W. Lutidine/B(C<sub>6</sub>F<sub>5</sub>)<sub>3</sub>: At the Boundary of Classical and Frustrated Lewis Pair Reactivity. *J. Am. Chem. Soc.* **2009**, *131* (10), 3476–3477. <https://doi.org/10.1021/ja900572x>.
- (45) Mahdi, T.; Stephan, D. W. Enabling Catalytic Ketone Hydrogenation by Frustrated Lewis Pairs. *J. Am. Chem. Soc.* **2014**, *136* (45), 15809–15812. <https://doi.org/10.1021/ja508829x>.

- (46) Légaré, M.-A.; Courtemanche, M.-A.; Rochette, É.; Fontaine, F.-G. Metal-Free Catalytic C-H Bond Activation and Borylation of Heteroarenes. *Science* **2015**, *349* (6247), 513–516. <https://doi.org/10.1126/science.aab3591>.
- (47) Mummadi, S.; Unruh, D. K.; Zhao, J.; Li, S.; Krempner, C. “Inverse” Frustrated Lewis Pairs – Activation of Dihydrogen with Organosuperbases and Moderate to Weak Lewis Acids. *J. Am. Chem. Soc.* **2016**, *138* (10), 3286–3289. <https://doi.org/10.1021/jacs.5b13545>.
- (48) Lensink, C.; Xi, S. K.; Daniels, L. M.; Verkade, J. G. The Unusually Robust Phosphorus-Hydrogen Bond in the Novel Cation [Cyclic] HP(NMeCH<sub>2</sub>CH<sub>2</sub>)<sub>3</sub>N<sup>+</sup>. *J. Am. Chem. Soc.* **1989**, *111* (9), 3478–3479. <https://doi.org/10.1021/ja00191a081>.
- (49) Tang, J.-S.; Verkade, J. G. [P(MeNCH<sub>2</sub>CH<sub>2</sub>)<sub>3</sub>N] as a Superior Catalyst for the Conversion of Isocyanates to Isocyanurates. *Angew. Chem. Int. Ed.* **1993**, *32* (6), 896–898. <https://doi.org/10.1002/anie.199308961>.
- (50) Dielmann, F.; Moore, C. E.; Rheingold, A. L.; Bertrand, G. Crystalline, Lewis Base-Free, Cationic Phosphoranimines (Iminophosphonium Salts). *J. Am. Chem. Soc.* **2013**, *135* (38), 14071–14073. <https://doi.org/10.1021/ja4080979>.
- (51) Buß, F.; Mehlmann, P.; Mück-Lichtenfeld, C.; Bergander, K.; Dielmann, F. Reversible Carbon Dioxide Binding by Simple Lewis Base Adducts with Electron-Rich Phosphines. *J. Am. Chem. Soc.* **2016**, *138* (6), 1840–1843. <https://doi.org/10.1021/jacs.5b13116>.
- (52) Chi, J. J.; Johnstone, T. C.; Voicu, D.; Mehlmann, P.; Dielmann, F.; Kumacheva, E.; Stephan, D. W. Quantifying the Efficiency of CO<sub>2</sub> Capture by Lewis Pairs. *Chem. Sci.* **2017**, *8* (4), 3270–3275. <https://doi.org/10.1039/C6SC05607E>.
- (53) Mehlmann, P.; Mück-Lichtenfeld, C.; Tan, T. T. Y.; Dielmann, F. Tris(Imidazolin-2-Ylidenamino)Phosphine: A Crystalline Phosphorus(III) Superbase That Splits Carbon Dioxide. *Chem. Eur. J.* **2017**, *23* (25), 5929–5933. <https://doi.org/10.1002/chem.201604971>.
- (54) *Gaussian 09, Revision A.02*, M. J. Frisch, G. W. Trucks, H. B. Schlegel, G. E. Scuseria, M. A. Robb, J. R. Cheeseman, G. Scalmani, V. Barone, G. A. Petersson, H. Nakatsuji, X. Li, M. Caricato, A. Marenich, J. Bloino, B. G. Janesko, R. Gomperts, B. Mennucci, H. P. Hratchian, J. V. Ortiz, A. F. Izmaylov, J. L. Sonnenberg, D. Williams-Young, F. Ding, F. Lipparini, F. Egidi, J. Goings, B. Peng, A. Petrone, T. Henderson, D. Ranasinghe, V. G. Zakrzewski, J. Gao, N. Rega, G. Zheng, W. Liang, M. Hada, M. Ehara, K. Toyota, R. Fukuda, J. Hasegawa, M. Ishida, T. Nakajima, Y. Honda, O. Kitao, H. Nakai, T. Vreven, K. Throssell, J. A. Montgomery, Jr., J. E. Peralta, F. Ogliaro, M. Bearpark, J. J. Heyd, E. Brothers, K. N. Kudin, V. N. Staroverov, T. Keith, R. Kobayashi, J. Normand, K. Raghavachari, A. Rendell, J. C. Burant, S. S. Iyengar, J. Tomasi, M. Cossi, J. M. Millam,

M. Klene, C. Adamo, R. Cammi, J. W. Ochterski, R. L. Martin, K. Morokuma, O. Farkas, J. B. Foresman, and D. J. Fox, *Gaussian, Inc., Wallingford CT, 2016.*

- (55) Stephens, P. J.; Devlin, F. J.; Chabalowski, C. F.; Frisch, M. J. Ab Initio Calculation of Vibrational Absorption and Circular Dichroism Spectra Using Density Functional Force Fields. *J. Phys. Chem.* **1994**, *98* (45), 11623–11627. <https://doi.org/10.1021/j100096a001>.
- (56) Vosko, S. H.; Wilk, L.; Nusair, M. Accurate Spin-Dependent Electron Liquid Correlation Energies for Local Spin Density Calculations: A Critical Analysis. *Can. J. Phys.* **1980**, *58* (8), 1200–1211. <https://doi.org/10.1139/p80-159>.
- (57) Becke, A. D. Density-Functional Exchange-Energy Approximation with Correct Asymptotic Behavior. *Phys. Rev. A* **1988**, *38* (6), 3098–3100. <https://doi.org/10.1103/PhysRevA.38.3098>.
- (58) Lee, C.; Yang, W.; Parr, R. G. Development of the Colle-Salvetti Correlation-Energy Formula into a Functional of the Electron Density. *Phys. Rev. B* **1988**, *37* (2), 785–789. <https://doi.org/10.1103/PhysRevB.37.785>.
- (59) E. D. Glendening, J. K. Badenhoop, A. E. Reed, J. E. Carpenter, J. A. Bohmann, C. M. Morales, C. R. Landis and F. Weinhold, *NBO 6.0, (2013) Theoretical Chemistry Institute, University of Wisconsin, Madison, WI.*
- (60) Lu, T.; Chen, F. Multiwfn: A Multifunctional Wavefunction Analyzer. *J. Comput. Chem.* **2012**, *33* (5), 580–592. <https://doi.org/10.1002/jcc.22885>.
- (61) Stephan, D. W.; Erker, G. Frustrated Lewis Pair Chemistry of Carbon, Nitrogen and Sulfur Oxides. *Chem. Sci.* **2014**, *5* (7), 2625–2641. <https://doi.org/10.1039/C4SC00395K>.
- (62) Dobrovetsky, R.; Stephan, D. W. Catalytic Reduction of CO<sub>2</sub> to CO by Using Zinc(II) and In Situ Generated Carbodiphosphoranes. *Angew. Chem. Int. Ed.* **2013**, *52* (9), 2516–2519. <https://doi.org/10.1002/anie.201208817>.
- (63) Sumerin, V.; Schulz, F.; Nieger, M.; Leskelä, M.; Repo, T.; Rieger, B. Facile Heterolytic H<sub>2</sub> Activation by Amines and B(C<sub>6</sub>F<sub>5</sub>)<sub>3</sub>. *Angew. Chem. Int. Ed.* **2008**, *47* (32), 6001–6003. <https://doi.org/10.1002/anie.200800935>.
- (64) Chase, P. A.; Gille, A. L.; Gilbert, T. M.; Stephan, D. W. Frustrated Lewis Pairs Derived from N-Heterocyclic Carbenes and Lewis Acids. *Dalton Trans.* **2009**, *0* (35), 7179–7188. <https://doi.org/10.1039/B908737K>.
- (65) Hounjet, L. J.; Bannwarth, C.; Garon, C. N.; Caputo, C. B.; Grimme, S.; Stephan, D. W. Combinations of Ethers and B(C<sub>6</sub>F<sub>5</sub>)<sub>3</sub> Function as Hydrogenation Catalysts. *Angew. Chem. Int. Ed.* **2013**, *52* (29), 7492–7495. <https://doi.org/10.1002/anie.201303166>.

- (66) Fasano, V.; Ingleson, M. J. Expanding Water/Base Tolerant Frustrated Lewis Pair Chemistry to Alkylamines Enables Broad Scope Reductive Aminations. *Chem. Eur. J.* **2017**, *23* (9), 2217–2224. <https://doi.org/10.1002/chem.201605466>.
- (67) Bergquist, C.; Bridgewater, B. M.; Harlan, C. J.; Norton, J. R.; Friesner, R. A.; Parkin, G. Aqua, Alcohol, and Acetonitrile Adducts of Tris(Perfluorophenyl)Borane: Evaluation of Brønsted Acidity and Ligand Lability with Experimental and Computational Methods. *J. Am. Chem. Soc.* **2000**, *122* (43), 10581–10590. <https://doi.org/10.1021/ja001915g>.
- (68) Scott, D. J.; Simmons, T. R.; Lawrence, E. J.; Wildgoose, G. G.; Fuchter, M. J.; Ashley, A. E. Facile Protocol for Water-Tolerant “Frustrated Lewis Pair”-Catalyzed Hydrogenation. *ACS Catal.* **2015**, *5* (9), 5540–5544. <https://doi.org/10.1021/acscatal.5b01417>.
- (69) Ashley, A. E.; Herrington, T. J.; Wildgoose, G. G.; Zaher, H.; Thompson, A. L.; Rees, N. H.; Krämer, T.; O’Hare, D. Separating Electrophilicity and Lewis Acidity: The Synthesis, Characterization, and Electrochemistry of the Electron Deficient Tris(Aryl)Boranes B(C<sub>6</sub>F<sub>5</sub>)<sub>3-n</sub>(C<sub>6</sub>Cl<sub>5</sub>)<sub>n</sub> (n = 1–3). *J. Am. Chem. Soc.* **2011**, *133* (37), 14727–14740. <https://doi.org/10.1021/ja205037t>.
- (70) Scott, D. J.; Fuchter, M. J.; Ashley, A. E. Metal-Free Hydrogenation Catalyzed by an Air-Stable Borane: Use of Solvent as a Frustrated Lewis Base. *Angew. Chem. Int. Ed.* **2014**, *53* (38), 10218–10222. <https://doi.org/10.1002/anie.201405531>.
- (71) Mahdi, T.; Stephan, D. W. Facile Protocol for Catalytic Frustrated Lewis Pair Hydrogenation and Reductive Deoxygenation of Ketones and Aldehydes. *Angew. Chem. Int. Ed.* **2015**, *54* (29), 8511–8514. <https://doi.org/10.1002/anie.201503087>.
- (72) Gyömöre, Á.; Bakos, M.; Földes, T.; Pápai, I.; Domján, A.; Soós, T. Moisture-Tolerant Frustrated Lewis Pair Catalyst for Hydrogenation of Aldehydes and Ketones. *ACS Catal.* **2015**, *5* (9), 5366–5372. <https://doi.org/10.1021/acscatal.5b01299>.
- (73) Légaré, M.-A.; Rochette, É.; Lavergne, J. L.; Bouchard, N.; Fontaine, F.-G. Bench-Stable Frustrated Lewis Pair Chemistry: Fluoroborate Salts as Precatalysts for the C–H Borylation of Heteroarenes. *Chem. Commun.* **2016**, *52* (31), 5387–5390. <https://doi.org/10.1039/C6CC01267A>.
- (74) Scott, D. J.; Phillips, N. A.; Sapsford, J. S.; Deacy, A. C.; Fuchter, M. J.; Ashley, A. E. Versatile Catalytic Hydrogenation Using A Simple Tin(IV) Lewis Acid. *Angew. Chem. Int. Ed.* **2016**, *55* (47), 14738–14742. <https://doi.org/10.1002/anie.201606639>.
- (75) Dorkó, É.; Szabó, M.; Kótai, B.; Pápai, I.; Domján, A.; Soós, T. Expanding the Boundaries of Water-Tolerant Frustrated Lewis Pair Hydrogenation: Enhanced Back Strain in the Lewis Acid Enables the Reductive Amination of Carbonyls. *Angew. Chem. Int. Ed.* **2017**, *56* (32), 9512–9516. <https://doi.org/10.1002/anie.201703591>.

- (76) Mosafari, E.; Ripsman, D.; Stephan, D. W. The Air-Stable Carbocation Salt [(MeOC<sub>6</sub>H<sub>4</sub>)CPh<sub>2</sub>][BF<sub>4</sub>] in Lewis Acid Catalyzed Hydrothiolation of Alkenes. *Chem. Commun.* **2016**, 52 (53), 8291–8293. <https://doi.org/10.1039/C6CC03970G>.
- (77) Mummadi, S.; Kenefake, D.; Diaz, R.; Unruh, D. K.; Krempner, C. Interactions of Verkade's Superbase with Strong Lewis Acids: From Labile Mono- and Binuclear Lewis Acid–Base Complexes to Phosphenium Cations. *Inorg. Chem.* **2017**, 56 (17), 10748–10759. <https://doi.org/10.1021/acs.inorgchem.7b01719>.
- (78) Berini, C.; Navarro, O. Ni-Catalysed, Domino Synthesis of Tertiary Alcohols from Secondary Alcohols. *Chem. Commun* **2012**, 48 (10), 1538–1540. <https://doi.org/10.1039/C1CC10826C>.